Inorganic Solid Acids and Their Use in Acid-Catalyzed Hydrocarbon Reactions

A. Corma

Instituto de Tecnología Química, U.P.V.-C.S.I.C., Universidad Politécnica de Valencia, Avenida de los Naranjos s/n, 46022 Valencia, Spain

Received December 5, 1994 (Revised Manuscript Received February 15, 1995)

Contents

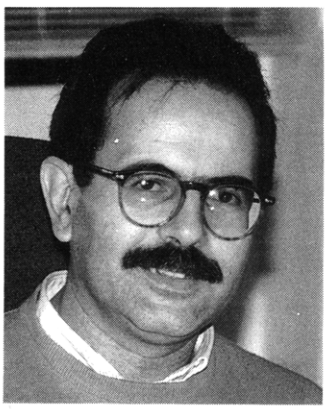

Avelino Corma Canos was born in Moncófar, Spain, in 1951. He studied Chemistry at the Universidad de Valencia (1967–1973), and received his Ph.D. at the Universidad Complutense de Madrid in 1976. The work was done under the direction of Professor Antonio Cortés on the Catalytic Isomerization of Xylenes at the Instituto de Catálisis y Petroleoquímica (C.S.I.C.). After two years postdoctoral stay with Professor B. W. Wojciechowski at Queen's University (Canada) working on catalytic cracking, he joined the Instituto de Catálisis y Petroleoquímica as an associated researcher. In 1987 he became a full Professor and was appointed as director of the Instituto de Tecnología Química (UPV-CSIC) at the Universidad Politécnica de Valencia in 1990. His current research field is zeolites as catalysts, covering aspects of synthesis, characterizations and reactivity in acid–base and redox catalysis. A. Corma has written about 200 articles on these subjects in international journals, three books, and a number of reviews and book chapters. He is a member of the Editorial Board of *Zeolites*, *Catalysis Review Science and Engineering*, *Journal of Molecular Catalysis*, and *Catalysis Letters*. A. Corma is coauthor of 20 patents, five of them commercialized.

It is possible to say that solid acid catalysis involves the largest amounts of catalysts used and the largest economical effort in the oil refining and chemical industry. From a research point of view, acid catalysts have the attractiveness that the nature of the active sites are known and its chemical behavior in acid-catalyzed reactions can be rationalized by means of existing theories and models. This makes these catalysts quite unique if they are compared with others such as metals, oxides, and sulfides in which the particular group of atoms which constitutes the catalytic active site is most of the time unknown. If one adds to all this, the fact that in solid acid catalysts it is frequently possible to modify the acid properties of the material in a predetermined direction through synthesis and post-synthesis treatment and furthermore it is possible to "confirm" those modifications by available characterization techniques, there is no doubt that one is in front of a potentially very rewarding research field.

In this review I have tried to describe perhaps the most important solid acids based on inorganic oxides, going from their preparation procedures and characterization, to their catalytic activity for a series of hydrocarbon reactions. The review starts with an introductory part in where the nature of the acid sites and their physicochemical characterization is de-

0009-2665/95/0795-0559$15.50/0

Table 1. Basic Indicators Used for the Measurement of Acid Strength

indicators	color		pK_a	equivalent (H_2SO_4) %
	base form	acid form		
neutral red	yellow	red	+6.8	8×10^{-8}
methyl red	yellow	red	+4.8	
phenylazonaphthylamine	yellow	red	+4.0	5×10^{-5}
p-(dimethylamino)azobenzene	yellow	red	+3.3	3×10^{-4}
2-amino-5-azotoluene	yellow	red	+2.0	5×10^{-3}
benzeneazodiphenylamine	yellow	purple	+1.5	2×10^{-2}
crystal violet	blue	yellow	+0.8	0.1
p-nitrobenzeneazo(*p'*-nitrodiphenylamine)	orange	purple	+0.43	
dicinnamalacetone	yellow	red	−3.0	48
benzalacetophenone	colorless	yellow	−5.6	71
anthraquinone	colorless	yellow	−8.2	90
2,4,6-trinitroaniline	colorless	yellow	−10.10	90
p-nitrotoluene	colorless	yellow	−11.35	
m-nitrotoluene	colorless	yellow	−11.99	
p-nitrofluorobenzene	colorless	yellow	−12.44	
m-nitrochlorobenzene	colorless	yellow	−13.16	
2,4-dinitrotoluene	colorless	yellow	−13.75	
2,4-dinitrofluorobenzene	colorless	yellow	−14.52	
1,3,5-trinitrotoluene	colorless	yellow	−16.04	

scribed. Then the classification to the different catalysts is initiated with the older amorphous silica−alumina and aluminium phosphates and followed by catalysts with more interest at present which are discussed in order of increasing acid strength: zeolites, heteropoly acids, and sulfated metal oxides. The aim of this review is to present an extended summary of the state of the art and the current and the future tendencies in the field.

I. Nature of Acid Sites on Solid Acid Catalysts

The acidity of a material is defined relative to a base used in acid−base interaction. In this sense the solid acid may be understood as a solid which changes the color of a basic indicator or as a solid on which a base is chemically adsorbed. From the point of view of Brönsted acidity, the solid acid is able to donate, or at least partially transfer, a proton which becomes associated with surface anions. By taking into account the Lewis definition, the solid acid must be able to accept an electron pair. Thus, when the acid surface reacts with a Lewis base molecule a coordinate bond is formed, and this is clearly different from oxidation−reduction reactions, in which a complete transfer of one or two electrons occurs.

There is a large number of reactions which are catalyzed by acid sites, and their importance has surpassed the interest in the fundamental chemistry. It can be said that solid acids are the most important solid catalysts used today, considering both the total amount used and the final economical impact. Then, when a solid acid catalyst is to be designed and optimized in order to carry out a certain reaction, the following questions have to be necessarily answered: What type of acid sites are needed, either Brönsted or Lewis? What is the acid strength required to activate the reactant molecule, and finally, how are the number of the required acid sites in a given solid acid catalyst maximized?

In order to answer these questions, different techniques have been developed to determine the surface acidity, and they will be briefly described in the next section.

II. Physicochemical Characterization of Surface Acidity

A. Titration Methods

Considering that the acidity of a solid catalyst is manifested by the conversion of an adsorbed neutral base into its conjugated acid, the simplest and most widespread method of the acid strength determination for a solid catalyst involves a collaboration of suitable color indicator adsorbed on its surface.

In order to apply this method it has to be accepted that the pH scale used to determine acid strength in dilute aqueous media can be extrapolated to very strong acid media by means of overlapping indicator comparison. By use of an appropriate series of indicators, the extrapolated pH scale is given by H_0 which is the Hammett acidity function.[1] Thus, when the indicator (B) reacts with a Brönsted acid (AH) to form the corresponding conjugated acid (HB^+) and base (A^-), the acid strength is expressed by the Hammett acidity function in the following way:

$$H_0 = pK_a + \log [B]/[BH^+] \quad (1)$$

In the case of the interaction with a Lewis acid site, H_0 is expressed by

$$H_0 = pK_a + \log [B]/[AB] \quad (2)$$

where [B] is the concentration of the neutral base which reacted with the Lewis acid or electron pair acceptor, A.

At this point, the acid strength of a solid catalyst can be estimated by noting which members of a series of Hammett indicators (Table 1)[2] are adsorbed in the acid form.[3] Thus, provided that those indicators are chosen whose acid colors are intense enough to mask their basic colors,[4] the determination can be carried out in the following way: each of a series of Hammett indicators in dilute benzene solution is added to separate samples of the dried solid and the resulting colors are noted. If the color is that of the acid form of the indicator, then the value of the H_0 function of the surface is the same or lower than the pK_a of the

conjugate acid of the indicator. Then, the lower the pK_a of the color changing indicator is, the greater the acid strength of the solid. Detailed information on the acid strength determination using colored indicators can be found in the literature.[5-13] Indicators of different pK_a values and amine titration can give the number of acid sites at various acid strengths. The method consists, in practice, of titrating a solid acid suspended in benzene with *n*-butylamine using an indicator. In order to have reproducible values by this titration techniques, variables such as titration time, volume of added indicator, pore size, and moisture should be carefully considered.[5]

Even in the case when all experimental precautions have been taken, the above titration method suffers from a large number of limitations, starting from the fact that equilibrium is rarely achieved,[14,15] and therefore acidity data from indicator methods should not be used straightforward to predict catalytic behavior. Moreover it should be taken into account that this method gives the sum of the amount of Brönsted and Lewis acids, and only if arylcarbinols are used as indicators, Brönsted acid sites can be specifically measured.[16] Another problem arises from the visual determination of the color change, which could be even more subjective when colored or dark catalyst samples are used. In order to alleviate this problem, spectrophotometric methods have been used,[17,18] and in some cases the spectroscopically measured titers are much lower than the visual titers, specially at high acid strengths.[4,16,19] However, it has been found[20-22] that the traditional Hammett measurements based on determination of the position of the protonation equilibrium of an indicator by UV–visible spectroscopy are not applicable to reallife catalysts. Indeed, when indicator methods are used there is the possibility that the color or the bond arising from the acid form of the indicator may also be produced by surface sites which are not catalytically active. It appears then that if a solid acid has a high acid strength, as measured with indicators, this does not necessarily imply that it is going to be catalytically active. This has been the case observed with sulfated zirconia catalysts[23] for which Hammett indicator technique showed that ZrO_2 is already in the superacid region, while it is inactive for *n*-butane isomerization. Moreover, even in the case of *n*-butylamine, quantitative measurements of band intensity can be misleading if there is considerable overlap of broadened absorption bands from both forms of the indicators.

In order to overcome the above limitations, calorimetric titration of solid acids with amines has been developed.[5,17,21,24,25] However, Farcasiu and Ghenciu[26,27] have shown that, besides the uncertainties associated with the thermal effects due to interactions other than the acid–base, the transfer of more than one proton can be involved. Thus, some molecules treated as simple bases in calorimetric studies[24,25] were later proven by NMR to be at least in part deprotonated in the acid used for calorimetry.[27,28]

The solid acid titration can also be followed catalytically. Indeed, one can measure the catalytic activity for a given reaction after adding different amounts of basic reagents such as alkali metal ions or volatile amines. A plot of the activity versus the amount of added base allows one to determine the minimum amount required for zero activity, and therefore the number of acid sites. The relative acid strength of solids for a given reaction can also be estimated from the slopes of the titration curves.[6,7,29,30] However, this method presents the limitation coming from the fact that the basic molecule used as poison can be adsorbed on both active and inactive acid sites.[31]

Despite the disadvantages of the solution phase titration methods, they are still used and further work is being carried out. More recent studies have been devoted to determine the Brönsted and Lewis site concentration by means of a dual sample titration method.[32] This method relies on the experimental observation that sterically hindered pyridines such as 2,6-dimethylpyridine or 2,6-di-*tert*-butylpyridine bind much more strongly to Brönsted than to Lewis acid sites.[33] Moreover, a sterically unhindered base such as pyridine or *n*-butylamine is able to displace the hindered base from the Lewis but not from the Brönsted acid site.[34,35]

It is better to carry out the titration in a dry box to avoid interference from water and other atmospheric contaminants,[32] and also ultrasonic treatment of the amine-treated catalyst slurry is useful to establish an equilibrium between adsorbed and solution-phase amine.[36] Nevertheless, it should be taken into account that ultrasonication can promote indicator decomposition and catalyst particle fragmentation.[37]

The dual sample titration method has been used in obtaining the number of Brönsted and Lewis acid sites and in the study of the influence of calcination temperature in amorphous silica–aluminas.[38] Despite the fact that this method represents a clear improvement over conventional amine titration with indicator methods, it still presents some limitations derived from the fact that 2,6-dimethylpyridine is not completely selective for adsorption on Brönsted acid sites,[39] and on top of that, it cannot be applied to molecular sieve catalysts because some of the amine titrants and indicators cannot access the acid sites located inside the channels and cavities.

Overall, it has to be said that even though the use of indicators and the Hammett acidity function (eq 1) is still used by many authors to measure the acid strength of solid acids, they should be aware that this is intrinsically inappropriate. Indeed, the use of the H_0 function is adequated for homogeneous aqueous solutions of acids, but in the case of heterogenous acids, neither a_{H+} nor the surface acidity function H_0 have an explicit physical meaning. Therefore, the application of Hammett indicators to characterize the catalytic properties of solid acids can be misleading.

B. Adsorption and Temperature-Programmed Desorption of Base Molecules

Adsorption of volatile amines such as NH_3, pyridine, *n*-butylamine, quinoline, etc., can be used to determine the number of acid sites on solid catalysts. An excess of the base is adsorbed, and what is

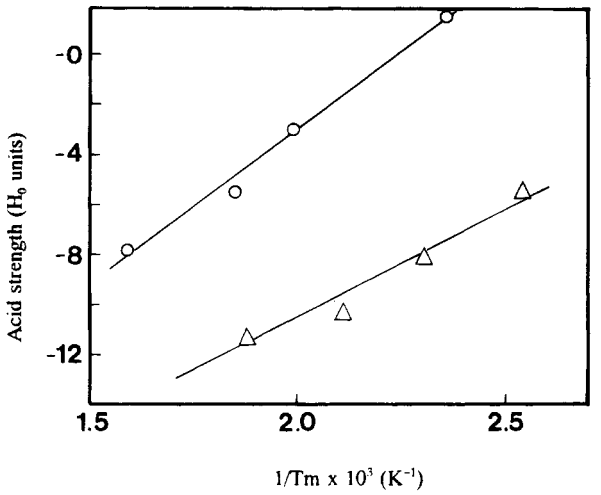

Figure 1. Relationship between Hammett acidity and reciprocal ammonia desorption temperature (T_m) for alumina (○) and silica–alumina (△) catalysts.

considered physically adsorbed is removed by prolonged evacuation. After this, whatever is left on the surface is accounted for as chemically adsorbed, and it measures the total amount of acid sites. The acid strength distribution can be found by direct calorimetric measurements giving the heat of adsorption at different base coverages, or by thermal desorption (TPD) of the preadsorbed base and calculation of the proportion of adsorbed base evacuated at various temperatures.[5-7,40-47] The relationship between temperature of peak maximum (T_m) and activation energy of chemisorbed base adsorption (E_d) is given by the following equation:

$$2 \log T_m - \log \beta = E_d/2.303\,RT_m + \log (E_d A_m/RK_0) \quad (3)$$

where β is the linear heating rate, A_m is the amount of base adsorbed at saturation, K_0 is the preexponential factor in the desorption rate expression, and R is the gas constant. Although TPD method does not give directly a plot of acid strength distribution expressed by the Hammett (H_0) or arylcarbinol (H_R) functions, a correlation has been established:[48]

$$H_0 = a + b/T_m \quad (4)$$

where a and b are empirical constants specific for the acid solid. Figure 1 shows for two systems, namely alumina and silica–alumina, this linear correlation between $1/T_m$ and acid strength as related to the H_0 scale.

In this sense, NH_3 TPD has been extensively used to measure the acidity of solid catalysts.[49] However, it has to be considered that this procedure may be misleading if ammonia dissociates giving NH_2^- and H^+ species which are adsorbed on both acid and basic sites and this depends on the kind of solid and on the adsorption conditions. To this respect Juskelis et al.[50] have shown that a nonacidic, but basic, solid such as calcium oxide does not only adsorb NH_3 but also strongly retains the ammonia even at high temperatures. Amines[50-55] have been recommended as more appropriate adsorbates than NH_3, for the

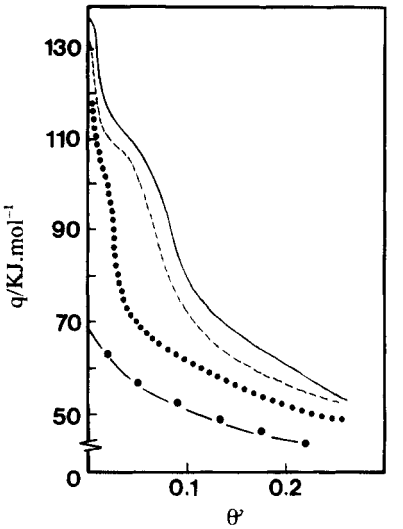

Figure 2. Heat of adsorption of NH_3 on SiO_2–Al_2O_3 at 298 K as a function of the surface coverage (θ) (—) 28 wt % Al_2O_3; (- - -) 13 wt %; (●) 0.7 wt %; (- ● -) 0.0 wt %.

acidity measurements by TPD. It then appears that the choice of the basic probe molecule is critical for the adequate estimation of acidity from the TPD results. For example, *tert*-butylamine has been used for acidity measurements on solid acids,[55] but it decomposes to olefins on strong acid sites at high desorption temperatures.[56] However on solids with medium acidity, alkylamines can be quite useful as the acidity probes.[57]

Furthermore, it has to be considered that basic molecules are adsorbed on both Brönsted and Lewis acid sites, and in those cases when only one of the two types of acid sites is catalytically active, the TPD results will not correlate with catalytic activity, unless the adsorption on the two sites is differentiated by spectroscopic techniques. This is well illustrated by the adsorption of NH_3 and desorption in the 100–400 °C range onto a series of amorphous silica–alumina catalysts containing various amounts (0–100%) of Al_2O_3.[53] From the NH_3 adsorption isotherms, free energies, entropies, and heats of adsorption were calculated. The results presented in Figure 2 show that the isosteric heat of adsorption drops rapidly with surface coverage. This could be interpreted by assuming that the strongest acid sites, i.e., those with a larger heat of adsorption are the first to adsorb NH_3. Moreover, the isosteric heat of adsorption was maximum for the pure Al_2O_3 sample, and systematically decreases with the increase of the SiO_2 content. From these data one should conclude that the 100% Al_2O_3 sample has the largest number of the acid sites having the highest strength and consequently that this should be the most active catalyst for acid-catalyzed reactions. However it is known that a maximum in activity for reactions such as catalytic cracking or C_8 alkylaromatic isomerization[54] occurs on silica–aluminas with 25% wt Al_2O_3. Then it appears that adsorption methods provide particularly misleading acidity values when a substantial amount of base is strongly adsorbed on sites which are catalytically inactive. On top of that, the results of Auroux[58] for various probe molecules on a medium-pore zeolite (ferrierite) show that the mea-

sured heat of adsorption is a function of the surface coverage, and therefore the acid strength population seems to be dependent on the nature of the basic probe molecule used for the calorimetric study.

In the case of solid superacids, e.g. the sulfated metal oxides, the conventional TPD method using desorption temperature to measure the acid strength is inadequate because of the decomposition of the sorbate occurring before the desorption. In order to overcome this problem, an approach has been presented[59] that utilizes TPD to monitor the acidity, in which the observation of a TPD peak with a base indicating a certain level of acidity is similar to the observation of a Hammett indicator color change registering a certain level of acidity. This is achieved by using alkyl- and fluoro-substituted benzenes to measure the relative strength of metal halide and zeolite acid catalysts,[60,61] while the probe basicities are fine-tuned at the molecular level by changing the ring substituents. However, Jatia et al.[62] have found no correlation between the TPD peak of adsorbed benzene and the catalytic activity for *n*-butane isomerization. These authors showed that the TPD peak at ca. 560 °C is from CO_2, SO_2, and O_2 indicating that the adsorbed benzene is totally oxidized in the catalyst samples. TPD can be used to monitor selectively Lewis acid sites when suitable probe molecules are used.[63] For instance the TPD of NO monitored by ESR gives a very specific measurement of the Lewis acid sites on solid catalysts.[64]

In general, it is recommended to analyze the exit gases during the TPD measurements, as well as to couple TPD acidity determinations with spectroscopic techniques in order to determine the bonding of the probe molecules with the different type of acid sites. However if one is willing to use the TPD of bases for the determination of heats of adsorption and from these values to deduce acid site strength, one should be aware that while eq 2 assumes that reabsorption and diffusion of the desorbed base are negligible, this is very seldom true.[65] Moreover the example described above[50] and which shows that CaO strongly retains NH_3, clearly indicate the dangers of using temperature of peak maximum to discuss heats of adsorption and acid strengths, unless the nature of the adsorption sites are perfectly known.

C. Vibrational Spectroscopy Methods

Infrared (IR) and Raman spectroscopy have been used to determine acidity of solid catalysts by studying adsorbed probe molecules.[66-69] The IR spectroscopy is a very powerful technique since it allows one to look directly at the hydroxyls present on a solid acid catalyst and consequently to see which of them can interact with basic molecules and therefore to find out which presents Brönsted acidity and which of them are, or are not, accessible to base molecules of different sizes. In principle, the concentration of hydroxyl groups, and therefore the concentration of potential Brönsted acid sites, could be obtained from the intensity of the corresponding IR band. However, for quantitative estimation the extinction coefficients of the different types of hydroxyls contributing the IR band are required, something which is very seldom possible.

Table 2. IR bands (1400−1700 cm^{-1}) Region of Pyridine Adsorbed on Solid Acids

hydrogen-bonded pyridine	coordinately bonded pyridine	pyridinium ion
1400−1477	1447−1460	
1485−1490	1488−1503	1485−1500
		1540
1580−1600	~1580	
	1600−1633	
		~1640

Attempts have been made to measure the surface concentration of different hydroxyl groups on the basis of the assignment of O−H stretching frequencies to specific types of hydroxyls,[68-73] with limited success in most of the cases. Then, it is not surprising that most of the information on acidity of solid catalysts obtained by IR comes from spectroscopic studies of adsorbed molecules. From this point of view two main groups of probe molecules have been used. The first one involves the adsorption of relatively strong basic molecules such as pyridine, substituted pyridines, quinoline, and diazines. Among them, 1,2- and 1,4-diazines are less basic than pyridines and are more appropriate for the selective detection of very strong acid sites and for the semiquantitative measurement of Lewis and Brönsted acid sites, but they are in general less informative than pyridine. The pioneering works of Parry,[74] Basila et al.,[75] and Hughes and White[76] showed that the pyridine molecule is able to simultaneously determine the concentration of Brönsted and Lewis acid sites. Moreover, when IR is combined with thermal desorption, it can provide estimation of acid strength distribution. In Table 2 the IR frequencies of the bands from pyridine adsorbed on solid acids are given. It can be seen there that the characteristic bands of pyridine protonated by Brönsted acid sites (pyridinium ions) appear at ~1540 and 1640 cm^{-1}, while the bands from pyridine coordinated to Lewis acid sites appear at ~1450 and 1620 cm^{-1}. Then, by measuring the intensity of those bands and from the values of the extinction coefficients given by several authors[76-78] it is possible to calculate the number of Brönsted and Lewis acid sites capable of retaining pyridine at certain desorption temperatures. When there are different types of hydroxyl groups on a solid acid, it is possible by looking at the stretching bands of the hydroxyl groups before and after the pyridine adsorption, as well as after desorption at different temperatures, to determine which hydroxyls are acidic and to characterize their relative acid strength. As an example, the results from Figure 3 show that in the ultrastable zeolite Y, the external and internal silanols (3746 and 3700 cm^{-1}, respectively) and hydroxyl groups from extraframework alumina (3670 cm^{-1}) are not acidic toward pyridine. On the other hand, the Si−OH−Al-bridged hydroxyl groups are acidic and they are able to retain pyridine at $T \geq 150$ °C and 10^{-2} Pa. It has been recently found[79] that at low pyridine coverages iminium ions can be formed on strong acid sites. They are produced at the expense of pyridinium ions and are characterized by a band at 1462 cm^{-1}.

Laser Raman spectroscopy can also be used to observe pyridine adsorbed on Brönsted and Lewis

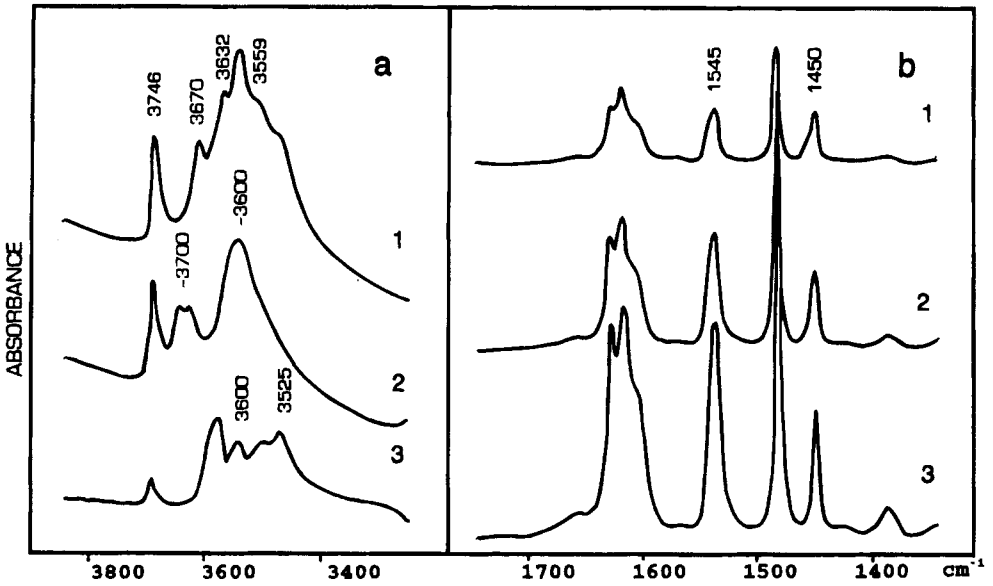

Figure 3. IR spectra of the USY sample: (a) Hydroxyl range (1) before and (2) after pyridine adsorption, and (3) difference spectrum; (b) spectra of pyridine adsorbed at room temperature and desorbed at (1) 523, (2) 623, and (3) 673 K.

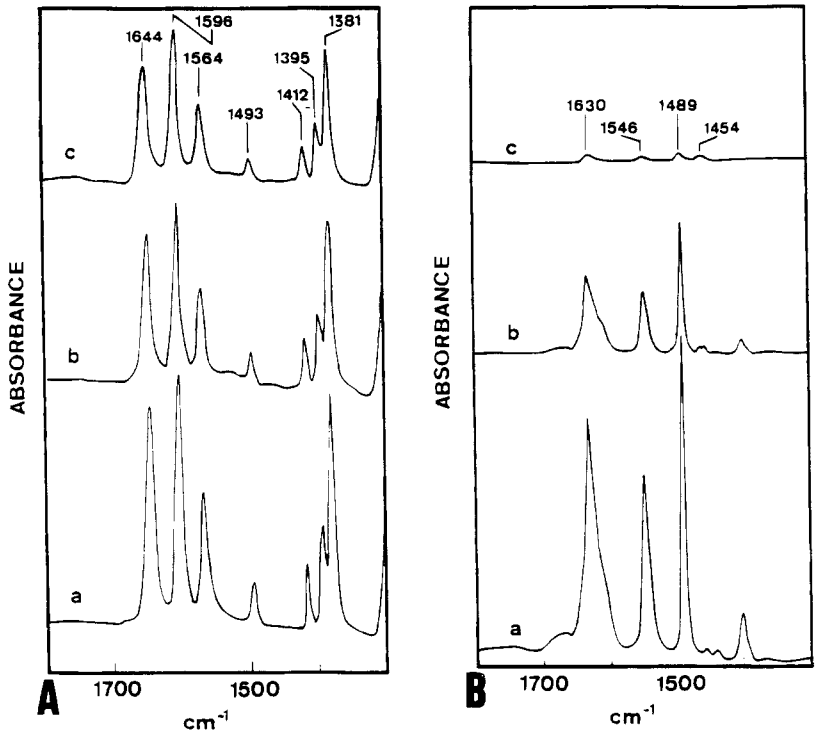

Figure 4. IR spectra of (A) quinoline and (B) pyridine adsorbed on NH_4Y: (a) degassed at 523 K and 10^{-2} Pa, 1 h; (b) degassed at 623 K and 10^{-2} Pa, 1 h; (c) degassed at 673 K and 10^{-2} Pa, 1 h.

acid sites and that H-bonded.[80] However it has to be pointed out that since Raman bands arise from polarizability changes which accompany skeletal and stretching vibrations, the protonation of pyridine is difficult to detect. Therefore, Raman spectroscopy has a low sensitivity for measuring Brönsted acidity. The Raman study of pyridine adsorbed on cation exchanged zeolites have shown the capability of this technique for determining the Lewis acid strength of metal cations. It has been found[81] that the band near 1000 cm^{-1}, arising from the symmetric ring breathing mode of adsorbed pyridine, shifts linearly to a higher frequency as a function of the electrostatic potential of the zeolite cation.

Quinoline is a more basic and larger molecule than pyridine and can also simultaneously distinguish between Brönsted and Lewis acids. The spectra given in Figure 4[82] show the characteristic bands associated with the presence of Brönsted and Lewis acid sites. Because of its larger size, quinoline can be used in some cases, and under controlled conditions, to measure the amount of external acid sites in microporous acid materials, with pores smaller than ~6 Å.

NH_3 can also be used to distinguish between Brönsted and Lewis acid sites, since it gives characteristic IR bands associated with NH_4^+ and NH_3 coordinated to Lewis acid sites.[83]

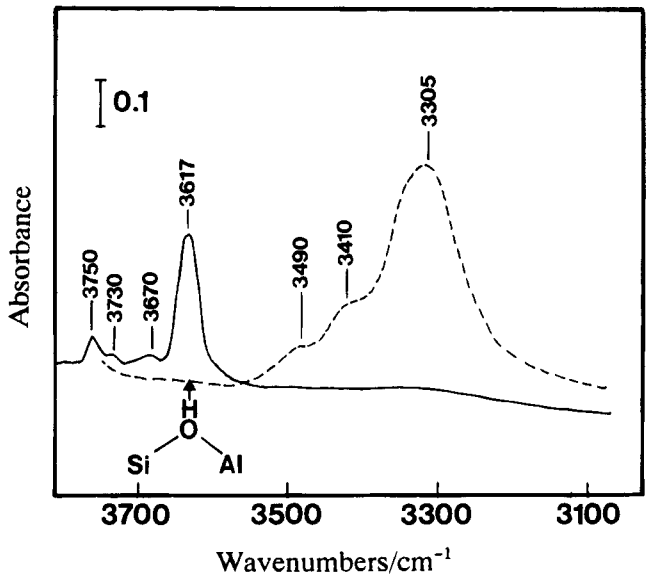

Figure 5. Hydroxyl region of IR spectra of HZSM-5 before (solid) and after (dotted) adsorption of CO at 77 K.

Brönsted acid sites can be selectively measured by IR, using substituted pyridines (2,6-dimethylpyridine) as probe molecules.[83,84]

Pyridine and NH_3 have been widely used as probe molecules, because they are quite stable and the IR spectroscopy can differentiate and quantify the amounts adsorbed on Brönsted and Lewis sites. However, owing to their strong basicity they adsorb strongly, and therefore, unspecifically even on the weakest acid sites. Thus, weaker bases have been used as probe molecules for solid acid catalysts, and quantitative IR data for systems involving CO, SH_2, acetone, benzene, olefins, acetonitrile, H_2, etc. have been reported.[85-88]

Adsorption of carbon monoxide at low temperatures (77 K) is largely used now, owing to the fact that this is a very weak soft base, which has a small molecular size which excludes steric hindrance, and CO is unreactive at low temperature. It specifically interacts with both hydroxyl acid groups and cationic Lewis acid sites. It has been demonstrated that CO interacts with surface hydroxyl groups via H-bonding.[89-94] The H-bond donor strength is considered as a qualitative measure of the acidity of the OH groups involved. Indeed, the H-bond formation will affect both the hydroxyl group and the CO molecule and this is reflected by the frequency shifts of the O−H and CO stretching bands.[90-92,95] An empirical correlation between the heat of adsorption of CO and the experimental frequency shift $\Delta\nu_{OH}$, has been found:[91]

$$\Delta H = 1.308(\Delta\nu_{OH\text{-}40} + Q)^{1/2} \qquad (5)$$

where Q is the heat of condensation (6.77 kJ mol^{-1}) of CO at 77 K. Alternatively, the heat of adsorption can be determined from the temperature dependence of the equilibrium adsorption constant.

When CO was applied as a probe molecule to determine the acidity of different hydroxyl groups such as silanols from silica and bridged hydroxyl groups from a HZSM-5 zeolite (Figure 5), a shift in the OH frequency of ~90 cm^{-1} [90] and ~312 cm^{-1}, respectively, was found. This gives adsorption enthalpies of 16 and 28 kJ mol^{-1} for silica and HZSM-5, respectively, indicating the stronger interaction of CO with bridged hydroxyls, and therefore their stronger acidity. Figure 5 also shows a smaller interaction of CO with other hydroxyl groups on zeolite such as those associated with hydroxylated extraframework (3670 cm^{-1}) or internal silanols (3500 cm^{-1}).

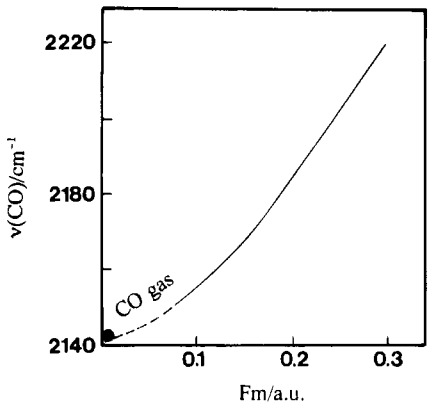

Figure 6. Correlation of carbonyl stretching frequency of adsorbed CO with modified electric field strength F_m.

If Lewis acidity associated to metal cations is involved, a σ bond becomes the dominating interaction. Comparably weak bond energies and higher carbonyl stretching frequencies than the gas phase are the consequences. For instance, in the case of γ-Al_2O_3 which presents a large amount of Lewis acid sites, the carbonyl IR bands of CO adsorbed at 77 K and 20 Torr, after evacuation at 77 K,[92] appears as a strong band at 2152 cm^{-1} with shoulders at 2140 and 2188 cm^{-1}. The 2152 and 2140 cm^{-1} bands are associated to H-bonded and CO physically adsorbed CO,[89,90] while the 2188 cm^{-1} band shifts to 2196 cm^{-1} on evacuation and its intensity does not seem to change significantly indicating that it corresponds to a stable surface complex which has been identified as a CO molecule held by a Lewis acid site Al^{3+}.[89,90,92-102] Therefore, together with the position, the stability of the various carbonyl bands has also to be considered in order to carry out the proper band assignation.

Data from different authors[98,103-105] using ν(CO) values free from shifts due to lateral interactions, show (Figure 6) a nonlinear dependence of ν(CO) on the modified electric field strength, F_m, which is given by

$$F_m = sR_m^{-2} \qquad (6)$$

where s is the ratio of the cation charge (Z) to its coordination number in the cus state (N), and R_m is calculated using effective ionic radii of the central ion in the considered coordination as they have been compiled.[106]

The CO adsorption is also used to detect defect sites,[96,98] as well as to study the effects of anionic modifiers such as SO_4^{2-}, Cl^-, and F^- on Lewis acidity. In this way, the introduction of anionic modifiers leads to enhanced Lewis acid strength as can be deduced from the increase of the carbonyl stretching frequency relative to its value for the unmodified

Table 3. Effect of Modifiers on Carbonyl Stretching Frequencies (cm^{-1}) of Adsorbed CO

oxide	modifier	%	ν(CO)
Al_2O_3			2190
	SO_4^{2-}	5	2210
	F^-	5	2208
	Cl^-	5	2203
	Na^+	3	2180
TiO_2			2192
	SO_4^{2-}	*a*	2196
	Na^+	2	2184

[a] Impurities from the preparation via the sulfate route.

surface (Table 3). The opposite effect can be observed when Na^+ is added.

It appears then that carbon monoxide is a highly specific probe which allows the establishment of the range of acidities when different types of hydroxyls and Lewis sites are involved.

The shifts of hydroxyl bands upon adsorption of aromatics and ethylene on solid acids indicate the strength of the Brönsted acid sites.[107-110] When using ethylene as a probe molecule, the adsorption should be carried out at temperatures as low as 210 K in order to avoid olefin polymerization on the acid sites. Hydrogen sulfide can also be used in a similar way as ethylene and has proved to be an excellent probe molecule to characterize strong acid sites in zeolites.[110] Finally, acetonitrile which is a small molecule with low basicity, $pK_B = 24$, and even better the deuterated acetonitrile which gives a less complex spectrum, is of great utility to measure strong acid sites. The formation of hydrogen bonds between CD_3CN and Brönsted acid sites gives, for instance, in the case of zeolites three IR bands at 2900, 2400, and 1700 cm^{-1}.[111,112] Under adequate adsorption conditions,[113] CD_3CN can be used to monitor Brönsted and Lewis acid strength.[114-116]

D. Nuclear Magnetic Resonance Methods

Nuclear Magnetic Resonance (NMR) is a powerful technique to study solid acid catalysts.[117-119] Advanced NMR methods such as cross-polarization (CP), magic-angle spinning (MAS) of solids, high-resolution and pulse-field-gradient magnetic resonance, multinuclear spectroscopy, and variable-temperature MAS NMR[120] have increased the capability of this technique to study acid sites in solid acid catalysts. Indeed, the total number of the acid sites and their relative strength can be measured by proton MAS NMR techniques in samples of solid acids containing as low as 10^{18} protons.[121-128] The dynamic character of Brönsted acidity has been established from the mean lifetime of protons calculated from NMR, before and after contacting the OH groups with base acting molecules such as water, benzene, pyridine, etc. Following the work of Freude, the ratio between the number of protons involved in a particular process (n), and the mean residence time of the proton at a lattice oxygen ion (τ), can be used as a relative measure of the acidity of OH groups. In a more direct way and by taking into account published quantum chemical calculations,[129-131] a relationship between the acid strength of the different Brönsted acid sites and its chemical shift has

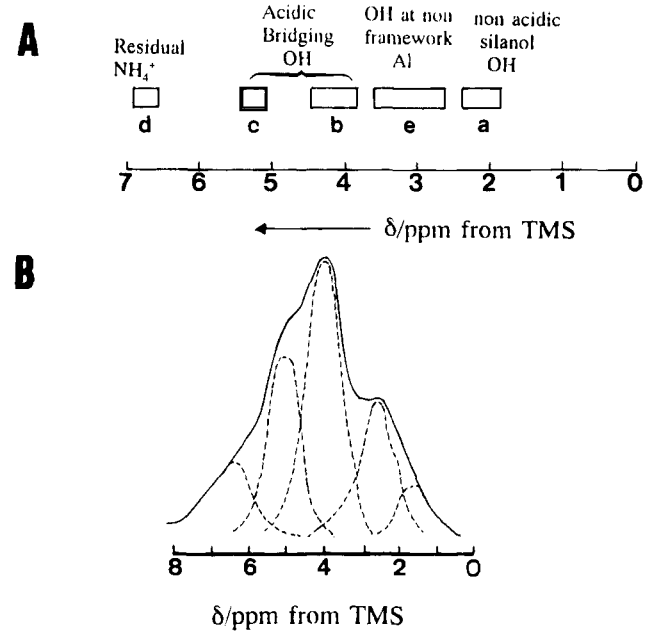

Figure 7. (A) The ^1H chemical shifts (δ) of various protonic species in aluminosilicates and (B) spectrum of zeolite Y showing a Gaussian deconvolution of the different protonic sites.

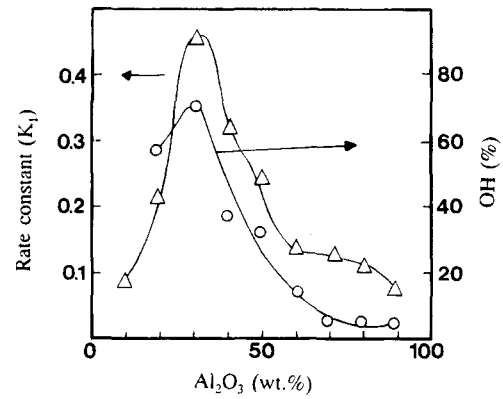

Figure 8. Rate constant for cumene cracking (A, left axis) and the relative percentage of structural acid, OH groups (○, right axis) as a function of Al_2O_3 content for a series of amorphous silica–alumina catalysts.

been found for the case of acidic zeolites (Figure 7). Band c corresponds to bridging OH groups, and the c resonance is due to steric modification of SiOHAl groups in, for example small cavities of zeolites.[125] To determine the number of protons of each type, a Gaussian decomposition of the spectrum is carried out (Figure 7B), and the adsorption intensity is compared with a standard with a known concentration of protons.[132,133] Thus, it is possible to measure the influence of zeolite treatments on the final concentration of all OH groups, including the acidic bridged hydroxyls. This procedure gives a good correlation between acidity and catalytic activity of solid acid catalysts (Figure 8).[134] Recently, two NMR techniques ^2H MAS NMR and echo Fourier ^{27}Al NMR have been applied to the investigation of Brönsted sites in dehydrated hydrogen forms of zeolites.[135] For a dehydrated sample of the H-ZSM-5 zeolite, the ^2H MAS NMR technique showed that in addition to the values of chemical shifts, the quadrupole coupling constants C_{qcc}, can be studied in order to characterize

Table 4. Protonation and Coordination Shifts of Alkyl-Substituted Pyridines

molecule	carbon	amine[a]	H^+ shift[b]	BF_3 shift[b]
pyridine	2	150.3	−8.3	−7.2
	3	124.0	4.4	2.5
	4	135.9	12.0	7.5
4-methylpyridine	2	150.0	−9.2	−7.9
	3	124.8	3.9	2.1
	4	146.7	15.3	10.1
	CH_3	20.6	2.3	0.4
4-ethylpyridine	2	150.2	−9.1	−7.9
	3	123.5	4.1	2.1
	4	152.6	14.5	9.5
	CH_2	28.3	1.3	0.1
	CH_3	14.5	−0.5	−1.15
4-*n*-propylpyridine	2	150.1	−9.0	−7.6
	3	124.0	4.0	2.0
	4	151.0	14.8	9.2
	α-CH_2	37.3	0.8	−0.1
	β-CH_2	23.8	−0.4	−0.8
	CH_3	13.7	0.1	−0.3

the hydroxyl groups. The values of C_{qcc} of the bridging hydroxyl groups increase along the framework Al content of faujasite owing to the decreased acid strength of the bridging OH groups. Meanwhile, the ^{27}Al signal of Si−OH−Al sites, which was "NMR invisible" becomes visible at 11744 T by means of the echo Fourier technique yielding a quadrupole coupling constant of 16.0 ± 1.0 MHz ($\eta = 0.1 \pm 0.1$) for the dehydrated zeolite H-ZSM-5.

A new method for measuring Brönsted acidity of solid acids has been presented by Batamack et al.[136] using wide-line ^1H NMR spectroscopy. This technique is based on the interaction between one molecule of water per one Brönsted site. Thus, samples with low acid strength give only hydrogen-bonded H_2O, while formation of H_3O^+ occurs when acidity is stronger.

The NMR technique can also be used to characterize the interaction of amines with acid sites, provided that the spectra of the protonated and unprotonated forms are significantly different. Good amine probes, from the NMR point of view, should have, at least, one carbon atom that responds differently to Brönsted and Lewis acid sites. Moreover, the lines should not overlap. When these conditions are fulfilled, the number and acid strength of OH acidic groups can be directly determined by the ^{13}C shifts of the adsorbed molecules. In Table 4 ^{13}C MAS NMR results for several amines after protonation by HCl and coordination with BF_3 are listed. It appears that better results are obtained when using symmetrically substituted pyridines, which have three, instead of five, lines in the ring carbon region. In the case of the probe molecules, ^{13}C MAS NMR allows accurate calculation of the sum of Lewis and Brönsted acid sites; however, the shift measurements are not precise enough to separate both types of acid sites. Better results for the discrimination between Brönsted and Lewis acid sites are obtained from ^{15}N and ^{31}P NMR of N and P surface-bound complexes.[137−142] In this way, ^{15}N CP/MAS NMR in the displacement titration of chemisorbed pyridine on silica alumina with *n*-butylamine has shown the potential of this technique.[137] However, the results are difficult to reproduce, and the presence of water strongly modifies the rate of the probe molecule exchange. $^{15}N_2O$ is a selective base probe molecule for Lewis acid sites.[143] ^{13}C NMR can also measure acidities from interaction of acid sites with weak bases such as alcohols, acetone, and acetonitrile.[144,145] The adsorption of other weak bases such as propylene and SH_2 have also been studied by ^1H and ^{13}C MAS NMR, giving additional information on the type of species formed as a function of the type and quantity of surface active sites.[143,146]

In the last decade, phosphorous-containing probe molecules such as trialkylphosphines and trialkylphosphine oxides[147−149] have been used to quantify the number of Brönsted and Lewis acid sites on solid acids by means of ^{31}P MAS NMR and CP/MAS NMR. These molecules can be very adequate to quantify the Brönsted and Lewis acid sites on the external surface of zeolite catalysts, since owing to their size they cannot penetrate the pores. Thus, the results could be correlated with catalyst activity when large organic molecules are involved. So far, this has not been achieved by using base probe molecules coupled with IR techniques. There is no doubt to us that MAS NMR technique will become as useful as IR techniques, if not more, to determine surface acidity on solid catalysts.

E. Photoelectron Spectroscopy Methods

Since XPS measures the kinetic energy of photoelectrons emitted from the core levels of surface atoms upon X-ray irradiation of the uppermost atomic layers, it can be of use to characterize surface acid sites, in combination with base probe molecules.[150]

For instance, the two N_{1s} lines arising from nitrogen atoms in chemisorbed pyridine, one arising from protonated pyridine and the other from pyridine coordinated to Lewis acid sites, could be used to characterize both, Brönsted and Lewis acidity. However, it can be easily understood that this technique cannot be as powerful as IR and NMR spectroscopy. Indeed, owing to the charging and contamination problems it is very difficult to obtain accurate measurements. Moreover, it cannot be used to determine the total acidity of microporous solid acids. On the other hand, it can be used to monitor acidity at external surfaces, and on solids which are opaque to IR radiation.

F. Surface Acidity from the Analysis of the Positron Annihilation Line Shapes

Positron annihilation spectroscopy (PAS) has been scarcely applied to the study of catalytic materials.[151] The method involves three techniques, i.e., positron annihilation lifetime (PAL), one- and two-dimensional angular correlation of the annihilation radiation (1D- and 2D-ACAR), and Doppler-broadened annihilation radiation (DBAR) measurements.[152] Very recently,[153] an alternative new method to measure the specific acidity of catalytic samples with large surface areas using PAS has been presented. The authors have presented results together with 2D-ACAR and DBAR measurements on the NH_4^+-ZSM-5 zeolite and have shown their utility by the line-shape measurements (parameter S) of PAS to monitor the specific acidity of the zeolite (Figure 9).

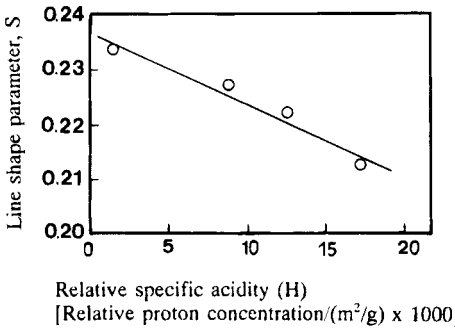

Figure 9. Plot of the line-shape (S) parameter obtained in positron annihilation spectroscopy versus relative specific acidity (*H*) for the NH_4^+–ZSM-5 sample.

G. Conclusions

In conclusion, it appears that the indicators can be used only to get approximate idea on the acid strength distribution of a given solid acid. When indicators are used together with titrating organic molecules the number of acid sites with different strengths could be determined. However, if those results are compared with catalytic activity, good correlations are not necessarily obtained. This is because of the overtitration since one uses more basic reagent than the stoichiometric equivalent of the catalytically active acid sites. Furthermore, only a small fraction of the total acid sites measured are usually active for a given reaction, and the low temperature at which acidity is measured favors indiscriminate adsorption of the basic molecules on all acidic sites. This can be partially overcome by using adsorption–desorption methods. Thermally programmed desorption of basic probe molecules, including sterically hindered ones, can be adequate measures of surface acidity, if coupled with spectroscopic techniques and if the products are analyzed in order to detect any decomposition. In general, it appears that a single technique is not sufficient for the solid acid characterization and interpretation, and for the prediction of catalytic activity and selectivity. However, IR and NMR, including the use of ^{15}N MAS NMR are particularly useful to determine simultaneously both Brönsted and Lewis acid sites. When those are combined with TPD, the relative strength of the acid sites can also be determined and consequently catalyst performance could be, then, related to acidity.

III. Solid Acid Catalysts

A. Amorphous Silica–Alumina and Aluminum Phosphate

The first solid acid catalysts commercially used on a large scale were acid-leached natural aluminosilicates such as clays. They were the first cracking catalysts in the Houdry's process.[154] However the negative impact of the impurities (Fe) on selectivity moved the researchers to prepare amorphous-like synthetic aluminosilicates such as amorphous silica–aluminas.[155] The acidity of these materials can be explained taking into account Tanabe's postulates:[156] (i) "The coordination number of a positive element of metal oxide, C1, and that of a second metal oxide, C2, are maintained even when mixed"; (ii) "The coordination number of a negative element (oxygen) of a major component oxide is retained for all the oxygens in a binary oxide". Indeed, if a silicon atom is replaced by a tetrahedral Al atom, the AlO_4 part is unsatisfied by a whole valence unit and this can be compensated by a proton.[157,158] Molecular orbital calculations were done on silica–alumina cluster models,[159–160] and it was concluded that the H in the hydroxyl group becomes protonic by coordination of Al to an oxygen atom (O_s) bridging the Si. The coordination of the Al atom to the O_s atom corresponds to a Lewis acid base interaction, and the stronger the interaction, the stronger the Brönsted acid strength of the O_s associated H. More recent quantum chemical calculations[161] have summarized that the Brönsted acid sites of binary silica–alumina oxides are bridged hydroxyl groups and water molecules coordinated on a trigonal aluminum atom.

From all the above, one can conclude that the most important goal to be achieved in order to maximize the number of acid sites, is to prepare silica–alumina samples with the maximum amount of tetrahedrally coordinated Al. In this way, one proton would be generated by each Al atom. To do this, the formation of Al–O–Al bonding should be avoided during the synthesis.

The two most common methods for preparing amorphous silica–alumina are as follows: starting from a silica hydrogel with an aluminum sulfate solution, the aluminum salt is hydrolyzed and precipitated by the addition of aqueous ammonia. Another type of preparation involves the interaction of sodium silicate and sodium aluminate. In both cases the global preparation process involves drying, exchange with NH_4^+, and calcination.

In the case of silica–aluminas as solid catalysts it is desirable to maximize not only the number of acid sites but also their accessibility to the reactant molecules by producing a material with the appropriate surface area and porosity. This can be done by controlling the concentration of reactants in the initial mixture, and the pH and aging time of the gel.[162–164]

Recently, it was found that if bulky organoammonium cations, such as tetraalkylammonium cations, are used during the synthesis of amorphous silica–alumina all the aluminum in a 13 wt % Al_2O_3 containing silica–alumina is in tetrahedral coordination and produces acid hydroxyl groups. Moreover, the pore size distribution could be controlled by selecting the size of the alkylammonium cation.[165,166] However, when the material was calcined, ^{27}Al MAS NMR showed that some octahedral Al is already formed.[166] This was more so when the silica–alumina was subjected to calcination and/or steaming at temperatures above 650 °C. Then, a strong reduction in tetrahedrally coordinated Al, acid hydroxyl groups, and surface area was observed.[166]

An improvement in the preparation of high surface area amorphous silica–alumina has been achieved[167] by using tetrapropylammonium hydroxide, in an alkali-free reaction mixture. The material was prepared from a precursor of a ZSM-5 zeolite, and it presents a high surface area with controlled porosity

in the 30–60 Å range. In the original preparation all Al was tetrahedrally coordinated. However, it turned into octahedral Al when calcination steaming at temperatures above 650 °C.

A very exciting recent discovery was the preparation of mesoporous molecular sieves.[168–170] Yanagisawa et al.[168] prepared mesoporous materials by intercalating long-chain alkyltrimethylammonium cations in the layered silicate Kanemite, followed by calcination to remove the organic. During this process it appears that silicate layers condensed to form 3D structure with pores of 30 Å. The acidity of the material was reported to be similar to that of an amorphous silica–alumina. At the same time, Beck et al.[169,170] synthesized nanotubes of amorphous silica–alumina named as M41S, and from which MCM-41 is perhaps the most popular, by using tetramethylammonium and cetyltrimethyl- or hexadecyltrimethylammonium as organics. The regularity of the pore structure has been illustrated by lattice images which show a honeycomb like structure.[170] An interesting thing about these materials is that the pore size can be varied in a wide range (20–100 Å) by choosing the appropiate surfactant chain length, by adding an auxiliary organic, and by using a post-synthetic treatment to reduce the pore size.[170,171]

It has recently been presented that when synthesized, all Al in the MCM-41 structure are in tetrahedral positions. However, as soon as the material is calcined, octahedral Al is observed. If calcination-steaming temperature is increased above 650 °C, then the pores collapse and the 800–1000 $m^2\ g^{-1}$ of the original material is reduced to less than 250 $m^2\ g^{-1}$.[172,173] The ^{29}Si MAS NMR, NH_3 TPD, and pyridine adsorption results[170,173] indicate that MCM-41 strongly resembles an amorphous silica–alumina with very regular tubes.

Amorphous silica–aluminas have been used as catalysts for a large number of hydrocarbon transformations. Among them, they have been particularly useful in isomerization of olefins, paraffins, and alkyl aromatics; alkylation of aromatics with alcohols and olefins; olefin oligomerization; and catalytic cracking. All these reactions will be described in more detail in the next section. Here the potential catalytic applications of the new amorphous silica–aluminas with regular pores ("nanotubes") will be presented. In this case, the amorphous silica–alumina with controlled pore size: i.e., those prepared from ZSM-5 precursors and called MSA,[167] and MCM-41[174,175] have been successfully used to oligomerize propylene to produce gasoline and middle distillate. When the results are compared with those obtained on regular amorphous silica–alumina and an H-ZSM-5 zeolite (Figure 10),[167] it can be seen that the largest conversions at the lowest temperatures are obtained on MSA and MCM-41 samples. In a similar way, MSA and MCM-41 samples show a very good activity and selectivity for benzene alkylation with propene (Table 5).[167] Other applications of these materials are in the field of catalytic cracking,[176,177] but in this case the catalyst regeneration can be critical taking into account the limited thermal–hydrothermal stability of the catalysts.

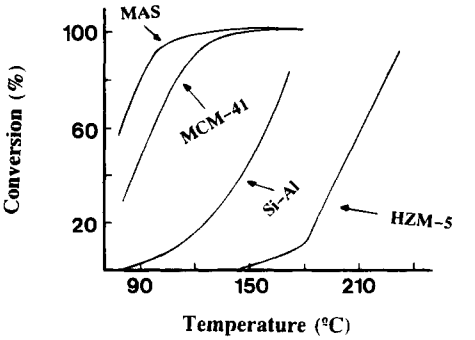

Figure 10. Propene oligomerization on different acid catalysts.

Table 5. Benzene Alkylation with Propene[a]

samples	cumene selectivity	
	referred to benzene	referred to propene
MSA	94.5	89.8
MCM-41	90.8	81.9
amorphous Si–Al	90.8	82.3

[a] T = 160 °C; P = 4 MPa, propene conversion = 90–95%; and benzene/propene = 14.4 (mol).

Amorphous aluminum phosphates have been much less used than amorphous silica–alumina in acid-catalyzed hydrocarbon reactions. This is due to the lower acid strength of the formers which limits its real possibilities to easier reactions. It has been found by IR spectroscopy of adsorbed NH_3 and pyridine that the acidity of stoichiometric amorphous aluminum phosphates (Al/P = 1), corresponds to both Brönsted and Lewis acid type.[178] Hydroxyl groups associated to P are mild Brönsted acid sites and their acidity is enhanced by hydrogen bonding to Al–OH groups. The Lewis acidity is associated to tricoordinated Al sites and/or Al_2O_3 segregated when the sample is heated at temperatures above 500 °C:

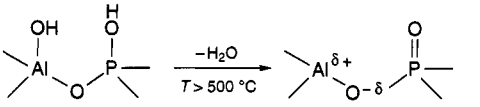

Acidic amorphous aluminum phosphates are usually prepared from an aqueous mixture of aluminum salts and phosphoric acid by precipitation with aqueous ammonia followed by calcination at 500 °C. The number of acid sites in the final material is controlled by the chemical composition (Al/P ratio), and precipitating agent (ammonia, ethylene oxide, and propylene oxide). The maximum number of acid sites as well as those with stronger acidity are obtained in samples prepared with aqueous ammonia,[179] when the Al/P ratio is below 1, and more specifically around 0.3.[180] The acid strength of amorphous aluminum phosphates, which includes sites with $H_0 \leq -5.6$, makes them active for olefin isomerization and aromatic alkylation reactions. However, more demanding reactions such as paraffin isomerization and cracking can hardly be catalyzed by these materials at low temperatures.

If both silica–alumina and aluminum phosphate amorphous materials were of importance in the 1950s and 1960s, they found their natural evolution when crystalline aluminosilicates (zeolites), aluminophos-

phates (ALPOS), and silica–alumina phosphates (SAPOS) were synthesized. These are most versatile materials which add to the acid characteristics of their predecessors amorphous materials, the benefits of larger surface area and controlled pore size within the dimensions of molecular reactants and products. On top of that, they have by far a larger thermal and hydrothermal stability. Today, zeolite type materials have become the largest used and a more versatile type of acid catalysts, and their acid characteristics and catalytic activity for selected hydrocarbon reactions will be described in the following section.

B. Zeolites and Zeotypes as Solid Acid Catalysts

1. Zeolites as Microreactors

General Considerations. Zeolites are tridimensional crystalline aluminosilicates with the following formula in the as-synthesized form: $xM_{2/n}O \cdot xAl_2O_3 \cdot ySiO_2 \cdot WH_2O$ where M is a cation which can belong to the group IA or IIA or can be an organic cation, while n is the cation valence, and W represents water contained in the zeolite voids. Crystalline structures of the zeolite type but containing tetrahedrally coordinated Si, Al, P, as well as transition metals and many group elements with the valence ranging from I to V such as, B, Ga, Fe, Cr, Ti, V, Mn, Co, Zn, Cu, etc., have also been synthesized with the generic name of zeotypes, including $AlPO_4$, SAPO, MeAPO, and MeAPSO type molecular sieves.[181-187]

The main characteristic of the zeolites and zeotypes is that the tetrahedral primary building blocks are linked through oxygens producing a three-dimensional network containing channels and cavities of molecular dimensions.

Considering the channel size they are conventionally defined as ultralarge (>12-), large (12-), medium (10-), or small (8-membered ring) pore materials depending on the smallest number of O or T atoms that limits the pore aperture of their largest channel, and whose diameter varies between 5 and 20 Å. A summary of zeolites and zeotypes with different pore size is given in Table 6.

The system of channels of these molecular sieves produces solids with very high surface area and pore volume, which are capable of adsorbing great amounts of hydrocarbons. This fact combined with the possibility to generate active sites inside of the channels and cavities of zeolites and zeotypes produces a very unique type of catalyst, which by itself can be considered as a catalytic microreactor.

In a catalytic reaction the reactant follows a sequence of events before it becomes a desorbed product. In the case of a zeolite, the sequence is diffusion of reactant through the zeolite micropores to reach an active site, adsorption of reactant on the active site, chemical reaction to give the adsorbed product, desorption of the product, and, finally, diffusion of the product through the zeolite channels.

Diffusion Effects. In the case of hydrocarbon reactions on zeolites and zeotypes, where the size of a molecule closely matches the pore size, it is reasonable to think that the first step in the catalytic process, i.e. the diffusion of the reactant, can play an important role in the overall rate of the reaction observed. Indeed, in such a case it is impossible to think in terms of molecular and Knudsen-type diffusion, so Weisz[188] introduced the term "configurational diffusion" to denote intracrystalline migration. The configurational diffusion is strongly dependent on the site and nature of the reactant, the type of molecular sieve, and temperature. In practice, intracrystalline diffusivities (D_c) in the range of 10^{-8} to 10^{-20} m^2 s^{-1} have been reported (Figure 11).[189] However, concerning the pore diameter of zeolites and zeotypes one should bear in mind that due to lattice vibration the effective pore size is somewhat

Table 6. Zeolites and Zeotypes and Their Ring Size for the Major Channel

molecular sieve type	framework struct.type (IUPAC CODE)	type species	window size
ultralarge pore	CLO	cloverite	20
		JDF-20	20
	UFI	VPI-5, MCM-9, $AlPO_4$-54	18
	AET	$AlPO_4$-8, MCM-37	14
large pore	FAU, EMZ	cubic and hexagonal faujasite, SAPO-37	12
	BEA	beta	12
	MOR	mordenite	12
	OFF	offretite	12
	MAZ	mazzite, omega, ZSM-4	12
	LTL	Linde Tpe L	12
	MTW	ZSM-12 MCM-22 SSZ-26, SSZ-23	12
	AFI	$AlPO_4$-5, $SAPO_4$-5	12
	ATO	$AlPO_4$-31, SAPO-31	12
	AFR	SAPO-40	12
	AFS	MAPSO-46	12
	AFY	COAPO-50	12
	ATS	MAPO-36	12
medium pore	MFI	ZSM-5, silicate	10
	MEL	ZSM-11	10
	FER	ferrierite	10
		ZSM-48	10
	MTT	ZSM-23	10
	TON	ZSM-222, theta 1	10
	HEU	clinoptilolite	10
	AEL	$AlPO_4$-11, SAPO-11	10
	AFO	$AlPO_4$-41	10
small pore	LTA	A	8
	ERI	erionite, $AlPO_4$-17	8
	CHA	chabazite	8
	KFI	ZK-5	8
	RHO	RhO, BeAsPO-RHO	8
	AEI	$AlPO_4$-18	8
	AFT	$AlPO_4$-52	8
	ANA	$AlPO_4$-24	8
	APC	$AlPO_4$-C, $AlPO_4$-H_3, MCM-1	8
	APD	$AlPO_4$-D	8
	ATT	$AlPO_4$-33, $AlPO_4$-12-TAMU	8
	ATV	$AlPO_4$-25	8
	AWW	$AlPO_4$-22	8
		$AlPO_4$-12	8
		$AlPO_4$-14	8
		$AlPO_4$-14A	8
		$AlPO_4$-15	8
		$AlPO_4$-21	8
	ATN	MAPO-39	8
	CHA	SAPO-34, COAPO-44, COAPO-47, ZYT-6	8
	GIS	MAPSO-43	
	LTA	SAPO-42	

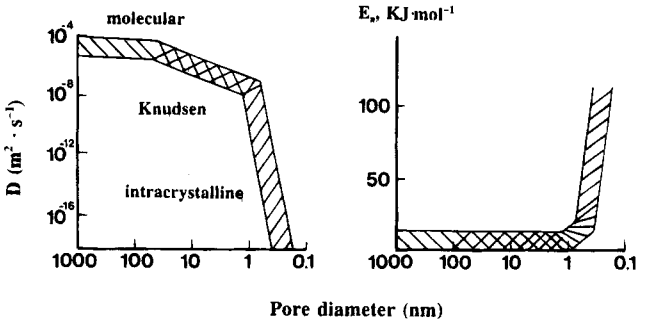

Figure 11. Effect of pore diameter on molecular diffusivities and energy of activation of diffusion.

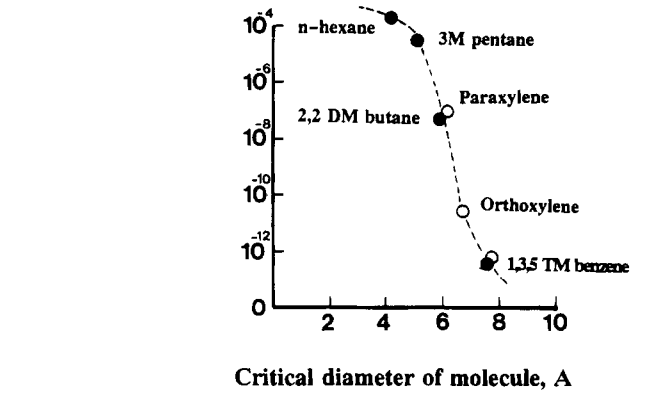

Figure 12. Diffusion coefficients in HZSM-5 for hexane isomers (at 500 °C) and several aromatics (at 315 °C): (○) aromatics and (●) aliphatics.

larger than the crystallographic one. For instance, the difference can be 0.6 Å for zeolite Y heated at several hundred degrees Celsius. In any case zeolites can act as real molecular sieves for reactants and a remarkable molecular discrimination can be attained, as shown in Figure 12.[190] From a practical point of view, it has been estimated[191] that an effective conversion rate of 10^{-6}–10^{-5} g mol of reactant(s) per cubic centimeter of reactor volume is needed for useful fuel or commodity chemical processes. These requirements set a lower limit to useful flow rates into and out of the zeolite crystals, and the rate of diffusion should be larger than the intrinsic chemical conversion rate if the inner surface area of a porous catalyst wants to be utilized to the full extent.

In those cases, where the size of the molecule and pore dimensions allow the diffusion of the reactant, the temperature has an important effect on the rate since molecular diffusion is an activated process. Then, it is not uncommon to find that in processes in which intrazeolitic pore diffusion is the rate-limiting step, the experimental activation energy exceeds values of 15 kcal mol^{-1}. This is because, as it was said above for the transport of molecules through zeolite cages and micropores, the traditional notion of diffusivity no longer applies. Thus, the activation energy of diffusion increases as the critical dimensions of the diffusing molecules approach the dimensions of the pores[192–194] (Figure 11). This in turn means that the energy of activation criteria cannot be used in the case of zeolites and zeotypes to find if diffusion through the pores is the reaction-controlling step.

From a practical point of view, what should be done when the diffusion of reactant is slower than the chemical reaction is to decrease the diffusion main path by decreasing the crystallite size of the zeolite. This should increase the reaction rate. On the other hand, in those cases where the rate of the reaction is not dependent on the crystallite size, one can be sure that the process is not controlled by intrazeolitic diffusion, so all active sites are in use.

Since diffusion of molecules within zeolites is thought to proceed by thermally activated jumps from one site to an adjacent site,[195,196] it is clear that the geometry of the zeolite pores will also play an important role. For instance, in the case of zeolites with unidirectional channels, diffusivities can be sharply reduced by small amounts of debris in the pores generated during zeolite synthesis or activation and also by small amounts of strongly adsorbed molecules. These problems are smaller in zeolites in which a bidirectional or tridirectional pore system exists. For instance, while counterdiffusion of benzene and cumene, which are reactant and product in propylene–benzene alkylation, exists in the relatively open tridirectional structure of Y zeolite,[197] it does not occur within the more restricted unidirectional channels of mordenite.[198] In a similar way, the strong interaction of phenol with the zeolite surface strongly affects the counter diffusion rates even in the case of open tridirectional zeolites such as faujasite, where the ratio $D_{toluene}/D_{phenol} = 10^4$.[197] Finally, tortuosity of the channels also has an important effect on the diffusion of molecules close in size to the diameter of the pores; in this sense it has been found[199] that diffusion is five times faster in the straight channels rather than in the sinusoidal channels of ZSM-5. This in turn bring us to the concept of "molecular traffic control",[200] which assumes that in zeolites with channels of different pore diameter reactants and products of different size can preferentially diffuse through one or the other channel.

After the discussion on diffusion in zeolites one might have the idea that the relatively slow diffusion rates in zeolites are always a handicap. This is not however the case, and one should take into account that differences in diffusivities can be used to increase selectivity to a given product by adequate selection of the pore size of the zeolite catalyst. This comes into the field of shape-selective catalysis[201] which will be discussed later when studying the role of zeolite geometry on catalytic performance.

Adsorption Effects. When a reactant molecule has diffused inside the zeolite channel, it becomes subjected to a series of interactions which involve the following energy terms:[202] dispersion energy (ϕ_D), close-range repulsion energy (ϕ_R), polarization energy (ϕ_P), field–dipole energy (ϕ_{FN}), field gradient–quadrupole energy (ϕ_{FQ}), dipole–dipole energy (ϕ_{NN}), dipole–quadrupole energy (ϕ_{NQ}), and quadrupole–quadrupole energy (ϕ_{QQ}). Thus, it can be easily understood that by changing the chemical composition and structure of the zeolite the relative contribution of these interaction energy terms will be changed and, consequently, the adsorption characteristics of a given molecule. This flexibility in changing the

Table 7. Adsorption Characteristics of Dealuminated Beta Zeolites

HNO_3 concentration (mol/L)	SiO_2/Al_2O_3	% crystallinity	adsorption capacity (wt %)	
			H_2O	*n*-hexane
2.2	46	100	5.0	17
2.9	56	100	4.5	17
4.3	74	100	4.1	18
5.7	164	80	2.6	19
7.2	270	85	1.5	16
11.5	850	80	1.0	14
12	>4000	80	1.0	12

adsorption characteristics of zeolites will also allow discrimination between competing reactants and products by modifying their relative adsorption interaction. Indeed, in the case of zeolites there are structures with low framework Si/Al ratios, and therefore with a large number of compensating cations which will produce very high electrostatic fields (ϕ_{FN}) and field gradients (ϕ_{FQ}) in the channels and cavities. On the other hand, samples can be synthesized with high framework Si/Al ratios in which mainly dispersion forces (ϕ_D) are present, while very little or no influence from electrostatic fields and polarization forces will exist. In other words one could prepare zeolites with a very strong hydrophilic character which would preferentially sorb polar molecules or, on the opposite, with strong hydrophobic properties. In this way, one can change not only the total sorption capacity but also the relative adsorption, within the pores of the zeolite, of molecules with different polarity. This can be achieved by simply changing the framework Si/Al ratio by either synthesis or postsynthesis treatments. By following this, it has been found that highly siliceous ZSM-5 zeolites, which are highly hydrophobic, are able to selectively adsorb organic compounds such as *n*-butyl alcohol[203] or phenol and cresols[204] from their water solutions. Changes in the total adsorption capacity, as well as in the relative adsorption of water and hydrocarbons, for various framework Si/Al ratio of a large-pore zeolite Beta are given in Table 7.[205]

Modifications of adsorption properties of the catalyst can have a strong impact on the reactivity of zeolites and zeotypes. For instance, if one takes a general reaction such as

$$R + S \rightarrow P$$

that follows a Langmuir–Hinselwood bimolecular type mechanism and the product competes for adsorption sites, the following kinetic rate expression for the process can be written:

$$r = \frac{K_o (S_o) K_R K_S (R) (S)}{1 + K_R (R) + K_S (S) + K_P (P)}$$

From this kinetic expression it can be deduced that the rate of the reaction can be varied by changing the intrinsic kinetic rate constant (K_o) which could be done by altering the nature of the active sites, by modifying the total number of active sites (S_o), and by changing the total adsorption capacity, or the adsorption capacity for a given reactant and product. This was illustrated by carrying out a complete kinetic study of the isomerization of *m*-xylene on a series of HY zeolites with different Si/Al ratios.[206] In that work, it was found that when the framework Si/Al ratio was increased by postsynthesis dealumination not only the total number of active sites has changed, but also the adsorption capacity of the zeolite measured from the values of the adsorption constants (K). In other words, it was established that the concentration of reactant molecules inside the pores was varied by modifying the chemical composition of the zeolite. This, besides catalyst activity effects, has strong implications when uni- (xylene isomerization), and bimolecular (alkylaromatic disproportionation) reactions are competing. It was found[206] that the reduction of the adsorption capacity affected more strongly the rate of the bimolecular than unimolecular reaction, increasing therefore the selectivity to isomerization.

Another example, in which the adsorption term in the kinetic equation can play an important role, is the alkylation of phenol by ethylene over acidic faujasite catalysts.[207,208] At reaction temperatures below 473 K phenol is strongly adsorbed on the acid sites avoiding the adsorption of ethylene to form the necessary $C_2H_5^+$ alkylating agents. This makes the adsorption constant for the reactant ethylene practically zero and from the above kinetic equation, the rate of phenol alkylation should be zero. However, alkylation occurs when more polar alkylating agents, such as ethyl chloride or ethanol, are used, which can now compete quite favorably with phenol for adsorption sites.[207,209–210] At temperatures higher than 473 K, and by taking into account the larger (negative) adsorption heat of phenol with respect to ethylene, some adsorption of ethylene already exists and the alkylation occurs.

Changes in hydrophilicity–hydrophobicity can also influence the reactivity in systems where there are differences in polarity between reactants, or reactants and products. For instance, in esterification reactions, where water is formed as a product and the reaction is equilibrium limited unless H_2O is continuously removed, conversions larger than those corresponding to the thermodynamic equilibrium were found when more hydrophobic zeolites were used as catalysts.[211] This was interpreted by assuming that in more hydrophobic catalysts, the concentration of water in the pores, and therefore inside of the microcatalytic reactors, is lower and allows the reaction to proceed further than expected from the thermodynamic data. In other words, the hydrophobicity of the surface assists in the removal of H_2O from the "true reaction media".

Finally, we give an example where modifications of the total and selective adsorption strongly affect the reaction selectivity. In the catalytic cracking of hydrocarbons on zeolites, together with the unimolecular cracking reaction, bimolecular hydride transfer reaction also occurs. When increasing the framework Si/Al ratio of USY zeolite the total adsorption decreases, while the ratio of alkane/olefin adsorbed increases.[212,213] Both features produce an increase in the ratio of cracking to hydride transfer when increasing the Si/Al, with the corresponding increase in the olefinicity of products, and therefore in the

research octane number (RON) of the gasoline.

From what has been said, it is clear that the crystalline structure and microporosity of zeolites and zeotypes introduce clear differences in reactants and product diffusion and adsorption behavior between these materials and their amorphous equivalents such as silica–alumina and aluminum phosphates. These facts, together with the stabilization and acidity gained because of the crystalline structure, make zeolites and zeotypes unique solid acid catalysts.

2. Nature of Acid Sites

Zeolite structure containing only SiO_2 tetrahedra would be electrically neutral and no acidity would be developed on its surface. Brönsted acid sites are developed when Si^{4+} is isomorphically substituted by a trivalent metal cation, for instance Al^{3+}, and a negative charge is created in the lattice, which is compensated by a proton. The proton is attached to the oxygen atom connected to neighbor silicon and aluminum atoms, resulting in the so-called bridged hydroxyl group which is the site responsible for the Brönsted acidity of zeolites.

A first description of the chemical structure of bridged hydroxyls in zeolites was proposed by Uytterhoeven et al.,[214] who envisaged it as a Si–OH group strongly influenced by a tricoordinated neighboring Al^{3+}:

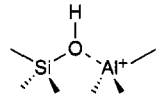

model I

This is one extension of the model proposed to explain the formation of strong Brönsted acid sites on the surface of amorphous aluminosilicates[215,216] and was supported by the two following facts: the number of bridged hydroxyls is the same as the number of Al^{3+}, and the decrease in the frequency of vibration of the bridged OH with respect to a terminal silanol can be explained by the interaction with a neighbor Al^{3+}.

The first model of acid sites in zeolites was improved by considering that the oxygen supporting the acidic hydrogen was chemically bonded to both Al^{3+} and Si^{4+} making a real bridge between them:[217–219]

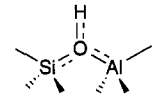

model II

The increase in acidity of the bridged hydroxyl with respect to the silanol group was explained[220] on the bases of the following rules established by Gutmann[221] to explain the interaction between atoms giving and accepting electron pairs:

The length of the nearest bonds to the site in where the donor–acceptor interaction occurs increases when increasing the strength of this interaction.

The bond length increases when its ionicity increases.

The lengths of the bonds generated in a coordination site increase when the coordination number increases.

Following this, it becomes possible to explain some of the properties of the zeolite Brönsted sites. On one hand, the coordination of the bridging oxygen will increase the length of the OH bond in the bridging hydroxyl with respect to the terminal silanol, something which is related with a stronger acidity of the bridged hydroxyl.[219] On the other hand, an increase of the electronegativity in the neighborhood of the OH will induce a transfer of electronic density from the less electronegative atom (H) to the most electronegative one (O). Then, and in agreement with Gutmann's second rule, an increase in the length of the OH bond should occur with the corresponding increase in acidity. We will return to these criteria to explain the influence of zeolite composition on acid strength.

On these bases and taking into account Gutmann's first rule, Rabo et al.[222,223] have proposed an interpretation to explain the acid strength differences between crystalline and amorphous silica–alumina. The interpretation is based on the idea that the protonated Al–OH–Si group prefers to form covalent O–H bonds by forming relatively low Al–O–Si bond angles. It was suggested that the decrease of the angles in the Al–OH–Si units, without affecting the nonprotonated Si–O–Si linkages, is prevented (or at least minimized) by the zeolite crystal in order to maintain long-range order. Thus, if long-range order in the crystal prevails over the short-range bonding preference of the Al–OH–Si group, then the original, large bond angles, will be retained. It would appear then that model I showed above could be more representative of the situation in an amorphous silica–alumina in where no stabilization by long-range symmetry exists, while model II would be more representative of the situation of the acid site in a crystalline zeolite structure.

While the above hypothesis explains a large number of experimental observations, there are still some questions to be answered. Indeed, there are no physical principles which can ascertain that more symmetric structures should be more stable. Then, it is not possible, on formal bases, to explain the rearrangement of the bridged hydroxyls by effects due to crystal symmetry. Moreover, it appears that large-pore zeolites and zeotypes have very flexible structures which can be deformed with little energy.[224,225]

Recent ^1H MAS NMR experimental results[226] have added more complexity to the modeling of acid sites in amorphous and crystalline aluminosilicates. Indeed, it has been observed that upon the removal of the hydration water the Si–O bond is broken in the amorphous material and a strongly covalent OH bond is formed. However, this is not observed in zeolite HY which maintains its original Al–OH–Si linkages. The presence of the Al–OH–Si linkages in zeolites is also confirmed by neutron diffraction studies[227] which have allowed the proposal of an averaged geometry for the protonic site which is in reasonable agreement with the geometry proposed on the bases of NMR[228] and theoretical[229] results (Table 8).

Table 8. Geometries of Bridged Hydroxyls

technique	distances (pm)			angles (deg)	
	OH	OSi	OAl	SiOAl	SiOH
NMR (HZSM-5) (ref 48)	96.5	168.4	184	124.4	114.5
RHI (ref 49)	96.4 ± 0.4	170 ± 0.2	194.5 ± 2	131.5 ± 5	117.5 ± 3
ND (HY) (ref 47)	105.1	164.8	164.8	141.3	108.5

At this point of knowledge, it appears that there are strong pieces of evidence in favor of the covalent character of the bridged hydroxyls.[230] The proton splitting energy is directly related to the acid–base properties of the hydroxyl groups. Thus, the acid–base properties should be correlated both with electronegativity of solids and with corresponding proton abstraction energies. The deprotonation energy is sensitive to lattice relaxation and depends on local geometric constraints due to the long-range ordered structure of the zeolites as well as the zeolite composition.[231] This, not only could explain the stronger acidity of crystalline aluminosilicates with respect to their amorphous counterpart, but also indicates that the proper way to distinguish hydroxyl groups of different acid strengths is to use the energy of their heterolytic dissociation. This can be indirectly estimated from the response of surface hydroxyls to their interaction with adsorbed bases.

3. Influence of Chemical Composition on Number and Strength of Acid Sites

In as-synthesized zeolites the negative charge present on the Al-substituted framework is compensated by organic and inorganic alkaline cations, and such zeolites show no Brönsted acidity. This is generated upon decomposition of organic cations by thermal treatment and by ion exchange of the synthesis cations by protons, or by NH_4^+ and di- or trivalent cations, either by liquid or solid state exchange followed by calcination.[232–238] Theoretically one proton should be introduced for each framework Al^{3+}, and therefore the larger the number of framework aluminum atoms, the higher the potential number of acid sites would be in a given zeolite. Thus, it is clear that the total number of Brönsted acid sites present in a zeolite catalyst will depend on the framework Si/Al ratio, or more generally speaking, on the ratio of framework M^{4+}/M^{3+} cations. In the case of SAPO-type materials they can be considered to be derived from the corresponding ALPO by introducing Si in the framework. The AlPO material is electrically neutral and therefore no charge-compensating Brönsted acid sites exist. The replacement of P^{5+} by Si^{4+} produces a negative charge in the framework which can be compensated by a proton in an Al–OH–Si center similar to that of zeolites. Therefore, in the case of SAPO the number of acid sites will be related to the presence of Si atoms but in this case, and owing to the different substitution mechanisms,[239] it is not possible to establish a direct correlation between the number of Si and the number of H^+, as could be done in the case of zeolites for the number of framework Al^{3+}.

It has been shown that the stretching frequency of the bridged hydroxyl groups in high aluminum containing zeolites decreases when decreasing the Al content of a given zeolite up to reaching a given framework Si/Al ratio (Figure 13).[240] This, together with the shift to lower field of the corresponding lines in the ^{1}H MAS NMR spectra, suggests that Brönsted acid sites in HY zeolites increase in strength when decreasing the Al content.[241] A decreasing heterolytic proton bond dissociation energy with increasing Si/Al ratio is also found from ab initio calculations on clusters with varying Si/Al content.[242] Thus, it is possible to conclude that the acid strength of a given site will increase when there is a decrease in the number of aluminum atoms in next nearest neighbor positions (NNN) of the aluminum atom which supports the acid site.[243] A completely isolated aluminum tetrahedron will have zero NNN (ONNN) and will support the strongest type of framework Brönsted site. Figure 14 shows the distribution of potential acid sites with different Al-NNN values in a Faujasite structure, that is, acid sites with different strengths.[243–246] The distribution shows that acid sites of different strengths can be found on the surface of HY zeolites, and it is possible to prepare a zeolite with the acid strength required for a given reaction, just by changing the framework Si/Al ratio. For instance, if a given reaction requires the participation of strong acid sites, a zeolite catalyst with less than five Al per unit cell should be used. On the other hand, for reactions demanding low acidity, better results from the point of view of activity and selectivity could be attained using zeolites with Si/Al ratios lower than six. It is clear that for framework Si/Al ratios >10 all tetrahedral Al should be isolated ONNN, and all acid sites should be equivalent, at least from the point of view of the chemical composition.

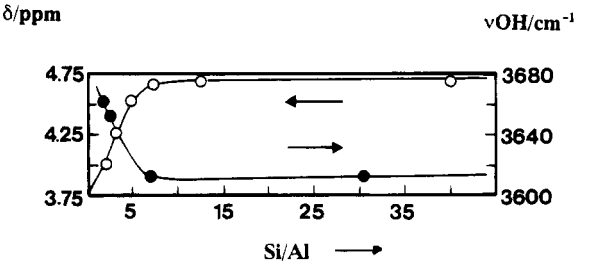

Figure 13. IR high-frequency OH stretching frequency (right axis), and chemical shift (○, left axis) of the corresponding line in the ^{1}H MAS NMR spectrum as a function of the Si/Al ratio of USY zeolites.

The influence of framework chemical composition on acid strength has been rationalized by noting that any change of the zeolite composition would modify the electronegativity of the framework, and the higher it is, the stronger is the acid strength. Thus, it has been found[247,248] that the mean Sanderson's electronegativy (s) correlates with different properties related to the acid strength of zeolites, such as the hydroxyl vibration frequencies in various protonated zeolites, the frequency shift of the high-frequency

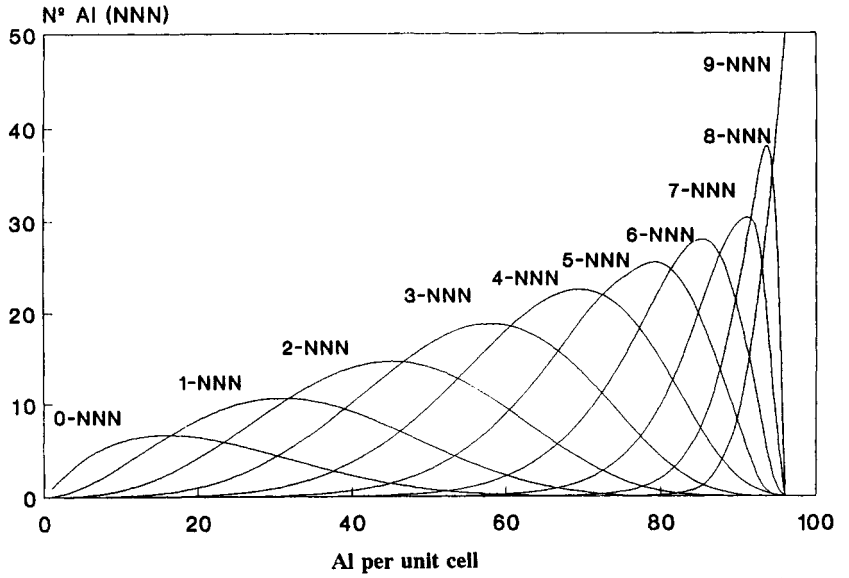

Figure 14. Distribution of the different types of framework Al as a function of the number of Al per unit cell in a Y zeolite.

hydroxyl band of H-zeolites upon interaction with benzene, and the turnover frequency for isopropyl alcohol dehydration on H-zeolites.

However, the use of the Sanderson's average electronegativity as the only parameter is not the most adequate since, as was said above, the acid strength of a given zeolite depends not only on the electronegativity, but also on the proton abstraction energy; and the deprotonation energy depends not only on the zeolite composition but also on the zeolite structure. Owing to this, the concept of "effective" electronegativity, which includes both structural and compositional variables, has been introduced.[249-251] In this way, the highest values of effective electronegativity were calculated for zeolites with the most open frameworks (lower framework densities).

The correlation between framework electronegativity and acid strength also applies to zeotypes[183,252,253] as it has been observed for zeotypes containing Ga^{3+}, Ge^{4+}, and B^{3+}.

Up to now, it has been evident that it should be possible to control the total number and strength of the acid sites in a zeolite by modifying the chemical composition of the framework. This offers the possibility to prepare tailor-made catalysts by changing the electronegativity of the zeolite framework following the acidity required to carry out a given reaction, always of course within the limits of the acidity range achieved in zeolites, and which correspond to $H_0 \geq -10$.

On the other hand, it is common that during zeolite activation, dealumination occurs to some extent and extraframework Al species can be generated. Indeed, it is known that the calcination of the NH_4^+ form of zeolites which is done in order to obtain the acid form, can produce some dealumination unless the decomposition of NH_4^+ is carried out in vacuum or, at least, in a shallow bed. This extraframework aluminum (EFAL) gives rise to the presence of Lewis acid sites as determined by pyridine adsorption.[254] On top of that, it has been claimed[255-257] that the presence of EFAL can enhance the acidity of framework Brönsted sites due to a polarization effect. This EFAL–Brönsted site interaction can also increase the catalytic activity of medium and large-pore zeolites beyond what can be expected from the composition of the framework Si/Al ratio.[255,258-265] Thus, it appears that not only the framework chemical composition, but the overall chemical composition which includes both framework and extraframework species, will affect acidity and therefore catalytic activity for carboniogenic reactions. According to this, there is no doubt that during dealumination of zeolites by post-synthesis treatment, the actual experimental procedure can have an important impact on the amount and type of EFAL formed. In this way, when dealumination is carried out on faujasites by steam treatment, the extracted framework Al remains as EFAL. Mild steaming (T < 600 °C) produces less polymerized cationic EFAL which may be responsible for the enhancement of the Brönsted acidity of some bridged hydroxyl groups. Harder steaming (T > 600 °C) forms pentacoordinated,[266] tetrahedrally coordinated,[267] and, in general, condensed alumina EFAL type species.

Steaming followed by acid treatment can extract a part of EFAL and to restore some of the high frequency (HF) and low frequency (LF) hydroxyl groups by removing cationic EFAL species which were in ion exchange positions.[268]

Dealuminated samples free of EFAL can be produced by using Al complexing agents such as EDTA[269] and $(NH_4)_2F_6Si$.[270,271] In the first case, the Al vacancies are partially left behind, while with the second reagent, the Al vacancies are healed by Si incorporation.

Finally, $SiCl_4$ has also been used to dealuminate zeolites.[272] This reagent removes some of the extracted Al as $AlCl_3$, but some part still remains in the zeolite.

By using one of the above dealumination procedures, or a combination of them, it should be possible to prepare zeolites, which can only be synthesized in a short range of Si/Al compositions, with an expanded

range of Si/Al ratios. Furthermore, one can control the presence or not of Lewis acid sites, as well as their nature and amount.

4. Influence of Structural Effects

It was said above that besides electronegativity, zeolite geometry also plays a role in determining the acidity of zeolites. In this way, it is claimed that the distances and bond angles in the Al−OH−Si group can affect the acidity of the hydroxyl group,[273] and strongly acidic zeolites have a range of T−O−T angles (ZSM-5, 137−177°; mordenite, 143−180°) larger than other less acidic (HY, 138−147°).

The effect of the bond angle and bond distances in Al−OH−Si on the acidity of the hydroxyl group has been studied by means of molecular orbital calculations.[274−277] Carson et al.[278] have calculated the energy required to deform the protonated and deprotonated Si−O−Al bridge, and found that the deprotonation energy decreases with the increase of the T−O−T bond angle, and consequently, the corresponding acidity increases. Other authors[279] arrive at similar conclusions since they found that in a cluster of the type $(HO)_3$ Si(OH) $Al(OH)_3$, the most stable T−O−T angles for the protonated and deprotonated forms are 134.2° and 179.3°, respectively. Experimental results seem to confirm this, and it can be illustrated with SAPO-37, which is isostructural with faujasite, and can be synthesized using tetrapropyl and tetramethylammonium as templates. In this structure the tetrapropylammonium cation is located in the supercavity, while tetramethylammonium cation is in the sodalite units.[280] When both templates are removed by calcination, acid sites are formed which correspond to hydroxyls pointing to the supercavity (3639 cm^{-1}) and to sodalite units (3573 cm^{-1}) and which are mildly acidic. However, if SAPO-37 is calcined at 400 °C in vacuum then the tetrapropylammonium (TPA) is removed while tetramethylammonium (TMA) is still present in the sodalite cages. In this case it has been found[225] that the high-frequency band at 3639 cm^{-1} was shifted at 3630 cm^{-1} indicating an increase in the acidity of the corresponding hydroxy group, as was confirmed by pyridine adsorption−desorption. This was explained by assuming that the presence of TMA in the sodalite cage can produce a deformation of the structure, opening the T−O−T′ angles and increasing the acidity of the associated protons.[225]

The zeolite structure may also cause preferential location of acid sites, i.e. preferential location on some particular oxygens. It was found by XRD that in faujasite the preferred oxygens for forming the bridged hydroxyls are O_1 and O_3, and then O_2, versus O_4 which are those with the lower T−O−T angles.[281,282] This has been confirmed by theoretical calculations.[242,274]

Neutron diffraction (ND) studies were also used to explain the distribution of protons dependent on the large range of effects, i.e. electrostatic forces between protons, framework oxygens, and cations.[227,283] ND has also confirmed that O_2 are preferred than O_4 positions for proton localization. This observation has been explained by assuming that although the bond angles for TO_2T and TO_4T are nearly the same, the proton localized on O_2 points to the 6-member ring window which communicates the supercavity with the sodalite unit, and is stabilized by four closely located oxygens. On the other hand, protons bonded to O_4 point to the supercage and are not stabilized by neighbor oxygens.

In conclusion, nowadays it is clear that zeolite geometry has an influence on acidity due to long-range effects as well as on the local structure of the acid sites. While long-range interactions have a clear effect on the strength of the OH bond and on its electronic properties, as has been demonstrated by IR and NMR, respectively, their effects on proton distribution have to be systematically investigated.

Besides its influence on acidity, the zeolite geometry plays an important role in the catalytic behavior of zeolites through the so-called "shape selectivity effects". Zeolite shape selectivity has been thoroughly discussed in the literature[188,201,284−295] and here will only be outlined.

The first type of shape selectivity is related to mass transport discrimination, and involves reactants and products selectivity. It occurs when the zeolite or zeotype acts as a true molecular sieve for potential reactants and products which, due to their different sizes, present significant differences in diffusivities through a given pore channel system. This type of selectivity is especially important for medium-pore zeolites and allows discrimination between linear and branched paraffins and olefins, as well as between different alkyl aromatic isomers.

When reactants can diffuse inside the zeolite pores and the reaction occurs within the crystalline structure, the size and shape of channels and cavities can also be used, in some cases, to select the desired reaction path by making use of the so-called "transition state shape selectivity". This occurs when the spacial configuration around a transition state located in the crystalline volume, is such that only certain configurations are possible.

There are other geometry-related effects on the product selectivity: "molecular traffic control" [200,295] in multidimensional pore zeolites and "channel tortuosity".[296] The former originates from the preferred diffusion in the crystalline volume of zeolites of molecules with different shape or size within one of two independent systems of pores. In the latter, the reactants will be subjected to more secondary reactions.

The more zeolite effects are discussed, the more and more similarities can be found between zeolites and enzymes. Although the zeolites are not as specific a catalysts as enzymes, they present some common features derived from their hydrophobicity−hydrophilicity, the response of their structure to the interactions of the reactant and the active site, and the shape selectivity effects. However, it is even more than that, and in the next chapter we will show that electronic confinement effects characteristic for molecular sieves, which are generally absent for amorphous mesopore catalysts, may introduce new effects which have an important impact on chemical reactivity.

5. Confinement Effects

When a reactant molecule diffuses through the micropores of a zeolite and starts to interact with its walls and acid sites, the sorption energy of the molecule will include, as was said above, the following energy terms:

$$E = E_D + E_R + E_P + E_N + E_Q + E_I + E_{AB}$$

where E_D and E_R are the attractive and repulsive contributions from the van der Waals interaction, respectively; E_P, E_N, and E_Q are the polar, field–dipole, and field gradient–quadrupole terms, respectively; E_I is the sorbate–sorbate intermolecular interaction energy; and finally, E_{AB} is the energy of the intrinsic reactant–acid site (acid–base) chemical interaction. If one assumes that under reaction conditions the sorbate–sorbate intermolecular interaction energy (E_I) is smaller than the other energy contributions, the interactions in the confined space of the pores are characterized by E_D, E_R, E_P, E_N, and E_Q terms. The first two energy terms will be mostly determined by the geometry of the environment of the acid sites, while the other three will be more sensitive to the chemical composition of the environment. Derouane[289] has proposed that owing to the confinement effect sorbate molecules in zeolites and zeotypes tend to optimize their van der Waals interaction with the surroundings and that the surface curvature of the pore walls interacting with the reactant amplifies the importance of van der Waals interactions. This effect makes zeolites even more similar to enzymes, since the confinement effect may lead to site recognition or molecular preorganization of specific sites of sorbates, reactants, and reaction intermediates or products.[297–299] Furthermore, because of the close size of reactants and zeolite pores, it can be considered that the molecules are "solvated" by the framework and therefore the electric fields generated by the zeolite must strongly affect the properties of the "solute" molecule.

Besides the confinement effect proposed by Derouane, when the size of a guest molecule approaches the size of the pores and cavities of the host, one must also consider an electronic confinement, which can strongly influence the energy levels of the reactant–guest molecule, making it more reactive. The electronic confinement[299] or boxing effect implies that owing to the partial covalent character of the aluminosilicate crystals,[300] electrons are not localized on the framework atoms, but they are partially delocalized through the bulk. Taking this into account, and when the size of the channels approaches the size of the molecule, the density of the orbitals (i.e. the probability for finding the electrons) of the guest molecule has to drop suddenly to nearly zero when reaching the walls of the zeolite. This is the consequence of the short-range repulsion with the delocalized electron clouds of the lattice. This implies that a contraction of the orbitals of the guest molecule will occur with the consequent changes in its energy levels. More specifically an increase in the energy, especially in the frontier orbitals, should be expected, something which may imply a preactivation of the molecule when residing in the pore of the microporous material.

Theoretical calculations made with the molecule of ethylene confined into a microscopic cavity show[299] that there is an increase in the energy of the HOMO orbital, and therefore, the electron shift to form a covalent bond will be more favored. Furthermore, it is deduced that the "basicity" of a confined guest molecule should increase with respect to that in the gas phase, and this may assist in explaining the stronger than expected acidity of zeolites. It should be noticed that the electronic confinement exists independently of the presence of electric field gradients, and as these, will contribute to the preactivation of molecules inside the pores of zeolites.

6. Soft–Hard Acidities in Zeolites

In 1963, Pearson[301] introduced the concept of hard and soft acids and bases (HSAB) in order to explain affinities between acid and bases that do not depend on electronegativities or other related macroscopic properties. A simple rule was established saying that soft acids prefer to react with soft bases and hard acids prefer to react with hard bases. Hard acids are defined[301–303] as small-sized, highly positively charged, and not easily polarizable electron acceptor, while soft ones are defined as those possessing the reverse properties. The fact that the bridged hydroxyl groups as well as the zeolite crystal have a strong covalent character, as was described above, makes it necessary to discuss the acidity of zeolites not only from the point of view of their acid strength but also from the point of view of their HSAB properties. The zeolite acidity considered from the softness point of view allows one to understand better the reactivity and, therefore, to explain the zeolite selectivity in reactions in which orbital control may exist and product distribution is not affected by diffusion limitations.

While the influence of zeolite composition and structure on acid strength has been thoroughly studied by theoretical calculations, as has been discussed above, only a few papers on the hardness of the acid sites have been published. Langemaeker et al.[304] have studied the variation of the Fukui function with changing electronegativity in the neighborhood of the zeolite acid site. The Fukui's function is related, by density functional theory,[305] to Fukui's frontier density[306] and can be interpreted as a local softness.[307] In a more recent work[308] the softness of zeolite structures was determined by semiempirical density functional methodology using the infinite solid model. Working with cluster structures, we have correlated the softness of the acid site and the softness of an adsorbed reagent on the basis of the LUMO energy obtained from both ab initio and semiempirical calculations.[309–312]

In our work it was found that by increasing the Si/Al ratio in the framework the acid softness increased. The effect on the energy of the LUMO orbital, and therefore on the softness, caused by replacement of Si by Al is due to long-range effects. The calculations show that the destabilization of the LUMO orbital is related to the spatial distribution of the negative charge in the Al-containing framework and the localization of the M^+ countercations.

It is known that the acid strength is affected when the nature of the framework atoms in the vicinity of the acid site is changed. With respect to the HSAB concept we found that the softness increases in the order of Al > Ga > B. From these results one may be tempted to correlate softness and acid strength, since in these cases the same tendency between the two parameters is observed. However, this should not be done since both parameters are not equivalent. Indeed, the acid strength is related to the inductive effect of the framework cations, while the softness is determined by the charge distribution in the framework. An example which shows that in some cases acid strength and acid softness can follow opposite tendencies, comes from the isomorphic substitution of Si by Ge, in the site supporting the bridged hydroxyl group.[313] Furthermore, it has been found with the Si–Ge system that the effect of the isomorphic substitution can be different and dependent on whether the substitution occurs at the same site supporting the OH acid group (increases softness) or in the second coordination sphere (decreases softness).

The catalytic implications of changes in acid softness–hardness have been observed for orbital-controlled reactions such as alkylation of toluene and *m*-xylene by methanol.[310–312,314,315] First, softness–hardness of the alkylating agent, i.e. the methoxyzeolite complex was evaluated theoretically for various zeolite compositions, and it was found that the softness of the acid sites and the softness of the methoxyzeolite complex increase with the framework dealumination. It was also observed that the softness of the alkylating agent is even larger due to the fact that during the activation of the electrophile–zeolite complex the energy of the LUMO orbital decreases and its density at the reaction site increases at the same time.[312] All this was reflected in the alkylation of toluene and *m*-xylene by methanol, by an increase in the para/ortho and 124/123 ratios with the increase of the softness, i.e. the increase of the Si/Al ratio of the zeolite, and when going from B-, to Ga- and to Al-substituted large-pore zeolites.[311]

The probability that orbital control exists in reactions occurring on zeolites is increased because when a molecule is introduced into a zeolite pore or cavity, the energy of the HOMO increases due to the presence of the electric field gradients and electronic confinement.[299] Then, and taking the electrophilic alkylation of aromatics as an example, if the energy of the HOMO orbital of the aromatic molecule is increased in the zeolite cavity compared to its value in the gas phase, it is obvious that the energy gap between the LUMO orbital of the electrophile and the HOMO of the aromatic substrate should be smaller in the confined space of zeolite than in an unconfined space. Consequently, a larger effect of the orbital control could be expected when reactions are carried out in zeolites. However, one should consider that the shape selectivity effects can be very important in zeolites, and they may lead to different results that the selectivity effects due to orbital control.[311]

7. Interaction between Hydrocarbons and Acid Sites: Carbocations as Intermediates in Acid-Catalyzed Reactions on Zeolites

At the beginning, the catalytic behavior of acid zeolites was compared to that of superacids in solution. It was supposed that as in the case of superacids in homogeneous phase,[316,317] carbocations would be formed on the surface of acid zeolites by protonation of olefins, aromatics, and even alkanes, by protonation and dehydration of alcohols, or by abstraction of hydride ions from saturated molecules. It was supposed that such carbocations would be the intermediate species in acid-catalyzed reactions of hydrocarbons. Since "free" carbocations were detected in a homogeneous solution of SbF_5–HF, one may expect to be able to detect them on the surface of an acidic zeolite. However, most of the attempts have failed[318] and the only carbocation positively identified on the amorphous silica–alumina and the HY zeolite is the very stable triphenylcarbenium ion. In this case the observed chemical shift is practically the same as that reported for the "free" carbocation with superacids in liquid media. Xu and Haw[319] have reported the NMR observation of indanyl carbenium ion intermediates in the reactions of hydrocarbons on acidic zeolites.

In the case of smaller potential carbocations possibly derived from alcohols and olefins, there is some indirect evidence of their presence at the zeolite surface.[319–323] Unfortunately, the high reactivity of such intermediate species with olefins to form oligomers, makes uncertain the interpretations based on the NMR assignments. Then, due to the lack of experimental evidence one may conclude that it is difficult to accept a direct analogy between the acid catalysis in zeolites and that of superacids in liquid media. The principal difference between the two types of systems would be the much larger stabilization of the intermediate carbocations by solvatation in the superacid media. This is so, despite of the fact that the zeolitic media are also able to solvate charged species, especially in zeolites with a high framework Al content, where the strong field gradients in the channels favor the polarization and ionization of guest molecules in a similar way as in highly polar liquids.[324]

Recently, it has been proposed[230,325,326] that the intermediate stable species in hydrocarbon reactions on acid zeolites must be alkoxy complexes. However, the species whose electronic structure and geometry could be assimilated to adsorbed carbenium ions would not be stable, but would correspond to activated species:

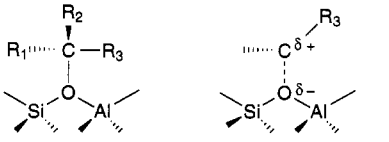

alkoxide (I) activated species (II)

Quantum chemical calculations show[325] that the intermediate II, which may represent the adsorbed carbenium ion is much less stable, even for small C–O distances, than the complex I. In the latter a

covalent bond between carbon and oxygen is formed, so the structure I could be identified with the real, stable, adsorbed intermediate, while the ionic system II requires an additional energy in order to exist. The energy needed to form II comes from thermal activation and/or from the stabilization achieved by its interaction with a basic oxygen (species III):

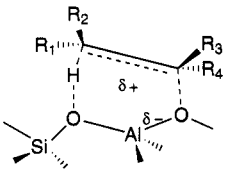

This type of intermediate III implies the existence and the important role of the acid–base pairs in zeolites. We have recently shown by detailed ab initio molecular orbital calculations[327] that in the case of C_3 and C_4 olefins this process is a concerted mechanism involving the proton transfer from the zeolite toward a carbon of the olefin double bond, and the simultaneous C–O bond formation at the adjacent oxygen on the zeolite structure. The reaction mechanism and the properties of the transition states are practically the same, irrespective of the framework T^{III} atom and the increase in branching when going from propylene to isobutene. This suggests that the geometric conformation of the transition state and the flexibility of the zeolite structure are determinant for the formation of an intermediate complex of type III.

The same type of stabilization effects have been observed when the stability of NH_4^+ formed by protonation of NH_3 by the acid sites of zeolites was compared with that of chemisorbed NH_3 on OH acid sites.[328] It was concluded that if NH_4^+ is coordinated to only one basic oxygen of the zeolite in its anionic form, the ionic pair type complex is less stable than that corresponding to the adsorption of NH_3 in where the H atom is still covalently bonded to the oxygen of the acid center:

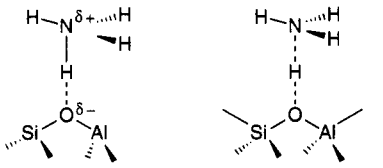

However, when the coordination of NH_4^+ is bidentate or tridentate to other basic oxygens, the ionic pair complex is more stable than the adsorbed complex. It was also found that the geometry around the tetrahedra changes when the proton is transferred. This would not be possible if the lattice was rigid. Consequently, proton transfer requires a flexible lattice that allows for local deformations.[231]

In conclusion, it appears that no "free" carbocations are formed as intermediates on hydrocarbon reactions catalyzed by zeolites, but in this case carbenium ions represent unstable ion pairs or transition states. In the case of zeolites those intermediate species are formed on acid–base pairs, and the flexibility of the zeolite is vital to allow proton transfer. There is no doubt that the electric fields present in zeolites, which are specially intense in Al-rich zeolites, can help to stabilize ionic pair complexes. However, it should be noticed that exactly the same type of reactions and at the same, or even lower, reaction temperatures occurs also on high Si/Al ratio zeolites, in where the stabilizations due to the "solvent" effect of the zeolite should be much lower.

8. Zeolites as Acid Catalysts for Hydrocarbon Reactions

Owing to the special characteristics of zeolites and zeotypes as acid catalysts, they have interesting catalytic properties for carrying out reactions with organic compounds.[329–335] Here, we are going to review a series of hydrocarbon reactions catalyzed by zeolites, wich are of fundamental and practical interest in the oil and chemical industry.

Isomerizations. **Alkenes.** When olefins are in contact with acid catalysts they can easily isomerize the double bond and interconvert the cis and trans isomers. These reactions proceed by breaking and formation of carbon–hydrogen bonds, on or next to the double bond, and are catalyzed by the acid sites.

In the case of catalysts with very strong acidity, proton addition to the double bond with the formation of a carbenium ion, followed by proton elimination has been observed in strong liquid acids:

$$CH_2{=}CH{-}CH_2{-}CH_3 \xrightarrow{+H^+} CH_3{-}CH^+{-}CH_2{-}CH_3 \xrightarrow{-H^+} CH_3{-}CH{=}CH{-}CH_3$$

A similar mechanism seems to work in the case of zeolites and other protonic solid acid catalysts, since when the catalyst is deuterated, the deuterium of the catalyst is incorporated into both reactant and isomerized butenes[336–340] with the following energy profile:[340]

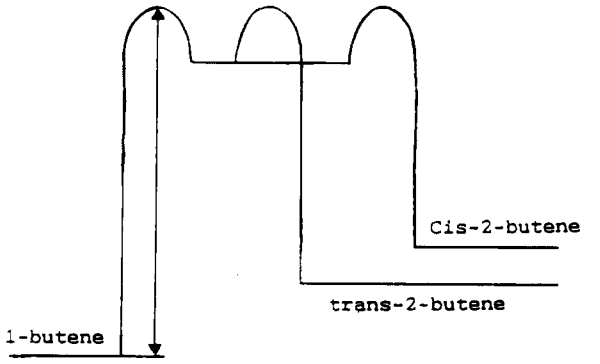

In the case of zeolite catalysts, it is supposed[230] that "free" carbenium ions are not formed, but some carbenium ion-like intermediate does form. This would evolve through a reaction coordinate involving a concerted mechanism in which the C–O bond stretching occurs at the same time as the proton of the carbenium ion-like intermediate is transferred to one of the vicinal basic oxygens:

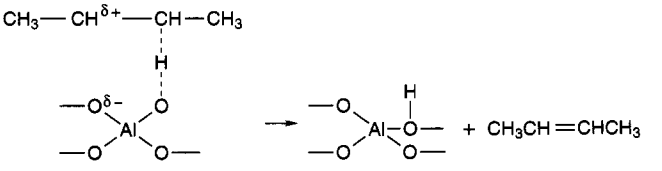

By following the mechanism proposed by Kazansky, it is clear that the activation energy of the double-bond isomerization should be the same as the energy required for the decomposition of an alkoxide group. Indeed, the calculated values for the alkoxide decomposition, and the value of the activation energy for the double-bond isomerization on zeolite catalysts are very similar and in the order of 15−20 kcal mol^{-1}.

In the case of the double-bond isomerization, weak acidity is required and NaHY zeolites with a $H_0 \leq +1.5$ can carry out the isomerization of double bond in long chain olefins with high activity and selectivity.[341] Stronger acid zeolites are less adequate, since besides the double-bond isomerization they can also carry out undesired reactions such as oligomerization and even cracking.

However in the case of olefins the most interesting type of isomerization, from the industrial point of view, is the production of branched olefins from *n*-olefins, especially in the C_4 and C_5 fraction. This is so because of the increasing interest in isobutene and isopentenes as starting materials for the production of methyl *tert*-butyl ether (MTBE), and methyl *tert*-amyl ether (TAME) which are used as oxygenated octane booster additives in the new reformulated gasolines.

The skeletal isomerization of olefins requires stronger acid sites than double-bond isomerization, and the activation energies involved are similar to those for olefin cracking, indicating that both reactions should share common steps.

By following a carbenium ion formalism, branching can occur through a protonated cyclopropane ring, which can give after ring opening and back proton transfer to the catalyst, a branched olefin:

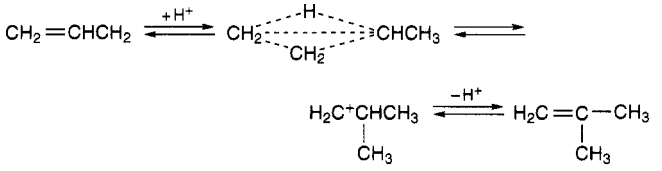

In this mechanism, and for hydrocarbons with less than five carbon atoms, a primary carbenium-like species is formed, and this would explain the need for stronger acidity for carrying out this reaction.

From the practical point of view the skeletal isomerization of short-chain olefins should be carried out at temperatures as low as possible, since at low temperatures the equilibrium is shifted toward branched products (Figure 15).[342] However, at lower temperatures the selectivity is decreased due to olefin oligomerization reactions.[343] If the reaction temperature is increased in order to avoid olefin oligomerization, then other reactions such as cracking, hydrogen transfer, and coke formation can compete, with the corresponding negative effect on selectivity and catalyst life. Thus, reaction temperature is an important variable which has to be adjusted together wich olefin partial pressure and catalyst acidity in order to optimize the process.

Large- and medium-pore zeolite and zeotype catalysts have been studied. In the case of large-pore zeolites such as Y, beta, and ZSM-12[344] higher selectivity for isoolefins and longer catalyst life were

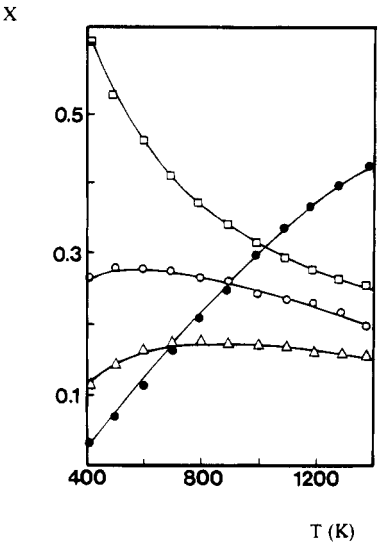

Figure 15. Temperature dependence of the equilibrium concentration of butene isomers: (●) 1-butene, (□) isobutene, (○) *trans*-2-butene, and (△) *cis*-2-butene.

obtained if the acidity of the zeolites is made mild by exchanging protonic sites by alkaline earth cations which may act as Lewis acid sites. Since hydrogen transfer and coke formation are competing undesired reactions, the density of acid sites in the zeolite can have an important effect on selectivity. This effect was studied[345] by means of two beta zeolites with Si/Al ratios of 51 and 28. As expected, a slower catalyst decay was obtained on the sample with the largest Si/Al ratio.

Since in alkene branching isomerization an adequate choice of the acid strength of the catalyst is important to control selectivity and catalyst deactivation, and thus, zeotypes of the AlPO, SAPO, and MeAPO type, whose acidity can be modified by introducing different elements at different concentrations into the framework, have been used as olefin isomerization catalysts. They are active and selective for *n*-butene isomerization if used at temperatures higher than 300 °C.[345-347]

The other factor which also plays a determinant role on the isomerization selectivity and the catalyst life, is the zeolite and zeotype pore size. In general, it can be said that medium-pore materials favor the skeletal isomerization with respect to double-bond isomerization and oligomerization. Moreover, geometrical restriction within the pores decreases the formation of coke precursors, and therefore increases the life of the catalyst. In this sense the adequate combination of acidity and pore size have made medium-pore Fe and Mn SAPO-11 and SAPO-31 suitable catalysts for commercial isomerization of *n*-butene. Results from Table 9[345] show that while SAPO-31 is already active and selective catalyst if used at high reaction temperatures, the selectivity to isobutene is strongly increased when Mn is introduced into the framework.

Another way to control acid strength is the synthesis of zeolites with T^{III} other than Al. When B instead of Al was introduced into ZSM-5 it was found that activity decreased but selectivity to isobutene increased. Thus, an improvement was claimed when ZSM-5 containing B and Al were synthesized.[348]

Table 9. Isomerization of 1-Butene over Substituted AlPO-31 Molecular Sieves at 743 K, 50% 1-Butene in N_2, WHSV = 4.5 h[a]

molecular sieve	conversion of 1-butene (%)	selectivity isobutene	product composition (vol %)			
			1-butene	*cis*-2-butene	*trans*-2-butene	isobutene
$AlPO_4$-31	69.8	6.6	30.2	28.0	35.2	4.6
MnAPO-31/2	73.4	19.1	26.6	24.6	31.2	14.0
SAPO-31	73.6	26.3	26.4	22.8	28.8	19.4
MnAPSO-31/1	76.6	32.9	23.4	21.6	27.8	25.2
MnAPSO-31/2	75.4	25.7	24.6	23.6	30.2	19.4
MnAPSO-31/3	71.9	14.2	28.2	26.2	33.2	10.2

[a] Samples taken after 6 h time on stream.

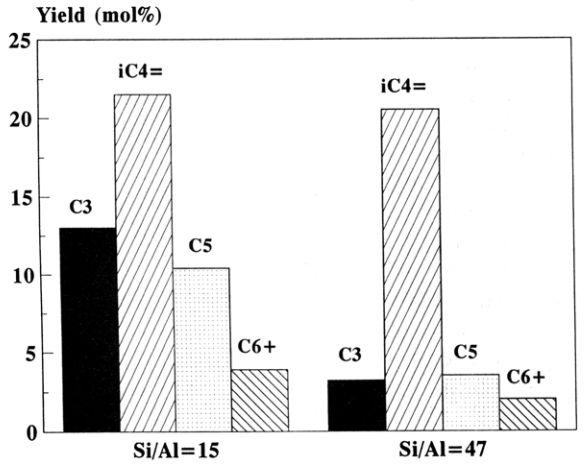

Figure 16. Product yields obtained during the isomerization of 1-butene on MCM-22 zeolite catalysts with two different Si/Al ratio. Reaction conditions: $T = 350$ °C, N_2/1-butene = 9/1, 1-butene WHSV = 28 h^{-1}, TOS = 30 min.

However, it should be taken into account that B can easily come out from the framework positions during the zeolite activation. If this happens, the B Al-ZSM-5 zeolites are equivalent to Al-ZSM-5 zeolites but with a higher Si/Al ratio. Indeed, the results presented in Figure 16 show that by increasing the framework Si/Al of MCM-22, which has 12 and 10 MR channels, the selectivity to isobutene increases, while the selectivity to oligomerization and cracking decreases.[349] Similarly, other medium-pore size zeolites with high Si/Al ratio such as ZSM-22 and ZSM-23, if used at high temperature and WHSV, give high activity and selectivities.[350,351]

The best results reported on skeletal isomerization of *n*-butene on zeolites correspond to ferrierite. This has a structure formed by unidirectional 10 MR channels with loobs. When the zeolite is optimized from the point of view of the framework Si/Al ratio and the crystallite size, selectivity to isobutene close to 70% at ~60% conversion is obtained.[352] It has been claimed[353] that the special channel structure of ferrierite is responsible for the high isomerization selectivity, which is achieved because cracking of the branched dimeric C_8 olefin intermediates which produce isobutene and *n*-butenes rather than C_3 and C_5 fragments.

Alkanes. Skeletal isomerization of paraffins with carbon numbers between 5 and 10 is important to improve the octane number of the gasolines, while isomerization of larger *n*-paraffins ($>C_{10}$) is also useful to decrease the freezing point of the diesel fuel. The skeletal isomerization of paraffins can be carried out on acid zeolites, and this process requires very strong acid sites. However, the use of monofunctional acid zeolites gives low selectivity to branched isomers because of extensive recracking of branched alkanes, which are easier to be cracked than the *n*-paraffins.

Conversion and selectivity is strongly increased when Pt or Pd are incorporated into the acidic zeolite, and the reaction is carried out in the presence of H_2. In this case, the proposed mechanism involves the formation of an intermediate olefin, which is produced by dehydrogenation of the alkane on the metallic site.[354] In the second step, the olefin diffuses to an acid site, where it is protonated to form a carbenium ion-like transition state, which can isomerize or even crack, depending on the hydrocarbon chain length, reaction temperature, and the average lifetime of the branched carbenium ion-like species on the catalyst surface. This in turn depends on both the acid strength and on the good hydrogen transfer–hydrogenation activity of the catalyst. An scheme of such a mechanism is as follows:

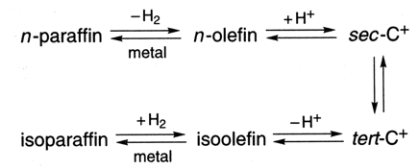

In the bifunctional mechanism described above and if the adequate balance between the metal and the acid function is achieved (Pt atom/acid site ≥ 0.15),[355] the rearrangement of the carbenium like-ion becomes the controlling step.

When shorter chain paraffins C_4–C_5 are to be isomerized very strong acid sites are needed since the reaction will go through primary carbenium ions. Thus, zeolites with stronger acidity, such as mordenite and ZSM-5, would appear as the most convenient. However, because of the small diameter of ZSM-5, the diffusion of branched isomers will be restricted in this zeolite, and therefore mordenite should be the preferred catalyst. When this is selected as the acid component, sites with maximum strength are produced by modifying the framework Si/Al ratio in post-synthesis treatments in order to obtain isolated tetrahedral Al atoms.[356,357] Thus, maximum activity is found for framework Si/Al ratios of ca. 10. However, it was pointed out, when discussing the influence of zeolite composition on acid strength, that an increase in the acid strength of bridged hydroxyl groups can be obtained by interaction with ex-

traframework species. This effect also occurs in mordenite, in which owing to the OH-EFAL interaction an increase in the activity of a Pt/Mordenite for isomerization of *n*-pentane and *n*-hexane was observed.[263]

Other large-pore zeolites in which strong acidity can also be produced are omega and beta. Indeed, bifunctional catalysts based on these two zeolites show good activity and selectivity for *n*-pentane and *n*-hexane isomerization.[358,359]

In the case of *n*-butane, zeolite catalysts can hardly work at temperatures below 270 °C and in this case most of the isobutane is formed by an alkylation–cracking mechanism, instead of by direct isomerization of *n*-butane.

When long-chain *n*-paraffins have to be isomerized, milder acidities and larger pores are desired in order to minimize recracking of the branched products formed. Thus, bifunctional catalysts based on zeolites such as faujasite, ZSM-3, CSZ-1, and L, or even zeolite mixtures as well as SAPOS and MEAPOS, show good selectivities for branching isomerization of long-chain paraffins.[360–366] In the case of open structures in where no shape selectivity effects exist, the product distribution can be predicted by taking into account the protonated cycloprane (PCP) mechanism.[367]

It can be concluded that when using zeolites as catalysts for isomerization of *n*-paraffins, one has to take into account the size of the reactant and products, as well as the acid demands to form the corresponding intermediates. Then, a zeolite or zeotype with the adequate pore size and acid strength could be selected. However, even with the best optimized zeolite catalysts, it is not possible to carry out the isomerization of *n*-butane to isobutane with good yields and selectivity. This reaction requires stronger acid sites than those obtainable in zeolites, and the possibilities of solid catalyst with stronger acid sites to carry out this reaction will be described later when discussing the acidic properties of heteropoly acids and sulfated metal oxides.

Alkyl Aromatics. Aromatic ring positional isomerizations are reactions of commercial interest where zeolites have demonstrated its superiority as catalysts. In Friedel–Crafts type of acid catalysts the isomerization of alkyl aromatics is always accompanied by the competitive transalkylation reaction. Zeolites have demonstrated that it is possible, by an adequate selection of the pore size and chemical composition, to optimize selectivity toward the production of the desired isomer. Taking the isomerization of xylenes as an example, the composition of the thermodynamic equilibrium at room temperature is approximately: 24, 60, and 16% for *p*-, *m*-, and *o*-xylene, respectively. Since the commercially most desired product is the para isomer, which is a raw material for production of terephthalic acid, there is a clear incentive for the selective isomerization of *m*- to *p*-xylene.

On solid amorphous catalysts, as well as on large-pore zeolites and zeotypes, the isomerization of *m*-xylene is accompanied by transalkylation to produce toluene and trimethylbenzenes:

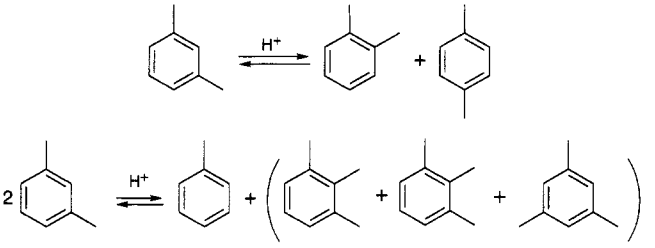

Furthermore, at high conversions, xylenes are produced with the thermodynamic equilibrium composition.

It is generally believed that isomerization of alkyl aromatics occurs by a 1,2 alkyl shift,[368] and the relative rate reflects the relative stability of the alkyl cation. However, when using large-pore zeolites, it has been found that even at low levels of conversion, isomers can also be formed through a bimolecular transalkylation mechanism from intermediates,[369–371] as it occurs for the transalkylation of xylenes to give toluene and trimethylbenzenes. Since the bimolecular transalkylation reactions should involve a bulkier transition state than that of the unimolecular 1,2 methyl shift it could be expected that by reducing the space available inside the channels, a situation may be reached where transalkylation could be suppressed by transition-state shape selectivity. This is what is observed when the reaction is carried out on zeolites with different pore sizes.[371,372] Results presented in Figure 17,[373] clearly show that transalkylation is strongly decreased in 10 MR zeolites. Besides geometrical effects, the chemical composition of the zeolite also has an effect on the ratio of uni- to bimolecular reactions. In this way, it was found by means of kinetic and isotopic studies[371] that by increasing the framework Si/Al ratio of a large pore HY zeolite, the ratio of uni to bimolecular reactions occurring during *m*-xylene isomerization increased.

If the suppression of xylene transalkylation achieved by using medium-pore zeolites is already a big improvement in the xylene isomerization process, zeolites can go further than this, and they can also improve the selectivity to the para isomer by product diffusion shape selectivity. As was presented before, in ZSM-5 zeolite the diffusion coefficient for *p*-xylene is more than 2 orders of magnitude higher than for *o*-xylene. This difference allows *p*-xylene to escape more rapidly outside the zeolite crystallite than the ortho isomer. Then the characteristic diffusion time for *o*-xylene is much greater than its characteristic isomerization time, so the diffusion of ortho will be selectivelly retarded within the pores, allowing time for isomerization toward *p*-xylene.[372] Results from Figure 18[373] show the effect of pore dimensions on the para to ortho ratio obtained during isomerization of *m*-xylene on zeolites with different pore sizes, and it shows the increased para selectivity obtained on medium-pore zeolites.

What has been said for xylene isomerization also applies to other alkyl aromatics such as ethyl-, methylbenzene,[374] diisopropylbenzene,[375] and 1-methylnaphtalene.[376–378] The relative ratio of the size of the molecule and the pore size seems to be the most important factor controlling the result of the isomerization.

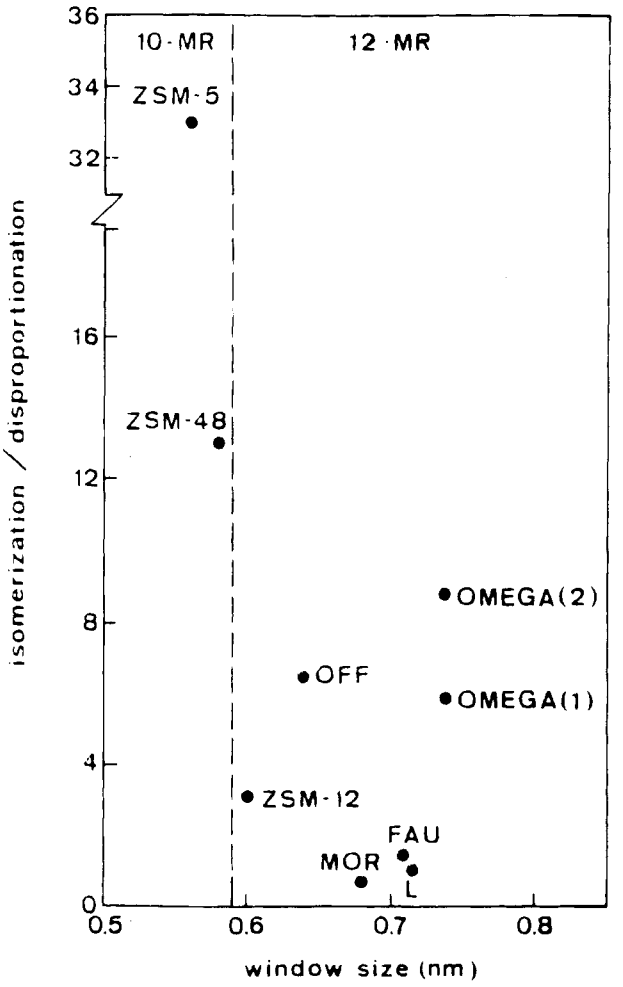

Figure 17. Ratio of the initial rates of isomerization to disproportionation of *m*-xylene over acid zeolites against the size of the windows of the intracrystalline cavities.

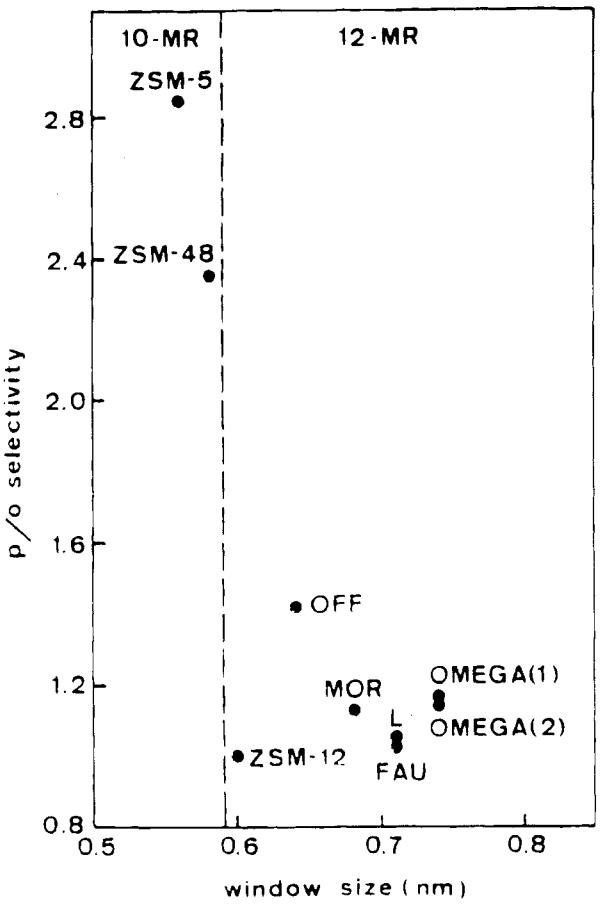

Figure 18. Initial *p/o* selectivity in the isomerization of *m*-xylene over acid zeolites against the size of the windows of the intracrystalline cavities.

The isomerization–transalkylation of alkyl aromatics is perhaps the best example to show the important role played by shape selectivity owing to the micropores of zeolites on hydrocarbon reactivity. This type of reaction is so determined by space restriction that they are widely used to test the pore topology of any new zeolite structure synthesized.[379]

Carbon–Carbon Rupture and Formation. **Catalytic Cracking.** Catalytic cracking of hydrocarbons is a field in which zeolites have been responsible for the largest revolution in oil refining in the last 30 years. Indeed, gasoil cracking is the basis for the production of more than 30% of the gasoline, while it also produces diesel, and olefins and isoparaffins for petrochemical uses. The substitution of amorphous silica–alumina catalysts by faujasite zeolites, toward end of the 1960s, allowed a strong increase in the production of gasoline.

From the point of view of cracking mechanism, the acid sites of the zeolite are believed to be the catalytic active sites. If cracking of hydrocarbons on liquid superacids proceeds through the formation of "free" carbenium and carbonium ions,[380,381] in the case of hydrocarbon cracking on zeolites, the formation of "free" carbocations has not been observed. However, and after considering the product distribution obtained during cracking of alkanes, alkenes, cycloalkanes, and alkyl aromatics, it appears obvious that carbenium and carbonium ion-like intermediates must also be formed on zeolites during catalytic cracking of hydrocarbons. In this way it is believed that when carbenium ion-like species are formed on the surface of the zeolite, one way to stabilize the short-lived ion pair is by a β-scission process which produces an olefin in the gas phase and a new alkoxy group which remains adsorbed:[230]

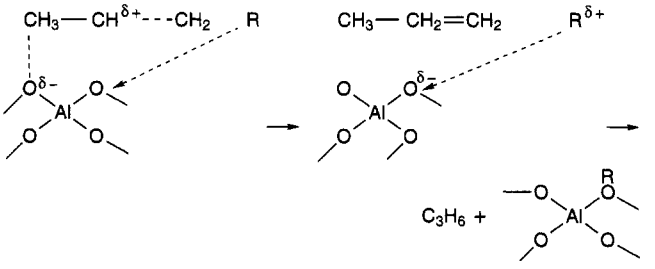

This reaction should involve a concerted mechanism that allows the compensation of the dissociating bonds by the new ones being formed. This, in turn, should produce a decrease in the activation energy with respect to a process involving the formation of "free" carbenium ions followed by cracking.

Recently, it has been suggested that similar to the mechanism of cracking proposed by Olah in superacids,[380] protolytic cracking could also occur on the surface of zeolites.[382,383] This mechanism started by protonation of a C–C bond by the acid site of the zeolite. Ab initio quantum chemical calculations

have been carried out to visualize the transition state of the protolytic cracking.[230] Even though the hydrocarbon molecule was small (C_2H_6) and the zeolitic active site was simulated by a very simple cluster, some interesting qualitative conclusions could be reached: the transition state appears as a two-point interaction of ethane with the OH and a neighboring oxygen. The reaction coordinate of protolytic cracking represents the concerted stretching of the O−H bond in the bridging hydroxyl group, combined with the heterolytic splitting of the carbon−carbon bond in the protonated ethane molecule. The final step is the formation of free methane and the formation of a methoxy group in the neighboring basic oxygen of the former acid site.

While there is no doubt that the initiation step in the protolytic cracking of paraffins and cracking of olefins is the formation of a carbocation or a carbenium ion-like intermediate on a Brönsted acid site of the zeolite, it is still under discussion if paraffin cracking initiation via carbenium ions also occur and, if so, on what zeolite sites are the carbenium ions formed.

Some authors have claimed that a carbenium ion can be formed on alkanes or cycloalkanes by abstraction of a hydride ion from the hydrocarbon by either a Brönsted acid site, which gives H_2 as a product,[384-388] or by a Lewis acid site from the catalyst.[389,390] Another hypothesis to explain the paraffin-cracking initiation, supposes that the cracking chain is initiated by Brönsted-site protonation of olefins that are either present in the feed or formed by thermal cracking.[391] A comprehensive discussion of the different initiation schemes can be found elsewhere.[392]

The current situation in the cracking of alkanes on zeolites appears to be the following: when cracking n-alkanes, the reaction is initiated by formation of a carbocation-like intermediate which cracks and gives a shorter alkane in the gas phase and an adsorbed carbenium ion-like species on the zeolite. This carbenium can either desorb giving one olefin in the gas phase and restoring the zeolite Brönsted site, or it may follow a chain mechanism by abstracting a hydride ion from another reactant molecule, and desorbing from the catalyst as a paraffin, while leaving a carbenium ion of the reactant molecule on the zeolite surface:

$$\text{zeol}^- - (C_nH_{2n+1}) + \longrightarrow C_nH_{2n} + H^+ - \text{zeol}^-$$
$$+ C_mH_{2m+2}$$
$$\longrightarrow C_nH_{2n+2} + \text{zeol}^- - (C_mH_{2m+1})^+$$

The adsorbed $(C_mH_{2m+1})^+$ can now crack following the β rule.

In summary, in the case of n-alkanes, it could be said that the first molecules of reactant are cracked by protolytic cracking. Then, when the shorter carbenium species remain on the surface, cracking can continue by two routes: (1) protolytic cracking, if the carbenium ion desorbs and regenerates the original Brönsted site, and (2) β-scission, if hydride transfer from a reactant molecule to the adsorbed carbenium ion occurs.

The relative extension of protolytic to β-scission mechanism or, in other words, the length of the cracking chain and hydrogen transfer, has an important impact on the quality of the products formed during the commercial cracking of gasoil in fluid catalytic cracking (FCC) units. Indeed, protolytic cracking is believed to favor the formation of undesired dry gas with respect to β-scission. On the other hand, hydrogen transfer is believed to be responsible for saturation of olefins, with the corresponding increase on gasoline stability and selectivity, but producing a decrease in the research octane number (RON).

Cycloalkanes, which are also present in FCC feedstocks,[393] play a determinant role in cracking chemistry for hydrogen transfer, and as precursors for aromatics and coke. They can also react on acid zeolites to give ring opening and cracking by protolytic and β-scission, as well as isomerization, and hydrogen transfer reactions.[394-396]

Alkyl aromatics, which are also constituent of FCC feeds,[397] also crack on zeolites by the complete cleavage of the side chain from the aromatic ring if that has less than five carbon atoms. Cracking can also take place along the side chain if this has more than five carbon atoms.[393,398-400]

Both, chemical composition and geometrical structure of zeolites play an important role on determining the product distribution obtained during catalytic cracking. In this way it has been shown that the ratio of protolytic cracking to β-scission increases when increasing the Si/Al ratio of the zeolite,[401] meanwhile hydrogen transfer and coke formation decrease. Thus, during gasoil cracking an increase in the framework Si/Al ratio of the zeolite produces a decrease in the selectivity to gasoline owing to a larger recracking, which yields C_1-C_4 gases, while also produces a decrease in the hydrogen transfer and coke formation, with the corresponding increase in RON and throughput, respectively.

The zeolite geometrical factors can be taken advantage of to selectively crack n-paraffins and n-olefins with respect to their branched isomers when using medium-pore-size zeolites. This effect is based on zeolite shape selectivity by mass transport discrimination, which arises because there are significant differences in diffusivities between branched and linear hydrocarbons within the pores of 10 MR zeolites, as for instance ZSM-5.[402-408] However, spatial constraints of reaction intermediates can also play an important role in determining the different cracking rates of monobranched and linear paraffins on ZSM-5 zeolite. Evidence of this was given by Frilette et al.[402] when showing that the relative rate of cracking n-hexane to that of 3-methylpentane was independent of the size of the individual catalyst crystal (Figure 19).[402]

The rate control by spatial constraints of reaction intermediates is due to the fact that a branched paraffin, by being a bulkier molecule than the unbranched isomer, requires more space to form the reaction intermediate, with possible limitations by the pore size of ZSM-5 zeolite. By carrying out this selective cracking of molecules in the gasoline range, the addition of ZSM-5 to FCC catalysts produces an increase in gasoline RON and also an increase in the production of propylene.

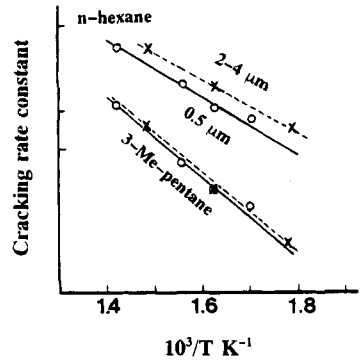

Figure 19. Arrhenius plot for the cracking of hexane isomers by HZSM-5 of different crystal size: (continuous line 0.5 μm, dashed line 2–4 μm).

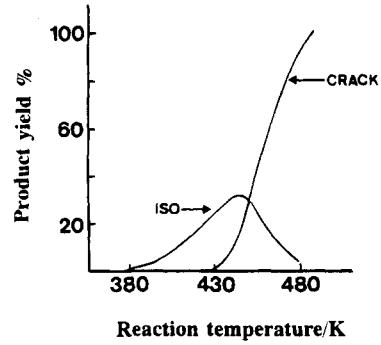

Figure 20. Yield of isomers (ISO) and cracked products (crack) for the reaction of *n*-decane over Pt/USY at various reaction temperatures.

Changes in the pore size of the zeolite additive, for instance by using beta or MCM-22 zeolites, allows one to keep a good gasoline selectivity while increasing the RON of the gasoline and shifting the C_4 and C_5 products to desirable isobutylene and isoamylene products.[409–411]

It can be concluded that by taking advantage of the high cracking activity of zeolites combined with the fact that different pore size zeolites may perform different type of cracking on the different products, leaves open the possibility to optimize cracking products by using multizeolitic cracking catalysts.

The effects shown by zeolites on catalytic cracking, also apply to hydrocracking of paraffins and gasoil. Thus, hydrocracking is slow for *n*-alkanes, but the rate strongly increases for branched isomers. It can be said that hydrocracking starts when the *n*-paraffin has undergone, at least, two isomerization steps. This can be seen when hydrocracking *n*-decane on a large-pore Pt/USY zeolite (Figure 20).[412]

As in the case of catalytic cracking, the channel structure of ZSM-5 has a strong effect on the relative rate of cracking and isomerization, as well as on the isomer distribution of *n*-decane, suppressing the formation of bulky di- and tribranched decanes and ethyloctanes.[412] The shape selectivity effect of medium- and small-pore zeolites for hydrocracking paraffins, has shown its practical utility in the selectoforming and catalytic dewaxing processes.

Carbon–Carbon Bond Formation by Alkane–Alkene Alkylation. Environmental concerns are driving forces to find solid acids which can be used instead of the unfriendly HF and H_2SO_4 catalysts for production of alkylation gasoline.[413] Acid zeolites were candidates for this,[414–416] and zeolite Y, either in the protonic form or exchanged with di- or trivalent cations, has been studied for alkylation of isobutane and butene. On the basis of the products formed, it appears that the general reaction mechanism operating on zeolites is the same as that on liquid acids.[413] This involves a chain mechanism in which the initiation step is the protonation of the olefin, followed by a hydride transfer from a molecule of isobutane to the *sec*-butyl carbocation:

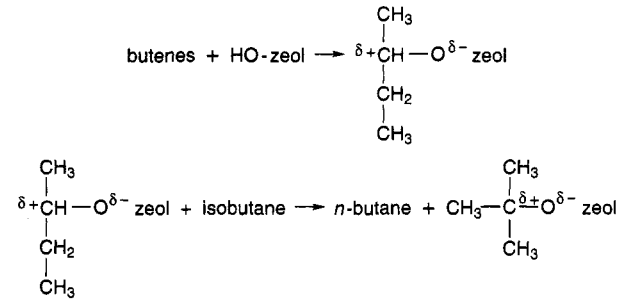

In a following step, the *tert*-butyl cation-like intermediate can attack an olefin to give the corresponding C_8 carbocation. Then, depending on the particular butene isomer the final will be different:

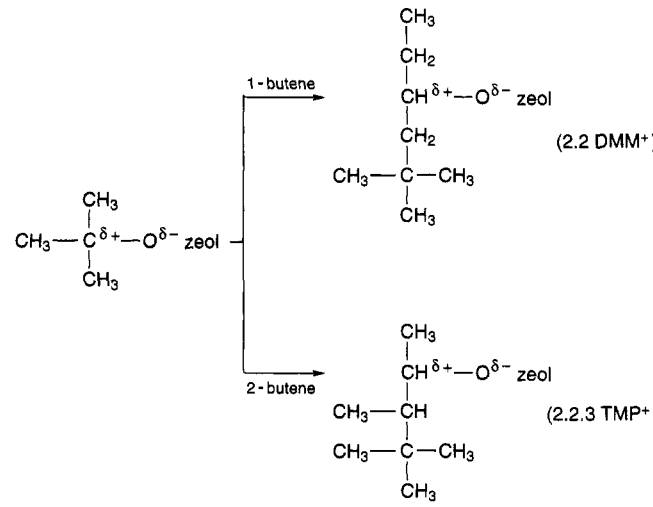

The chain is transferred by hydride transfer between the adsorbed C_8 carbocation-like intermediate and the isobutane reactant. In this way a C_8 branched alkane is desorbed while an adsorbed *tert*-butylcarbenium ion is formed.

The chain is finished by desorption of a carbocation giving the corresponding olefin and restoring the Brönsted acid site.

This simplified mechanism only applies in a first approximation. When the product distribution is analyzed in detail, it can be deduced that other isomerization and olefin oligomerization reactions also occur.[413] The most important pathway competing with the desired alkylation is the dimerization of the olefin which in the case of 2-butene would give dimethylhexanes (DMH). This is a much less desired reaction owing to the much lower octane number of dimethyl derivatives with respect to trimethylpentanes (TMP).

In the case of zeolites, high activity and selectivity to TMP are obtained in the first moments of the

reaction. However, after a few minutes on stream the activity of the zeolite for hydrogen transfer, which is the reaction responsible for chain propagation, is lost, and then the reaction enters a critical stage in which product distribution is better explained in terms of olefin oligomerization instead of isobutane–butene alkylation.[417,418]

Since zeolite composition and structure have an influence on acidity as well as on hydrogen transfer activity, different REHY and USY preparations have been studied.[419,420] It has been found that while maximum activities were obtained for framework Si/Al ratios of ~6, the ratio of TMP/DMH, which can measure the ratio of alkylation to oligomerization, continuously increases when decreasing the framework Si/Al ratio.[421] This is not surprising since it is known that the concentration of reactants in the pores, the extent of hydrogen transfer, and the distribution of acid sites, strongly depend on the zeolite framework composition. The results obtained with steam dealuminated USY were compared to those on another large-pore high Si/Al ratio zeolite, such as beta, with different crystal sizes.[421] It has been seen that, at least in beta zeolite, limitations in the diffusion of branched products may exist at the relatively low reaction temperatures used, as can be deduced from the increase in conversion, observed when decreasing the crystal size of the zeolite. Moreover, the beta zeolite is less selective to TMP due to its lower hydrogen transfer activity.

The pore size of the zeolite is critical for diffusion of the branched products as well as for allowing the bulky transition state involved in the hydrogen transfer reaction between TMP and isobutane. When zeolites with different structures were compared at the same level of total conversion, it was found[422] that alkylate yield increases from ZSM-5, which is formed by 10-member ring channels, to MCM-22 with 12-member ring cavities connected between them by 10-member ring windows, and an independent 10-member ring channel system,[423] and from this to large-pore zeolites such as mordenite, beta, and Y.

In conclusion, it can be said that even though the zeolites are active and selective catalysts to carry out the alkylation of isobutane with olefins, their practical use is limited, during to the fast catalyst deactivation if conventional reaction systems are used. In the next sections we will discuss the possibilities that offer stronger solid acid catalysts, such as heteropoly acids and sulfated metal oxides for this important reaction.

Carbon–Carbon Bond Formation by Olefin Oligomerization. Olefins can easily oligomerize in the presence of acid catalysts, and they also do so on acidic zeolites. ^{13}C "in situ" NMR studies indicate that the reaction may proceed via a carbenium-like type mechanism, and alkoxides were identified as intermediates.[424–428] Together with oligomerization, other consecutive reactions such as transmutation and hydrogen transfer also occur and the oligomers may be converted to secondary olefinic and paraffinic products.[429] Secondary reactions are so fast that a rapid equilibration of olefins to a composition determined by the temperature and pressure of the system occurred.

It is clear that in a system involving several bimolecular and unimolecular reactions, as well as products with different sizes, the final product distribution could be affected by the pore size of the zeolite. In general, and as it could be expected, the amount of branched products increases when increasing the pore size of the zeolite or zeotype (SAPO).[426–428,430–432]

The practical importance of olefin oligomerization is illustrated by the fact that this reaction, together with transmutation-disproportionation and aromatization of C_2 to C_{10} olefins, are the basis of Mobil's olefin to gasoline, distillate process (MOGD).[432–435] The process is quite flexible and allows, on the one hand the production of isoolefins, when the reaction is carried out at high pressures and low temperatures, and the hydrogenation of the 165 °C+ olefins produces a premium quality low-pour-point jet fuel and distillate fuel. On the other hand, when the process is operated at higher reaction temperatures aromatics are produced.[432] Zeolite ZSM-5, either in its acid form, with supported Ni, or with supported Ga, and in combination with aluminum phosphate/alumina are good catalysts for the oligomerization of C_2–C_{10} olefinic products.[436–442] Compositional (Si/Al ratio), textural (crystal size), and catalyst conformational parameters (extrudation and pelletization) of the ZSM-5 zeolite play an important role on the final catalytic performance.[442] Diffusional problems are important in this reaction, and therefore, a decrease in crystallite size produces an increase in activity and catalyst life. In the same way, if intercrystalline diffusion resistance is increased by high-pressure pelletization, a decrease in conversion and catalyst life is observed.

New zeolitic structures containing 12- and 10-member ring channels (MCM-22) have been claimed as adequate olefin oligomerization catalysts,[443,444] and multifunctional catalysts involving MCM-41 plus MCM-22 have been claimed to carry out oligomerization plus cracking.[445]

Reactions involving olefins or even paraffins which can be cracked and/or dehydrogenated to form olefins which then can react, is an open field where the structure of the zeolite pore plays a determinant role, and consequently the product composition can be controlled by using the adequate zeolite or zeotype structure.

Alkylation of Aromatics. Electrophilic alkylation of aromatics can be carried out by a variety of reactants such as olefins, alcohols, and halogenated hydrocarbons.[330] Commercial catalytic processes leading to the formation of ethylbenzene, *p*-xylene, propylbenzenes, ethyltoluene, and 4,4′-isopropylbiphenyl are based on alkylation of benzene, toluene, and biphenyl.

Early studies on the alkylation of benzene and related aromatics with olefins on large-pore acid zeolites found that a Langmuir–Rideal-type mechanistic kinetic equation can adequately represent the chemical process. In such a scheme, it was supposed that an anionic lattice-associated carbenium ion was formed by attack of a proton on an olefin, and this is then attacked by a free or weakly adsorbed aromatic.[329,446–448] However it has to be taken into

Table 10. Alkylation of Benzene with Dodecene at 200 °C and 14.6 atm on ZSM-12 Zeolite

dodecene conversion (wt %)	phenyldodecane isomer distribution (%)				
	2-Ph	3-Ph	4-Ph	5-Ph	6-Ph
54	92	8	0	0	0

account that it is difficult in the case of zeolite catalysts to assume a Langmuir–Rideal-type mechanism in the strict sense, i.e. adsorbed olefin and aromatic in the "gas phase", since any molecule within zeolite pores is going to be subjected to the electric field gradients and even to electronic confinement effects. Thus, one has to consider that at least some degree of weak chemical adsorption of the aromatic must occur.

Zeolites in which no diffusional or transition state shape selectivity exist behave like liquid acids or mesoporous amorphous solid acids, i.e. there is a predominance of ortho–para orientation in electrophilic substitution reactions on aromatic rings containing ortho–para-directing substituents. Moreover the stronger the increased electron density at the ortho and para position generated by the ring substituent, the easier will be the alkylation.[329,449] However, in the case of aromatics alkylation the concept of shape selectivity has been very useful in designing new improved alkylation catalysts based on zeolites. In this way, the Mobil–Badger ethylbenzene process is based on the use of a ZSM-5 zeolite catalyst to produce ethylbenzene, for the production of styrene, by alkylation of benzene with ethylene.[450] By an adequate choice of the benzene to ethylene ratio it is possible to limit the formation of diethylbenzene, and an overall yield of 99% of ethylbenzene is obtained.

Due to pore constraints medium-pore zeolites strongly limit the formation of coke, allowing cycles of up to 60 days between regenerations.

Product diffusion shape selectivity is responsible for the selective formation of *p*-ethyltoluene (97% of the three isomers formed) during the alkylation of toluene with ethene on modified ZSM-5 zeolites.[451] Production of *p*-xylene by alkylation of toluene by methanol (TAM Process)[452] is also based on the faster diffusion of the para isomer, with respect to *o*- and *m*-xylenes, which enriches the product in the most desired *p*-xylene.

Longer chain olefins have also been used for selective formation of monoalkyl products. In this way, isopropylbenzene is formed by alkylation of benzene with propylene on HZSM-5, with polymerization of propylene as the only serious competing reaction. Nevertheless, very little amounts of polyalkylated products are observed unless total pressure is increased.[453]

Long-chain alkyl aromatics are useful molecules for production of surfactants, and they are produced by alkylation of benzene with long-chain *n*-olefins on HF acid. The 12-member ring unidirectional ZSM-12 zeolite gave unique product distribution in the alkylation of benzene with long chain olefins, forming preferentially 2-phenylalkanes (Table 10),[454] owing to spatial restriction in the pores of this zeolite.

Larger polyaromatic molecules have been alkylated on amorphous solid acids as well as on large-pore zeolites.[455,456] An interesting example in which shape selectivity has been found in large-pore zeolites is the 4,4′ alkylation of biphenyl by propylene. Table 11[457] shows the isopropylation of biphenyl on large- and medium-pore zeolites, such as mordenite (HM), HY, HL, and HZSM-5, as well as on amorphous silica–alumina (SA). Results show that mordenite gives the largest selectivity to 4-isopropylbiphenyl (IPBP), and to 4,4′-diisopropylbiphenyl (DIPBP). This last product has commercial interest for liquid crystals and high-performance polymers. When the mordenite was further dealuminated to Si/Al ratios of 2600, it gave biphenyl conversion of 98% with a selectivity to the 4,4′ isomer of 73.5% at 523 K, propylene pressure of 8.43 kg cm^{-2}, and 20 of reaction. Dealumination decreased polymerization and coke formation, as well as reactions occurring on the external surface of the zeolite. The higher selectivity observed on H-mordenite with respect to other large-pore zeolites is believed to be due to the geometry of the channels in mordenite, which consist of 12-member ring crossed by 8-member ring channels. Then, the packed biphenyl molecules adsorbed in the 12-member ring channels would be alkylated by the propylene which would diffuse through the 8 MR channels.[458]

Acid mordenite catalysts also show shape selectivity for the alkylation of naphthalene, anthracene, dibenzofuran, and *p*-terphenyl with propylene,[459–462] due to steric restriction at the transition state in the pores and differences in diffusion rates of reactants and products.

Alkylation of aromatics is a good example of reactions where the diffusion and transition shape selectivity play a predominant role in controlling the selectivity of zeolite catalysts. Furthermore, it shows that depending on the size of the reactant and product molecules, shape selectivity applies to either medium- or large-pore size zeolites, and selective

Table 11. Alkylation of Biphenyl by Propylene on Different Zeolites and Amorphous Silica–Alumina (SA)

catalyst (SiO_2/Al_2O_3)	reaction temp (°C)	conv (%)	product. distribution (%)		isomer distribution of IPBP (%)			isomer distribution of DIBP (%)		
			IPBP	DIBPP	2-	3-	4-	4,4′-	3,4′-	3,3′-
HM(23)	180	16	89	11	7	20	74	75	16	2
	250	48	73	27	5	24	71	78	14	2
HY(5.8)	200	76	60	40	36	23	41	5	8	7
	250	83	61	33	7	48	45	11	22	13
HL(6.1)	200	82	54	36	39	18	43	10	8	6
	250	84	53	47	29	25	46	10	13	6
SA(4.3)	180	67	62	38	36	15	49	16	9	5
	250	84	48	39	18	32	50	25	26	8
HZSM-5(50)	300	6	100	0	16	30	54			

alkylation processes have been developed using both types of zeolites.

From the results reported on zeolite reactivity for acid-catalyzed reactions, it is clear that the combination of pore structure and acidities, which can be as strong as $H_0 = -10$, allows one to carry out a large number of catalytic reactions of hydrocarbons on these materials. However, zeolites are useless either to catalyze reactions at low temperatures or for processes requiring acidities stronger than $H_0 = -10$. In those cases, other more acidic inorganic solid catalysts are needed, and the possibilities of heteropoly acids and sulfated transition metal oxides will be discussed in the following sections.

C. Heteropoly Acids

1. Composition, Structure Preparation, and Textural Properties

Heteropoly compounds involve a large class of coordination-type salts and free acids which are formed by the condensation of more than two different types of oxoanions as for instance:

$$12WO_4^{2-} + HPO_4^{2-} + 23H^+ \rightarrow PW_{12}O_{40}^{3-} + 12H_2O$$

In this section the terms heteropoly compounds and heteropoly anions will be used for heteropoly acids (acid forms) and their salts.[463-465]

The anion contains a central atom, typically Si or P (Table 12), tetrahedrally coordinated to oxygens and surrounded by oxygen-linked hexavalent 2−18 peripheral metal atoms. These are usually Mo or W but can also be others such as V, Nb, Ta, single, or in combination. It is possible to prepare heteropoly anions with different structures.

Table 12. Elements Capable of Acting as Central Atoms in Heteropoly Compounds[3]

periodic group	element
I	H, Cu^{2+}
II	Be^{2+}, Zn^{2+}
III	B^{3+}, Al^{3+}, Ga^{3+}
IV	Si^{4+}, Ge^{4+}, Sn^{4+}, Ti^{4+}, Zr^{4+}, Th^{4+}, Hf^{4+}, Ce^{3+}, C^{4+}, and other rare earths.
V	N^{5+}(?), P^{3+}, P^{5+}, As^{3+}, As^{5+}, $V(?)^{3+}$, V^{5+}, $Sb(?)^{3+}$, Sb^{5+}, Bi^{3+}
VI	Cr^{3+}, S^{4+}, Te^{4+}, Te^{6+}
VII	Mn^{2+}, Mn^{4+}, I^{7+}
VIII	Fe^{3+}, Co^{2+}, Co^{3+}, Ni^{2+}, Ni^{4+}, Rh^{3+}, Pt^{4+}(?)

The structure of the fundamental units is called the primary structure. Secondary structures are formed when the primary units are joined to form a solid. For instance, for the heteropoly anion with a Keggin structure[466] the primary structure (Figure 21a) is formed by a central PO_4 tetrahedron surrounded by 12 WO_6 octahedra which are arranged in four groups of three edge-shared octahedra W_3O_{13}. These W_3O_{13} units linked by shared corners to each other and to the central PO_4. In this case, the secondary structure is formed by packing the polyanions into a *bcc* structure in which the protonated water dimer $(H_2O)_2H^+$ is connected to four anions by hydrogen bonding at the terminal oxygen atoms of

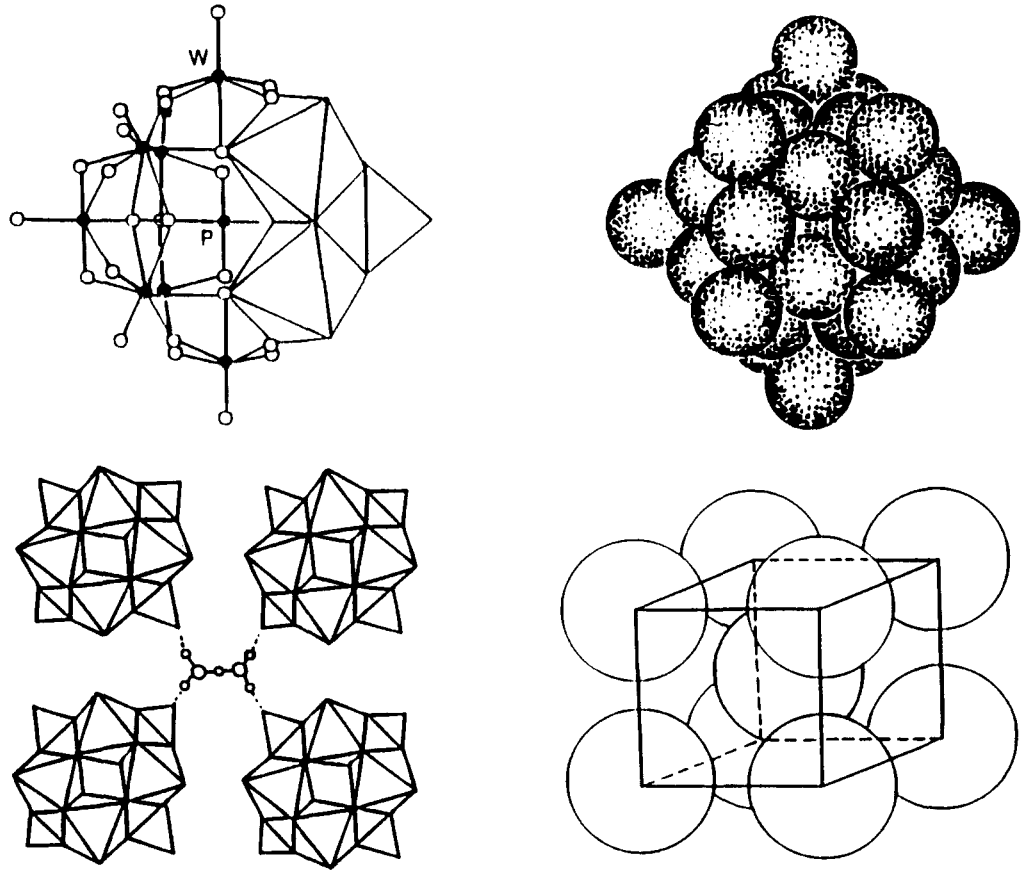

Figure 21. Heteropoly anion with the Keggin structure, $PW_{12}O_{40}^{3-}$: (a) primary structure; (b) secondary structure ($H_3PW_{12}O_{40}{\cdot}6H_2O$).

Table 13. Some Crystal Forms of the Keggin Structure

formula	crystal type
$H_3PW_{12}O_{40}\cdot 29H_2O$	cubic Type B, Fd^3m
$H_3PW_{12}O_{40}\cdot 24H_2O$	rhombohedral type B, $R3m$
$H_3PW_{12}O_{40}\cdot 14H_2O$	triclinic, P_1
$H_3PW_{12}O_{40}\cdot 5H_2O$	cubic type A, $Pn3m$

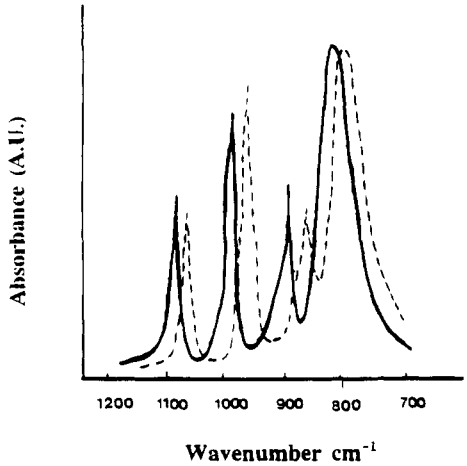

Figure 22. IR spectra of Keggin anions: (—) $[PMo_{12}O_{40}]$; (···) $K_3[PW_{12}O_{40}]$.

the anions (Figure 21b). Then, depending on the amount of hydration water and on the countercation, several crystallographic arrangements exist. For instance, the Keggin heteropoly acid $H_3PW_{12}O_{40}$ adopts different forms (Table 13), when hydration water content is changed from 5 to 29 molecules. In the case of heteropoly acids, the hydration water can be replaced by polar molecules, and as will be shown later this becomes crucial for the catalytic activity shown by solid heteropoly acids.

It can be said[463] that the structures of the heteropoly anions are governed by two general principles. Firstly each metal atom occupies a MO_x coordination polyhedron in which the metal atoms are displaced, owing to the M–O bonding, toward the polyhedral vertices that form the surface of the structure. The second principle establishes that structures with MO_6 octahedra that contain three or more free vertices are in general not observed.[467]

Different techniques have been used to characterize the primary and secondary structure of heteropoly anions, in solution, as solids or supported on different carriers. In this way, IR spectroscopy[468–474] can distinguish different types of oxygen atoms present in typical heteropoly acids, i.e., oxygen connecting species that binds central to peripheral atoms (O_c), bridging oxygens which bind adjacent peripheral atoms (O_b), and terminal species attached to a single peripheral atom (O_t). The IR spectrum of a Keggin anion (Figure 22)[471] shows bands at 1064 and 1079, 963 and 983, and 900–700 cm^{-1}, which correspond to P–O, Mo=O and W=O stretching bond vibrations, and to M–O–M bridging bond vibration, respectively. Laser Raman spectroscopy has also been used to study the structure of heteropoly compounds in solution[470,475,476] as well as in the form of solids, and supported.[470,472,473] An example of a Raman spectrum of a solid heteropoly compound is given in Figure 23. Very similar spectra are obtained in solution, indicating that the primary structure is preserved in the solid. Surface Raman scattering, useful for the characterization of heteropoly anions, is also a powerful technique to determine reactive species in "in situ" performed catalytic reactions, using the secondary structures, and individual anions in dilute supported systems.[477,478]

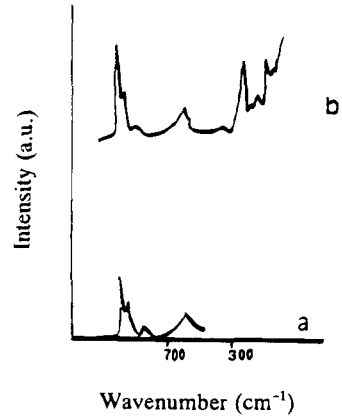

Figure 23. Raman spectra of $PMo_{12}O_{40}$: (a) solid state and (b) solution spectra.

Most of the elements found in heteropoly acids have nuclides (^{183}W, ^{95}Mo, ^{51}V, ^{31}P, ^{17}O, ^{1}H) which are suitable for the NMR spectroscopy. Therefore, it is not surprising that NMR has been extensively used for the characterization of heteropoly compounds by matching their NMR spectra to those of standards whose structures have been previously determined by other methods such as X-ray or neutron diffraction. NMR is also used to characterize their acidity, the state of adsorbed molecules, reaction intermediates, and even the microporosity.[479–509] Other spectroscopic methods such as visible and UV absorption and ESR are also used for the structure characterization, since they give indirect information about the bonding in heteropoly compounds.[465,504,510,511]

Heteropoly acids are synthesized under acidic conditions by apparently simple inorganic reactions of the type:

$$[PO_4]^{3-} + 12[MoO_4]^{2-} + 24H^+ \rightarrow [PMo_{12}O_{40}]^{3-} + 12H_2O$$

$$[SiO_4]^{4-} + 12[WO_4]^{2-} + 24H^+ \rightarrow [SiW_{12}O_{40}]^{4-} + 12H_2O$$

Unwanted side reactions and the presence of complex equilibria are possible, so caution must be taken during preparation in order to avoid hydrolytic decomposition of polyanions and nonhomogeneity of the metal cation to polyanion ratio in the solid. For instance, failure to recognize the hydrolytic instability of 12 molybdophosphoric acid and the formation of heteropoly species containing atomic ratios lower than 12 to 1 has led to the development of incorrect preparative procedures and misleading physicochemical results. Good results were obtained by either extraction of acidified solutions of sodium molybdate and sodium phosphate,[512] or by a non-ether route, by boiling molybdenum trioxide and phosphoric acid.[513,514] Details of the preparation procedures of heteropoly

Table 14. Elements That Are Potential Peripheral Atoms for Heteropoly Acids (ionic radii 53 pm < r < 70 pm; charge > 4+)

meet charge criteria	meet Size criteria	meet Both criteria
Mn^{7+}, Tc^{7+}, Re^{7+}	Ti^{4+}	V^{5+}, Nb^{5+}
	Mn^{4+}	Mo^{6+}, Ta^{5+}
	Fe^{3+}	W^{6+}, Os^{6+}
	Co^{2+}	
	CO^{3+}, Zn^{2+}	
	Ni^{2+}, Cu^{2+}	
	Ga^{3+}, Tc^{4+}	
	Ru^{4+}, Rh^{3+}	
	Pd^{4+}, Re^{4+}	
	Ir^{4+}, Pt^{4+}	

acids and their salts in aqueous and non aqueous solutions, are given in a number of reviews and papers.[515-526]

In order to introduce an element into the framework during the synthesis of the heteropoly acid, it has to have ability to rapidly exchange coordination in solution between tetrahedral and octahedral;[527] it should have a smaller size than that required for octahedral coordinated oxygen anions, and finally, elements supporting a high positive charge are required. The first characteristic indicates the necessity of having soluble precursors for the synthesis of the heteropoly anions. The high positive charge is required to avoid an excess of negative charge on the anion, while the small size of the framework atoms allows the structure to achieve a stable form. Strong ion-induced dipole forces between terminal oxygens and metal ions cause the exterior oxygens to be highly polarized toward the center of the complex, and consequently the protons are loosely attached, giving strong acidities. Moreover, it causes the good solubility in various solvents, and prevents condensation of the oxyanion monomers into infinite oxide lattices, giving instead discrete polyanions with definitive structures. Then, those requirements could be made more specific by noting that the framework atoms must have an ionic radius between 53 and 70 pm and a charge $>4^+$. In Table 14 the elements which meet those criteria are given.

With respect to the stability of heteropoly compounds, it can be said that the nature of the central atom is critical for the stabilization of the primary structure. The larger the central atom, the more stable the heteropoly anion structure is.[528] In the case of the secondary structures, water molecules connect the individual heteropoly anions through weak hydrogen bonds. In the case of $[PW_{12}O_{40}]^{3-}$, its radius is only 5-6 Å while the spacing between ions is ~23 Å, leaving therefore a considerable space between ions. From this arrangement it is not surprising that porous structures of considerable surface area can be formed by the loss of some crystallization water. In this way, it has been shown[529] that the surface area of 1-12 molybdophosphate $H_3[PMo_{12}O_{40}]$ increases from 0.1 to 10 $m^2\ g^{-1}$ when subjected to a moderate heat treatment in a dry He stream.

The amount of water and therefore the porosity and thermal stability can be controlled by formation of salts with different cations. In this way, Niiyama et al.[530] have classified the salts into two groups on the basis of their solubility (group I and II). The so called group II is hydrophobic and involves large monovalent cations (Table 15), which interact strongly with the anions, and maintain a rigid structure, which resists solvation in water at high temperatures. Water associated with the cation is held strongly until the decomposition temperature is reached. Under these conditions zeolitic water is the only water lost from the structure, this giving surface area over 100 $m^2\ g^{-1}$. In the case of salts of group I, hydration water is relatively easy to remove and then heteropoly ions are maintained close resulting in the absence of open pores and this gives surface area under 10 $m^2\ g^{-1}$.

Table 15. Physical Properties of Cation Salts of 1-12 Molybdophosphates

group	cation	crystal ionic radius (å)	surface area ($m^2\ g^{-1}$)
I	H^+		3.8
	Li^+	0.68	4.9
	Na^+	0.97	5.9
	Ag^+	1.26	1.3
	Mg^{2+}	0.66	1.4
	Ca^{2+}	0.99	0.3
	Co^{2+}	0.72	8.3
	Ni^{2+}	0.69	5.6
	Cu^{2+}	0.72	4.1
	Zn^{2+}	0.74	2.0
	Pd^{2+}	0.80	11.2
	Al^{3+}	0.51	3.3
	Cr^{3+}	0.63	3.3
	Fe^{3+}	0.64	2.2
	La^{3+}	1.02	3.9
	Ce^{3+}	1.03	6.1
II	K^+	1.33	183.6
	Rb^+	1.47	176.9
	Cs^+	1.67	132.7
	Tl^+	1.47	178.5
	NH_4^+	1.43	163.0

The effect of the ion-exchange procedure on the pore structure and morphology of the heteropoly salts has been studied by McGarvey and Moffat,[531] by means of N_2 adsorption-desorption isotherms and X-ray powder diffraction. They have demonstrated that the ion-exchanged salts have microporous structures, and the structure is retained after ion exchange, and quantitative aspects of the structure are, for a given anion, largely controlled by the size and nature of the cation. It has to be remarked that the microporosity found in heteropoly oxometalates can play an important role in shape-selective catalysis. However, considering the textural results[531,532] one should not expect to control pore size to the same extent as in zeolites since heteropoly oxometalates suffer from the disadvantage of having relatively broad pore size distributions, and consequently, the fraction of the surface area with potential shape selective effects will be considerably smaller than expected in a solid with pores of similar and uniform cross section.[532] However, Bonardet et al.[533] have recently investigated the microporosity of 12 polyoxometalate salts by the ^{129}Xe NMR method proposed by Ito and Fraissard,[534] and they confirmed for NH_4^+, K^+, and Cs^+ salts the presence of microporosity, and found that it is homogeneous and organized. This is generated by the introduction of certain cations which leads to the translation or the rotation of the

Keggin anions in such a way that the interstitial volumes become interconnected, creating homogeneous microporosity in which nonpolar molecules such as Xe can be adsorbed.[533]

It appears then, that the heteropoly acids salts of group II may offer interesting properties as catalysts considering their favorable textural properties. The group I heteropoly acid salts having the low surface area can be of interest in those reactions in which consecutive steps are to be avoided. In any case if required in large surface area form, they can be prepared by supporting the heteropoly acids on large surface area carriers.[505,535-539] However solid supports with surface basicity should not be used in order to avoid decomposition of polyanions.

2. Nature of Acid Sites

The pH values of aqueous solution of heteropoly acids indicate that they are strong acids, and their strong acidity is related to the large size of the polyanion having a low and delocalized surface charge density, causing a weak interaction between polyanion and proton. They present strong acidic properties also in the solid state and are very sensitive to countercations as well as the constituent elements of polyanions.[540-542] The origin of the acidity in heteropoly oxyanions is multiple (Table 16). In the case of heteropoly acids, protons are directly compensating for the negative charge of the anions. The states of proton and crystallization water in the acid form were studied by high-resolution solid-state ^{31}P NMR and IR,[543] and by ^{1}H NMR.[544] In the free polyanions in solution, bond length–bond strength correlations and ^{17}O NMR[545,546] indicate that the preferred protonation sites are the bridging oxygen atoms which have a larger electron density than the terminal atoms. In solid state, as was mentioned above, the protons are involved in the formation of the crystal structure of the heteropoly acid, and in the protonation of the more accessible terminal oxygens leading to the $H_5O_2^+$ species which links four neighboring heteropoly anions by forming hydrogen bonds with terminal W=O oxygens:[547]

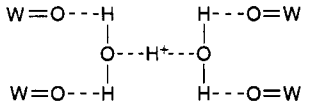

In the case of bulk dehydrated heteropoly anions it has been recently observed by ^{17}O NMR of solid molybdophosphate, that the terminal oxygen atoms are the predominant protonation sites in the dehydrated solid.[536]

Table 16. Aqueous Solutions of Heteropoly Salts

compound	pH of 2% solution
$La_3[PMo_{12}O_{40}]\cdot 10H_2O$	1.84
$Co_3[PMo_{12}O_{40}]_2\cdot 34H_2O$	2.05
$Ni_3[PMo_{12}O_{40}]_2\cdot 34H_2O$	2.01
$Mn_3[PMo_{12}O_{40}]_2\cdot 41H_2O$	2.11
$Co_2[PMo_{12}O_{40}]\cdot 24H_2O$	3.77
$Ni_2[SiMo_{12}O_{40}]\cdot 21H_2O$	3.68
$Mn_2[SiMo_{12}O_{40}]\cdot 22H_2O$	3.90
$Cu_2[SiMo_{12}O_{40}]\cdot 20{\cdot}5H_2O$	3.72
$La_4[SiMo_{12}O_{40}]_3\cdot 71H_2O$	3.16

In the case of metal salts, different mechanisms have been proposed to explain the origin of their acidity. In this way, and based on the correlation between catalytic activity of metal salts of dodecamolybdophosphoric acid in an acid catalyzed reaction (2-propanol dehydration) and the electronegativities of the metal cations (except for alkaline-metal salts), Niiyama et al.[548,549] have proposed that water coordinated to metal cations (M^{n+}) can become hydrolyzed generating H^+:

$$M^{n+} + mH_2O \rightarrow [M(H_2O)_m]^{n+} \rightarrow [M(H_2O)_{m-1}(OH)]^{n-1} + H^+$$

However, this mechanism, probably valid for cations with a large charge to size ratio, i.e., relatively acidic cations, fails to explain the nature of acid sites generated when cations with low electronegativity, such as Ag^+, are introduced. Nevertheless, it has been observed that in salts with reducible cations such as Ag^+ and Cu^{2+}, the presence of H_2 enhances the carboniogenic activity. This was attributed to the formation of protons after the following cation reduction:[550,551]

$$Ag^+ + {}^1/_2H_2 \rightarrow Ag^0 + H^+$$

This was later proved by pyridine adsorption on $Ag_3PW_{12}O_{40}$ and $Cu_3(PW_{12}O_{40})_2$ before and after treatment with H_2.[552] Before the H_2 treatment only the IR band at ca. 1445 cm^{-1} associated to Lewis acid sites was observed, indicating the interaction of adsorbed pyridine with Ag^+ and Cu^{2+} cations. The salts were then exposed for 1 h at 5.7 and 7.1 kPa, and at 300 °C to H_2 and after that evacuated. The IR spectrum of adsorbed pyridine gave a band at ca. 1535 cm^{-1} from pyridinium ions, thus indicating the presence of Brönsted acid sites formed in the reduction reaction (see above).

The acid characteristics of heteropoly acids and their salts have been studied by many of the methods described above. Note that the acid strength of heteropoly acids cannot be determined by the indicator method, except for heteropoly tungstates which have only a weak color. In the case of 1–12 tungstophosphoric acid $H_0 > 8.2$ was determined.[553] At present, many efforts are devoted to the characterization of the acidic properties of heteropoly acids by means of adsorption and thermal desorption of basic molecules[554-556] as well as by NMR.[505]

Stepwise thermal desorption of pyridine showed that a significant amount of protons from the bulk was still retained on $H_3PW_{12}O_4$ at 573 K. On the other hand, no pyridinium ions were detected on amorphous silica–alumina at this temperature.[557] In general, the amount of acid sites in heteropoly anions has been titrated by pyridine[558-560] and ammonia.[561] Figure 24[562] shows the acidic properties of a series of heteropoly compounds measured by thermal desorption of pyridine absorbed at 25 °C. In those cases only pyridinium ions were detected, and the amount of pyridine hold by the solid after evacuation at 130 °C agrees with the number of protons present in the free acids. Moreover, the change in the amount of pyridine retained by the solid at different desorption

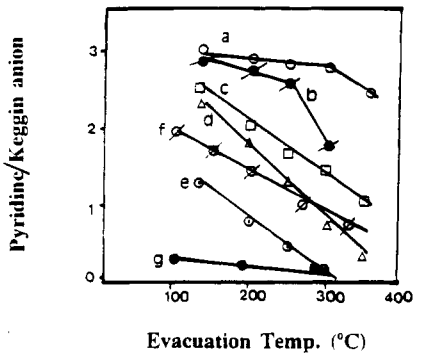

Figure 24. Thermal desorption of pyridine from several 12 heteropoly compounds: (a) $H_3PW_{12}O_{40}$; (b) $H_3PMo_{12}O_{40}$; (c) $NaH_2PW_{12}O_{40}$; (d) $Na_2HPW_{12}O_{40}$; (e) $Na_3PW_{12}O_{40}$; (f) $Cu_{3/2}PW_{12}O_{40}$; (g) $Cs_3PW_{12}O_{40}$.

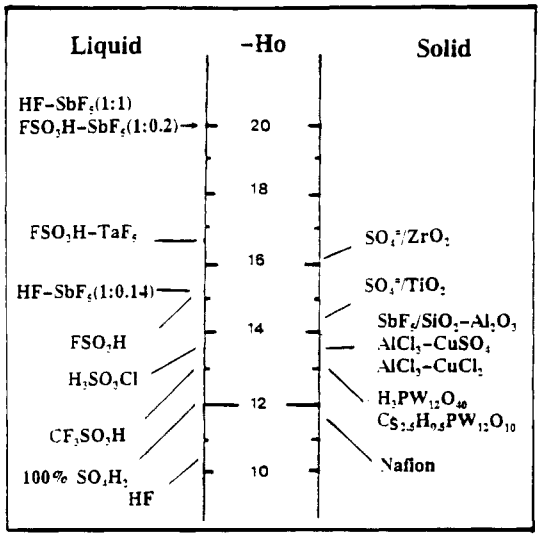

Figure 25. H_0 scale of superacidity including acid strengths of some common liquid and solid acids.

temperatures gives an indication of the relative acid strength of the different compounds.

It appears that partial substitution of H^+ by Na^+ decreases both the number and strength of the acid sites. In general, the acidity increases with increasing cation electronegativity. However, caution must be paid when the acidity of salts is compared since they are sensitive to slight changes in stoichiometry, reduction of the metal ion, hydrolysis during preparation and the degree of hydration.[563]

It appears then that heteropoly compounds have a relatively large number of strong acid sites (mainly of Brönsted type), which are accessible to bases. More specifically, it has recently been presented[564] that $Cs_xH_{3-x}PW_{12}O_{40}$ is a superacid and its performance can be modified by changing the extent of Cs substitution. Figure 25 provides a comparison of the relative acid strength of some solid superacids. Therefore, especially the high surface area materials should provide new opportunities for using them as solid acid catalysts in hydrocarbon reactions.

3. Acid-Catalyzed Hydrocarbon Reactions by Heteropoly Compounds

The acid catalysis of heteropoly compounds in the solid state is classified into "surface type" and "bulk type" catalysis. The former occurs on those compounds which are able to adsorb reactants only on the external surface. In this way hydrocarbons are adsorbed in amounts lower than that corresponding to the monolayer. In the case of "bulk type" catalysis, the heteropoly compound can take up polar molecules in amounts which correspond to more than 100 surface layers.[565,566] In case the uptake of polar molecules such as alcohols, ethers, and amines gave integral multiples of the number of protons, and the rate of their adsorption was primarily determined by the polarity and secondarily by the molecular size (Figure 26).[565] The amount adsorbed can be controlled by changing the cation in the salts.[567]

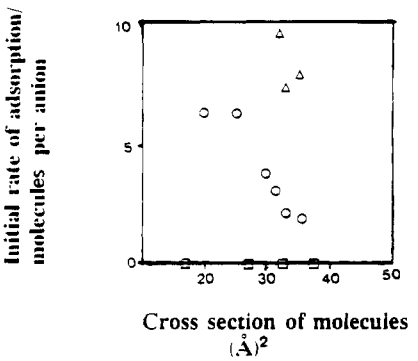

Figure 26. Initial rate of adsorption on $H_3PW_{12}O_{40}$ of various molecules vs molecular size: (1) ethylene; (2) dicloromethane; (3) benzene; (4) toluene; (5) methanol; (6) ethanol; (7) 1-propanol; (8) 2-propanol; (9) 1,4-dioxane; (10) 1-butanol; (11) 1-propanamine; (12) 2-propanamine; (13) 1-butanamine; (14) pyridine.

Considering the bulk adsorption properties, it turns out that catalytic reactions involving polar molecules occur not only at the surface but also in the bulk solid of certain heteropoly acids. The practical effect of this is that the catalytic system behaves like a highly concentrated solution. This explains why these solids have been named pseudoliquids.[568] Under such circumstances all the acid sites are available to the reactants and therefore high catalytic activity could be expected. A schematic diagram of the two types of catalysis is given in Figure 27. The pseudoliquid phase is characterized by uniformity, mobility, three-dimensional reaction field, and other qualities which are very convenient in the study of the catalytic phenomena by using in situ characterization techniques. In this way, Misono and Okuhara[564] have detected by NMR and IR spectroscopies several reaction intermediates during the dehydration of ethanol in pseudoliquid. The comparison of the chemical shift of the hydroxyl proton of the dimer species $(C_2H_5OH)_2H^+$ detected in $H_3PW_{12}O_{40}$ and in HSO_3F-SbF_5, supports the idea that $H_3PW_{12}O_{40}$ is a superacid.

After all this it is not surprising that heteropoly compounds have found large and practical applications in olefin and acetylene hydration, as well as in dehydration of alcohols.

Dehydration of Alcohols and Hydration of Olefins. The dehydration of alcohols to give ethers and olefins is a well-known acid-catalyzed reaction, and therefore, it also occurs on heteropoly acids and

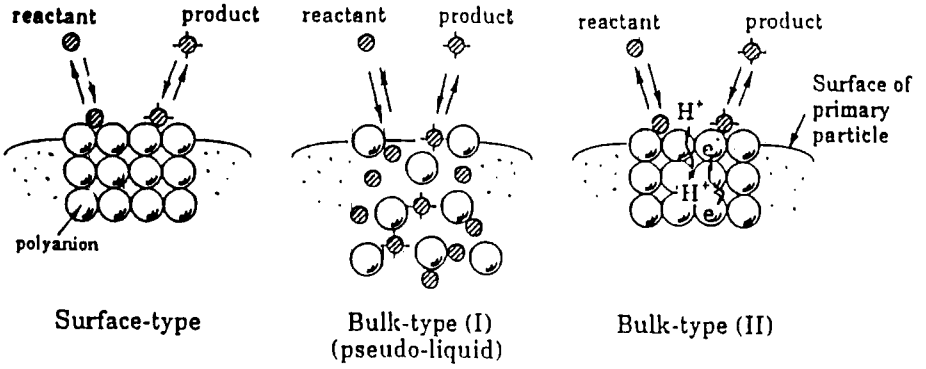

Figure 27. Two types of heterogeneous catalysis.

Table 17. Diffusivities of Alcohols on Ammonium Heteropoly Compounds Oxometalates and ZSM-5 Zeolites

		diffusivity: $10^{11}D$ (cm^2 s^{-1})			
diffusing species	T (K)	NHPW $L = 0.117$	NHSiW $L = 0.583$	NHPMo $L = 0.208$	ZSM-5 (Si/Al = 990) $L = 0.541$
methanol	298	1.0	24.1	4.2	57.5
	308	1.6	34.6	6.3	82.8
	323	2.2	47.1	8.5	113
ethanol	298	0.7	15.4	2.7	13.2
	308	1.0	22.5	3.7	23.5
	323	1.3	30.9	5.2	40.6
1-propanol	293	0.5	12.9	2.1	5.9
	308	0.8	16.7	3.1	13.2
	323	1.2	22.5	4.4	23.5
1-butanol	293	0.4	9.6	1.6	4.5
	308	0.6	12.9	2.3	7.4
	323	0.8	16.7	3.1	11.1
2-methyl-2-butanol	293	2.2	54.1	10.3	1.5
	308	3.0	72.3	13.5	2.8
	323	4.0	96.2	17.1	5.2
1-hexanol	293	0.05	–	0.5	0.8
	308	0.09	–	0.8	1.9
	323	0.13	–	1.1	3.3

their salts. On these materials the diffusivities of different alcohols have been measured in a series of heteropoly acids and the results are compared to those obtained in a ZSM-5 zeolite (Table 17).[531] It has been observed there that the diffusivity of *n*-alcohols decreases with the decrease of their molecular weight, and furthermore the hydrogen bonding has a substantial influence on diffusivity. Indeed, while in ZSM-5 the pore size restriction may be dominant it is apparent that in the large-pore heteropoly compounds the electric field potential plays an important role.

As was said before, owing to the flexible nature of the acid forms and of some salts, alcohols are readily absorbed into the bulk by substituting water molecules and/or by expanding the distance between polyanions. Under such circumstances the system behaves like a concentrated solution ("pseudoliquid phase"), and corresponds to a bulk-type catalysis.[560,563,569-571] If this is so, the reaction should take place in the three-dimensional bulk solid, and a catalyst effectiveness factor close to unity should be expected. Therefore, the rate of reaction should be proportional to the catalyst weight regardless of its specific surface area. Indeed, a linear correlation between the catalytic activity of a series of heteropoly compounds and their bulk acidity has been found and the results are given in Figure 28.[560] A kinetic proof of the bulk type catalysis for dehydration of 2-propanol over $H_3PW_{12}O_{40}$ has been obtained by a transient response analysis.[572] By using ethanol-d_0 and -d_6 this method has proved that, under reaction conditions, there is a large number of ethanol molecules absorbed in the catalyst bulk. Moreover, the amount of absorbed molecules depends on the partial pressure of ethanol, and the reaction proceeds in the catalyst bulk phase.

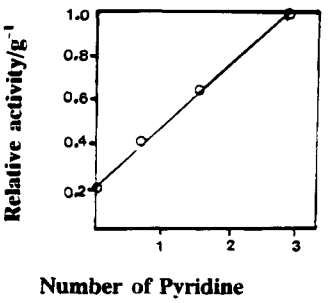

Figure 28. Relationships between strong acidity measured as the pyridine retained after evacuation at 573 K and catalytic activity for acid-catalyzed reactions of $Na_xH_{3-x}PW_{12}O_{40}$.

The IR spectra of $H_3PW_{12}O_{40}$, which has adsorbed $(C_2H_5)_2O$, and their changes with temperature,[573,574] together with the ^{31}P, ^{13}C, and ^1H solid-state NMR[575] have detected the presence of protonated ethanol dimer $(C_2H_5OH)_2H^+$, monomer $C_2H_5OH_2^+$, the cationic ethyl group coordinated to the oxygen of poly-

anion and protonated ether. On this basis the following reaction mechanism has been proposed:[574]

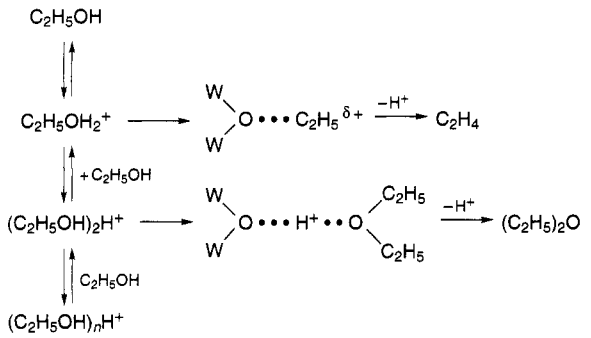

This mechanism is not only consistent with the general knowledge and with the intermediate species detected, but can also explain the unusual[576] dependence of ethylene and ether selectivities on the partial pressure of C_2H_5OH.[577,578]

The activity of heteropoly compounds in the alcohol dehydration reaction is much higher than that of silica–alumina[576,579] and their activity strongly depends on the temperature of the pretreatment,[580] on the amount and nature of the cations in the salts,[567,568] and, if supported, on the nature of the support (carrier).[581–583] Indeed, the type of cation, size, and its electronegativity does not only change the number of acid sites but also can dramatically change the absorption capability of the original heteropoly acid causing, in the limit, the alcohol dehydration reaction to occur at the surface of the salt instead of in the bulk phase. Besides being a source of protons, the interaction between the reactant and the heteropoly anion of the catalyst can be important for the overall process, as demonstrated by the catalytic action of the chiral 2–18 molybdophosphate. Indeed, this catalyst has been shown to promote the acid-catalyzed reaction of nonchiral benzyl alcohol to chiral polybenzyl.[584] The chirality of the products shows that the interaction between the reactant and the heteropoly anion plays an important role in the formation of the final product. It has been reported that when heteropoly acids are supported on silica, alumina, or activated carbon, they strongly interact with the support surface thus changing their behavior[505,581–584] and acting as a condensed solution at the surface of the support.[585] Recently, Hashimoto et al.[583] have obtained a supported heteropoly acid PW, highly dispersed by intercalation into a Zn aluminum carbonate hydroxide by an anion-exchanging technique. This was a very active catalyst for the dehydration of *n*-butanol having the turnover numbers for the intercalated PW/Zn-Al catalyst twice of the unsupported PW_{12} heteropoly acid.

In conclusion, it turns out that heteropoly acids are very adequate alcohol dehydration catalysts, owing to their very special absorption properties for polar molecules. Furthermore, their activity and selectivity can be tailored by introduction of metal cations and by changing the partial pressure of the reactant.

There is no doubt that if a catalyst is highly active for a given reaction (dehydration), it should also be very active for the opposite reaction (hydration of olefins to alcohols), provided that the reaction conditions are adequate. This basic catalytic principle is clearly illustrated by the case of heteropoly acids, on which industrial hydration processes of C_3–C_4 olefins have been developed (Table 18).[586] Using this type of catalysts, isopropyl alcohol was produced by hydration of propylene (Tokuyama Soda) with a conversion of 70% and selectivity of 99%.[587–590] The use of heteropoly acids in this process avoids the use of sulfuric acid, with the corresponding advantage in waste stream disposal.

Table 18. Industrial Processes for Hydration of Olefins Using Heteropoly Acids as Catalysts

reactant	phase	capacity (10^3t/year)	start	remarks
propene	liq(aq)	50	1972	first process (dil HPA)
n-butene	liq(aq)	40	1985	TO MEK
isobutene	liq (aq-C_4)	56	1984	C_4 separation (ConcHPA)

The hydration of isobutene is carried out selectively in the presence of *n*-butene in a highly concentrated aqueous solution (0.05–0.8 M) of 12 heteropoly acids at 60–80 °C. The isobutene hydration is so selective that it allows separation of butenes present in the C_4 streams produced by steam or catalytic cracking. When the process is carried out in a multistage reactor, isobutene is 100% converted, while less than 1% of the *n*-butene is hydrated. In this case the heteropoly acid not only acts as a strong acid catalyst but is also capable of increasing the solubility of butenes while stabilizing the reaction intermediates by the coordination to the polyanion.[591] The competitive coordination of isobutene, *n*-butene, and water to polyanions promotes the high selectivity for isobutene hydration.

The kinetic expression for hydration of isobutene when using heteropoly acids as catalysts continuously increases from first to second order:

$$\text{rate} = K[\text{polyanion}][\text{proton}][\text{isobutene}] = K[\text{polyacid}]^2[\text{isobutene}]$$

While in the case of mineral acids a first-order dependence is found.

Finally, it should be remarked that in this process the decomposition of heteropoly acid was suppressed by partial reduction of Mo or W and by coexistence of organic base with phosphoric acid, rendering the catalyst life longer and decreasing corrosion.

Another way of separation of isobutene from mixed C_4 hydrocarbon streams, such as Raffinate-1, involves the use of heteropoly acids in the etherification of the C_4 mixture with diols, such as ethylene glycol or 1,2-propylene glycol, to obtain the corresponding glycol mono-*tert*-butyl ethers. This is followed by deetherification of monoether at higher temperatures to yield pure isobutene and the regenerated glycol[592]

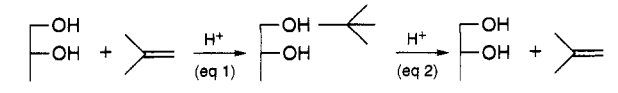

For this process heteropoly acids dispersed on group IV oxides, such as 12 tungstophosphoric acid on titania, are the adequate catalysts.[592]

Esterification and Hydrolysis. Esterification of alcohols with saturated and unsaturated acids is a reaction of industrial importance. Liquid-phase acid catalysts such as sulfuric acid, *p*-toluenesulfonic acid (PTSA), methanesulfonic (MSA), hydrochloric acid, etc. have been used. They however produce waste products as well as undesired byproducts such as ethers and olefins. For certain esterifications, non-acidic tetrabutyltitanates and -zirconates produce lower amounts of byproducts than the liquid acids, but their activity is much lower than that of the Brönsted acids.[593] In this sense heteropoly acids performed well for simple esterifications with carboxylic acids.[594-598] Izumi and Urabe[594] have obtained 95% of conversion and 100% selectivity for the esterification of acetic acid with ethanol to form ethyl acetate, at 150 °C and 1 atm.

Heteropoly acids may have the following advantages compared to other catalysts: the absence of byproducts produced in reactions of the conjugated base of the acid; the high activity which allows one to work at low temperature; the possibility to adjust their acidity by varying the counterion or by varying the heteroatoms or metal atoms; and the possibility to recycle the catalyst by acidifying the alkaline wash water followed by extraction with the feed alcohol.

The catalytic activity for esterification is similar to that of H_2SO_4 and PTS, suggesting that these catalysts were equally strong in solution due to the leveling effect of the basic reactant (Table 19).[598] However, for the hydrolysis of isobutyl propionate the catalytic activities of heteropoly acids were 60−100 times higher than those of H_2SO_4 and PTSA.[598]

The performance of the heteropoly acids for esterification of alcohols can be improved by supporting the heteropoly acids on activated carbon. This not only increases the catalyst life, but also the formation of the corresponding ether is remarkably suppressed.[594]

Heteropoly acids were used as catalyst for the production of phthalic acid diesters in the acid catalyzed diesterification of phthalic anhydride and the corresponding alcohols. The reaction proceeds in two stages. For instance, in the diesterification of phthalic anhydride with 2-ethylhexanol:[599]

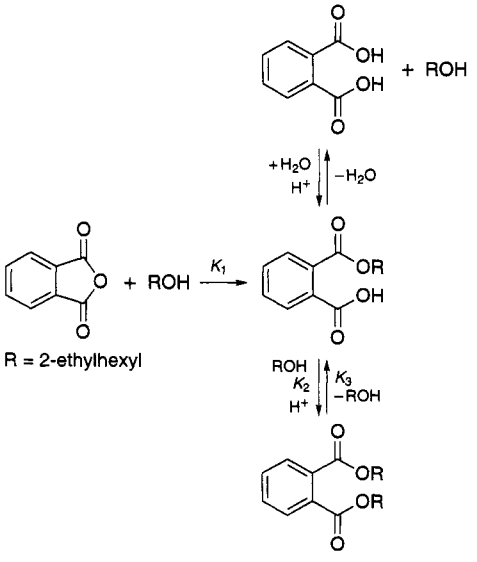

Table 19. Rate Constants for the Esterification of Propionic Acid with Isobutyl Alcohol at 70 °C

catalyst	n^a	rate constant (mol^{-1} dm^3 min^{-1} H^+-mol^{-1})
$H_3PW_{12}O_{40}$	30	3.8
	6	4.8
	0	4.9
$H_4SiW_{12}O_{40}$	22	3.3
$H_4GeW_{12}O_{40}$	7	3.3
$H_5BW_{12}O_{40}$	15	3.2
$H_6CoW_{12}O_{40}$	19	2.3
$H_6P_2W_{18}O_{62}$	32	2.7
PTSA		6.4
H_2SO_4		3.2

The first step is a fast and complete reaction of the anhydride with one molecule of alcohol, proceeding without the addition of catalyst. The second stage is the esterification of the resulting monocarboxylic acid with a second molecule of alcohol while forming one molecule of water. The equilibrium is shifted by the continuous removal of water.

The kinetics of the esterification reaction on heteropoly acids is given by the following equation:

$$-\mathrm{d[Alc]}/\mathrm{d}t = K_1[\mathrm{HTP}][\mathrm{Alc}][\mathrm{PA}] + K_2[\mathrm{HTP}][\mathrm{Alc}][\mathrm{ME}] - K_3[\mathrm{HTP}][\mathrm{DE}][\mathrm{H_2O}]$$

and the reaction shows a lower activation energy on heteropoly acids than on H_2SO_4 or PTSA. This allows the reaction to be performed at lower temperatures (100−120 °C) using the heteropoly acids catalyst with the corresponding low rate of formation of ethers and olefins. Ether formation depends on the structure of the alcohol, being lower for bulkier alcohols in agreement with a S_N2 mechanism. On the other hand the size of the alcohol has little effect on the rate of esterification.[599] In order to achieve better catalyst recovery, the reaction has been carried out on heteropoly acid supported on carbon, silica, alumina, and titania,[599,600] but in all cases leaching of the heteropoly acid was found, together with a decrease in the catalyst activity.

In conclusion, it appears that heteropoly acids are active and selective catalysts for carrying out both, esterification and hydrolysis reactions providing that reaction temperature could be kept low in order to diminish dehydration reactions. When this is achieved then the removal of water in order to shift the equilibrium becomes difficult unless the reaction is carried out at very low pressure, or in the presence of a cosolvent forming an azeotrope with water, which has lower boiling temperature.[599] Finally, complete recovery of the catalyst will be required if these reactions are to be used in practice.

Isomerization Reactions. Double-bond isomerization in olefins is a well-known acid-catalyzed reaction which involves the Brönsted sites of the catalyst. For instance, in the case the double-bond isomerization of *n*-butene a protonation of the double bond occurs in an initial step and a *sec*-butyl cation is formed.[601-603] The heteropoly acid will be in this case a supplier of the acid site, and any acidity modification may affect the catalytic activity. It has been found[604] that the nature of the central atom (Si or P) has little influence on the activity of heteropoly

Table 20. First Reduction Potentials of Various Heteropoly Acids

compound	first red. potential (eV)
$H_4SiW_{12}O_{40}$	− 0.19
$H_3PW_{12}O_{40}$	− 0.02
$H_4SiMo_{12}O_{40}$	+ 0.28
$H_3PMo_{12}O_{40}$	+ 0.30

molybdates, but it does have (Si < P) in the case of heteropoly tungstates. Interestingly, the value of the first reduction potentials of these compounds correlates very well with their catalytic activity (Table 20), which may indicate that for heteropoly acids with the same peripheral atom the reduction potential may be, at least in this case, correlated with acidity. The importance of the acidity of the heteropoly acid in the relation to the rate of olefin isomerization is proven by increasing the electronegativity of the cation. However, for the acidic salts, the correlation is not so direct.[604]

A more acid-demanding type of isomerization, is the isomerization of *n*-paraffins, and specially *n*-butane and *n*-pentane. The isomerization of *n*-butane is an important reaction since it produces isobutane which is a desirable reactant for the production of alkylation gasoline, as well as for the production of isobutylene required for methyl *tert*-butyl ether formation. The skeletal isomerization of *n*-butane involves the formation of a primary carbocation as intermediate. In order to do this very strong acid sites, whose conjugated anion can stabilize the unstable primary carbocations are needed. Thus, SbF_5-HF and oxide supported SbF_5[605,606] are used to carry out that reaction. Heteropoly acids, especially the strongly acidic $Cs_{2.5}H_{0.5}PW_{12}O_{40}$ salt,[607] have been proven to be selective catalysts for the formation of isobutane. However, temperatures as high as 300 °C are required to be of practical use.

In analogy with commercial bifunctional Pt catalyst on fluorinated alumina, Pd salts of heteropoly acids or Pd−heteropoly acid systems have been used for isomerizing *n*-pentane and *n*-hexane, in the presence of H_2.[608,609] The total conversion of hexane and the distribution of the products in hexane isomerization over Pd salts of $H_3PW_{12}O_{40}$ were much higher on the Pd salt than on the parent acid. In the case of pentane isomerization, 40% of conversion with 97% selectivity was obtained on the Pd salt at 180 °C. When the reaction temperature was increased to 200 °C, the conversion strongly increased (92%) but the isopentane selectivity appreciably decreased (58%). The results were improved when the Pd−$H_3PW_{12}O_{40}$ catalyst was supported on active carbon.

These results indicate that the isomerization of short-chain alkanes on bifunctional catalysts based on heteropoly acids deserves further attention.

Carbon−Carbon Bond Formation and Breaking. **Alkylation−Dealkylation of Aromatics.** As was said above, the conventional acid Friedel−Crafts catalysts involving proton donor-promoted Lewis acids such as aluminum chloride−hydrogen chloride, and proton containing molecular sieves are active catalysts for the alkylation of aromatics with alcohols, olefins, and alkyl halides. Heteropoly acids and their salts have also been used to alkylate aromatics by olefins.[537,610-613] In this area the pioneer work was done by Sebulsky et al.,[610] who reported the alkylation of benzene with 1-dodecene on a bench scale using a series of supported silicotungstic acid catalysts, with the purpose of producing a precursor of a biodegradable linear alkyl benzene sulfonate. The use of a solid catalyst such as the supported heteropoly acid should have sound environmental and technical advantages over more conventional catalysts such as aluminum chloride or hydrogen fluoride. Kinetic studies show that the following reactions occurred on the silicotungstic acid supported on Al_2O_3, SiO_2, and SiO_2−Al_2O_3:

$$\underset{\text{benzene}}{C_6H_6} + \underset{\text{dodecene}}{C_{12}H_{24}} \xrightarrow{r_1} \underset{\text{phenyldodecane}}{C_{18}H_{30}}$$

$$\underset{\text{phenyldodecane}}{C_{18}H_{30}} + \underset{\text{dodecene}}{C_{12}H_{24}} \xrightarrow{r_2} \underset{\text{heavy alkylate}}{C_{30}H_{54}}$$

$$\underset{\text{dodecene}}{2C_{12}H_{24}} \xrightarrow{r_3} \underset{\text{dodecene dimer}}{C_{30}H_{54}}$$

$$\underset{\text{benzene}}{C_6H_6} + \underset{\text{dodecene dimer}}{C_{24}H_{48}} \xrightarrow{r_4} \underset{\text{heavy alkylate}}{C_{30}H_{48}}$$

In other words, together with benzene monoalkylation other undesired reactions leading to the formation of dimers and heavy alkylates also occur. The kinetic rate constants for the different reactions were obtained[610] (Table 21), and the results clearly indicate that a second dodecyl alkyl group adds to the aromatic ring as rapidly as the first. Thus, the steric hindrance for the second alkylation does not seem to operate. Moreover, since the activation energies are also the same for the two reactions, it appears that the only control of selectivity can be done from the benzene to 1-dodecene ratio in the feed. In this way, a conversion of 99% and selectivity of 91% was obtained at 150 °C, at 14 atm of total pressure and a benzene to 1-dodecene ratio of 9.0. This result was indeed very promising, but the presence of heavy alkylates in the products (8%) indicates that some catalyst deactivation has already occurred.

Solid phosphorotungstic acid ($H_3PW_{12}O_{40}$) has showed a better performance than liquid (H_2SO_4, CF_3-COOH) or solid (Amberlyst-15, SiO_2-Al_2O_3) catalysts for the selective alkylation of *p*-xylene with 2-methylpropene.[614] This is an interesting reaction since the product, *tert*-butyl-*p*-xylene (BPX), is an important precursor for liquid crystalline polyesters and poly-

Table 21. Specific Rate Constants (h^{-1}) for Alkylation (K_1) and Dialkylation (K_2) of Benzene by 1-Dodecene, and Dimerization of 1-Dodecene (K_3)

type of reaction	specific rate constant (h^{-1}) at reaction temperature (°C)		
	64	121	150
K_1	0.99	17.8	52.5
K_2	0.99	17.8	52.5
K_3	1.10	19.8	59.0

Table 22. Selectivity for Alkylation of *p*-Xylene with 2-Methylpropene by Various Acid Catalysts[a]

catalyst	conversion (%)	selectivity (mol %) BPX	oligomers	OPX	PXM
$H_3PW_{12}O_{40}$	90	74.6	11.5	6.3	7.6
$H_4SiW_{12}O_{40}$	91	26.6	70.2	0.4	2.8
$H_5BW_{12}O_{40}$	97	6.1	93.9	0	0
$Cs_{2.5}H_{0.5}PW_{12}O_{40}$	89	50.5	48.0	0.8	0.7
SO_4^{2-}/ZrO_2	86	50.9	26.0	3.4	19.7
amberlyst-15	92	4.2	95.8	0	0
SiO_2 Al_2O_3	75	1.3	98.7	0	0
H_2SO_4	86	7.2	92.8	0	0
CF_3COOH	10	0	100	0	0

[a] 30 °C for 30 min; 0.45 g of cat; *p*-xylene, 0.28 mL; 2-methylpropene, 0.37 mmol min^{-1}.

amides having low melting points and good solubilities.[615] When H_2SO_4, $AlCl_3$, and acidic clays are used as catalysts the insertion of *tert*-butyl group into the ortho position of the *p*-xylene was very slow, and meta position was preferred.[614] Results from Table 22,[614] show that high selectivities are obtained when using $H_3PW_{12}O_{40}$ as catalyst. Moreover, with increasing of the acid strength of the heteropoly acid by increasing the valency of the central atom, the selectivity to BPX significantly increases, while the conversions of 2-methylpropene are at similar levels.

It was mentioned before that the acidic and adsorption properties of heteropoly compounds can be modified by synthesizing different salts. The results of these changes are reflected in the alkylation of 1,3,5-trimethylbenzene by cyclohexene. For this reaction a $Cs_{2.5}H_{0.5}PW_{12}O_{40}$ was remarkably more active than $H_3PW_{12}O_{40}$.[616,617] This activity difference cannot be explained only on the basis of total acidity and acid strength distribution, and the higher hydrophobicity of Cs salts with respect to the heteropoly acid form, with the corresponding beneficial adsorption of nonpolar molecules such as aromatic and cyclohexene has been claimed as an additional activity factor.[617] On top of that, the soft basicity of the heteropoly anion,[596] which can be changed by the presence of Cs^+, gives the system a special acid–base bifunctionality which enhances the catalytic activity of the heteropoly acid salt. The following scheme shows the acid–base bifunctional mechanism where polyanion stabilizes the cyclohexyl cation and/or the cyclohexyl 1,3,5-trimethyl proton from the latter cation:[617]

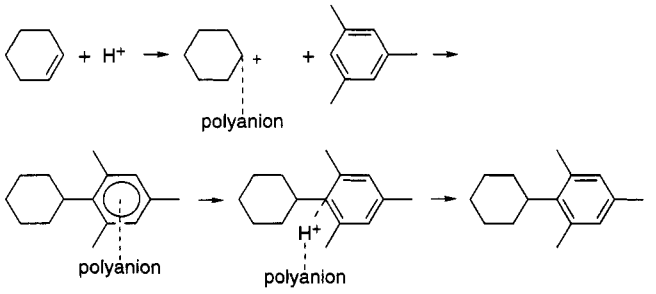

Since heteropoly acids can catalyze the alkylation of aromatics, they should also catalyze dealkylation and transalkylation. Indeed, Nowinska et al.[618] have shown that 12 tungstophosphoric acid supported on γ-Al_2O_3 and SiO_2 was active for cumene cracking at 250 °C, and for toluene disproportionation at 250–400 °C. In this sense the acidity of heteropoly acids is strong enough to catalyze the acylation of aromatics by benzoyl chloride.[611,612,619]

Table 23. Alkylation of Isobutane and Butene on Salts of $PW_{12}O_{40}$ Polyoxianions

catalyst salts	reaction temp (°C)	yields of products (%) C_5–C_7	TMP	other C_8	C_9^+	C_5^+
$Cs_{2.5}$	50	41	98	4	25	163
$Rb_{2.5}$	50	58	109	7	14	188
$K_{2.5}$	50	53	127	7	10	197
$Tl_{2.5}$	50	64	106	7	18	195
$(NH_4)_{2.5}$	50	64	115	8	12	199
$Cs_{2.7}$	100	21	36	8	65	130
$Cs_{2.5}$	100	56	59	21	13	149
$Cs_{2.3}$	100	108	50	29	9	196
$Cs_{2.5}$	20	28	73	2	58	161
H_3	100	0	0	23	112	135
ultra strong acid-zirconia	20	9	11	1	81	102

Alkylation of Isoparaffins and Olefins. The increasing demand for high-octane paraffinic gasolines has compelled the refiners to look for the appropriate isoparaffin alkylation process. However, in order to widely expand such process the actual acid mineral catalysts, i.e. HF and H_2SO_4 have to be substituted by solid acid catalysts. Owing to their strong acidities, heteropoly acids have been explored as potential catalysts for alkylation of isobutane with butene but the literature on this subject is scarce.[620,621] In these cases, K^+, Rb^+, Cs^+, and NH_4^+ salts of tungstophosphoric heteropoly acid were preferred as catalysts and they could form tribranched products in good yields at relatively low temperatures (Table 23). Moreover, it appears that they give better results than superacid SO_4^{2-}/ZrO_2 catalysts. However, little is known about an important feature of alkylation catalysts such as the catalyst deactivation–regeneration. The preliminary results[621] indicate that a strong deactivation of the catalyst can occur with time on stream.

Isobutane alkylation is a field of sufficient interest to justify further research on the application of heteropoly acids and their salts, as insoluble catalysts or supported on SiO_2, γ-Al_2O_3, carbon, etc. The special hydrophobic-hydrophilic properties of heteropoly acids as well as the stabilizing character of the polyanions can give, if properly tuned, interesting results.

D. Sulfated Metal Oxides

About 15 years ago, it was shown that by a sulfate treatment of oxides such as ZrO_2, TiO_2, SnO_2, Fe_2O_3, HfO_2, etc., a remarkable increase in the surface acidity and in the catalytic activity for carbenium ion reaction of the starting metal oxides was achieved.[622–627] These catalysts were claimed to present superacid sites with acid strengths, measured by the indicator method, of up to $H_0 < -16.04$ which have opened new perspectives in the use of friendly solid catalyst for carrying out, under mild conditions, reactions involving very strong acid sites. In this section the preparation, acid characteristics, and the carboniogenic catalytic activity for hydrocarbon reactions will be reviewed.

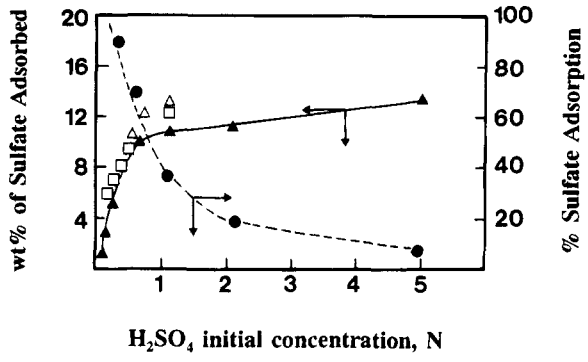

Figure 29. Sulfate adsorption (●) and percentage of sulfate adsorption (△) with solutions of varying initial H_2SO_4 concentration.

1. Preparation of Sulfated Metal Oxides

Different procedures for preparation of sulfated metal oxides have been reported.[622-628] The sulfated metal oxides are usually prepared by first precipitating the hydroxides, and after washing and drying, they are treated with a solution of H_2SO_4. The treatments with $(NH_4)_2SO_4$, SO_2, H_2S, and SO_3 also promote the catalytic activity.[626]

In the case of sulfate-treated superacids of Fe, Ti, Zr, Hf, and Sn, superacid sites were not created by the treatment of sulfate ion on the crystallized oxides but on the amorphous hydroxide forms followed by calcination and crystallization. However, in the case of superacid of Al_2O_3, better catalysts were obtained when the crystallized oxide rather than the amorphous one was treated with H_2SO_4.[630] Thus, it appears that the nature of the starting metal oxide hydroxide,[631] as well as each one of the posterior treatments, can be of importance for the final properties of the acid catalyst[632] and they will be discussed here.

After the dried hydroxide is impregnated with a solution of H_2SO_4 or $(NH_4)_2SO_4$, the resulting solid is dried and calcined to temperatures of 500–650 °C. A variable to be considered during the preparation is the normality of the H_2SO_4 solution. Indeed, it has been found[633-635] that the amount of sulfate adsorbed by the solid increases rapidly with the concentration of sulfuric acid in contact with the solid (Figure 29) and higher sulfur contents are obtained, for any calcination temperature, for higher H_2SO_4 normalities, in the case of SO_4^{2-}/ZrO_2 catalysts (Figure 30).

After H_2SO_4 impregnation, the calcination temperature of the resulting material also plays an important role on the subsequent textural, acidity, and catalytic activity.[636] The sulfated materials show larger surface areas than the pure metal oxides[637] (Table 24).

The XRD spectra of SnO_2, ZrO_2, and TiO_2 show the degree of crystallization of the sulfated oxides to be much lower than that of SnO_2 without the sulfate treatment. Furthermore, the presence of sulfate[638] retards the conversion of the tetragonal to the monoclinic form in the case of ZrO_2, and from anatase to rutile in the case of TiO_2. For instance, the XRD pattern of SO_4^{2-}/ZrO_2 heated at 650 °C was completely a tetragonal form, while the pure ZrO_2 was

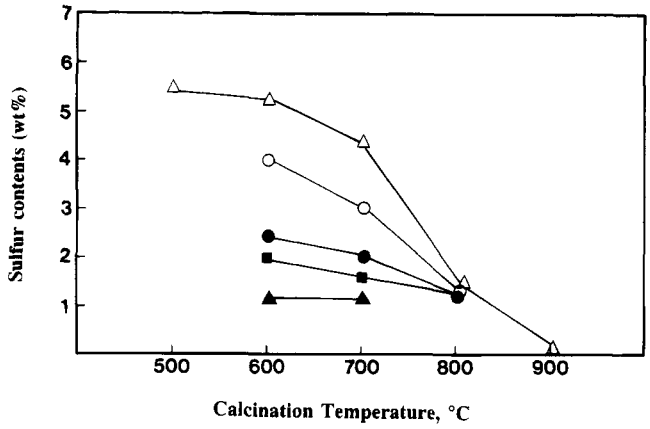

Figure 30. Variations of SO_4^{2-}/ZrO_2 sulfur content with respect to the calcination temperature for the various H_2SO_4 normalities used.

Table 24. Surface Area of Oxides and Sulfated Oxides

catalyst	calcination temperature (°C)	surface area ($m^2\ g^{-1}$) with SO_4^{2-}	surface area ($m^2\ g^{-1}$) without SO_4^{2-}
ZrO_2-I	500	187	100
	650	124	50
	800	41	28
ZrO_2-II	575	136	64
	650	84	44
TiO_2-I	500	112	87
	525	144	63
	600	100	55
TiO_2-II	500	117	75
	525	90	71
SnO_2	500	147	29
	550	166	28
	600	135	21
Al_2O_3-1	650	161	250
Al_2O_3-2	650	151	253
Al_2O_3-3	650	110	149

almost completely converted in the monoclinic form.[637] In the case of TiO_2, it is found that the temperature of crystallization or phase transformation of the anatase to rutile form in SO_4^{2-}/TiO_2 is ~200 °C higher than that of pure TiO_2.[639,640]

The slow down of the crystallization rate and phase transformation, together with the observed fact that samples with the sulfate treatment were cracked into fine particles in comparison to those of the samples without the sulfate treatment, can be the reason why specific surface areas of the catalysts are much larger than those of the oxides which have not undergone the sulfate treatment.

At calcination temperatures above 650 °C the sulfated species start to decompose probably following the reaction:[636]

$$2Zr^{4+} + SO_4^{2-} \rightarrow 2Zr^{3+} + SO_2 + O_2$$

Indeed, the formation of SO_2 by sulfate decomposition has been detected for sulfated ferric oxide.[641]

It can be concluded that the preparation of catalytically active sulfated oxides is not trivial, and the different preparation steps need to be optimized for each oxide: the starting salt and the precipitation procedure, the selection of the sulfating agent and procedure of sulfation, and calcination conditions.

2. Nature of Acid Sites

It was said above that much better catalysts are obtained with sulfated samples obtained from zirconium hydroxide rather than from zirconium oxide. Then, it can be assumed, in a first approximation, that the formation of acid sites involves a two-step chemical reaction between the superficial hydroxyl groups of zirconium hydroxide and adsorbed H_2SO_4:[636]

first step: impregnation–drying step

$$Zr_n(OH)_{4n} + xH_2SO_4 \leftrightarrow Zr_n(OH)_{4n-2x}(SO_4)_x + 2xH_2O$$

second step: calcination above 400 °C

$$Zr_n(OH)_{4n-2x}(SO_4)_x \rightarrow Zr_nO_{2n-x}(SO_4)_x + (2n-x)H_2O$$

Several observations support this reaction scheme.[636] In this way, the presence of SO_4^{2-} anions in the zirconia framework may explain the sintering resistance and the stabilization of the tetragonal phase. The existence of an optimum for the catalytic and ionizing properties as a function of the sulfur content may be due to the maximum covering of the hydroxide surface. However, the nature of the high acidity of the sulfated metal oxides is still controversial. Thus, several authors[627,631,642-645] have proposed that the very strong acidity is due to an increase in the number and strength of Lewis acid sites, and Yamaguchi[643] has offered the following scheme to describe the formation of an active catalytic site:

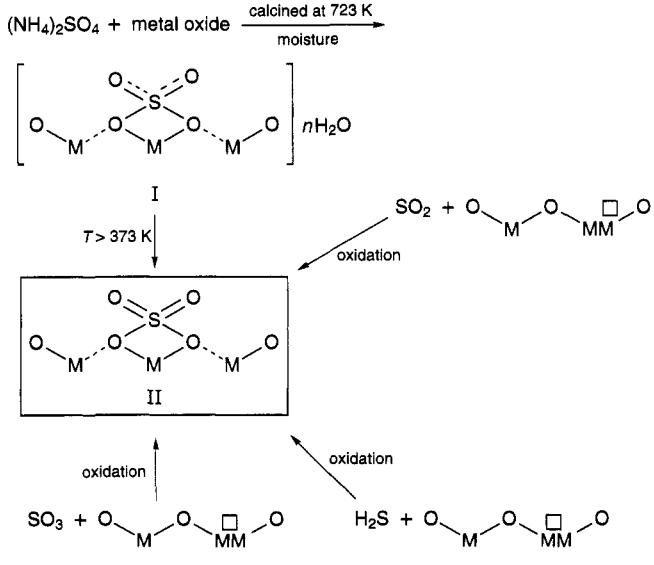

This author proposed that whatever the starting sulfur materials are, once they are oxidized at the surface of metal oxides, they form structure II. Thus the structure II is essential for the acid-catalyzed reactions as a common active site on the sulfur-promoted oxidized samples, and it is suggested that structure II may develop at the edge or corner of metal oxide surfaces. Sulfate-promoted ZrO_2 exhibit a strong IR band at 1370 cm^{-1} which has been assigned to an asymmetric stretching vibration of S=O. The adsorption of pyridine caused a large shift in the S=O band to 1330 cm^{-1}, which was explained[646] by assuming that the sulfur complex in the highly acidic catalysts has a strong tendency to reduce the bond order of SO from a highly covalent double-bond character to a lesser double-bond character when a basic molecule is adsorbed on its central metal cation. The strong ability of the sulfur complex with structure II to accommodate electrons from a basic molecule, i.e. to act as a Lewis site, is a driving force in the generation of highly acidic properties. However, chelation of the metal would leave it 8-coordinated and not a Lewis acid site.[632] Thus, while this scheme provides an illustration on the formation of active sites, it does not permit SO_2 or SO_3 to be eliminated from structure II without introducing problems with the oxidation states of the elements and compounds involved in the reaction:[634]

Arata and Hino[630] have proposed a different structure for the active site, in where sulfate bridges across two zirconium atoms:

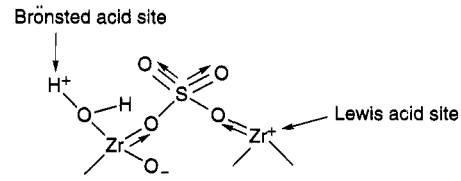

This model implies the formation of Brönsted acid sites, and it has been observed by IR that there is an easy conversion of Lewis to Brönsted acid sites by sorption of water molecules. The presence of those Brönsted acid sites would allow catalytic reactions to occur at much lower temperatures with the same rate as they occur at higher temperatures without the presence of Brönsted sites.

While the above structure is widely used to discuss the catalytic activity of these materials since it illustrates the presence of Brönsted and Lewis acid sites in the active catalyst, Davis et al.[634] have shown that it does not appear possible to make it conform with the chemical bonding, due to the valence or structural changes that occur during catalyst preparation and activation by heat treatment. Indeed, when losing sulfur upon heating above 650 °C, the following reaction will occur depending on whether SO_3 or SO_2 is lost:

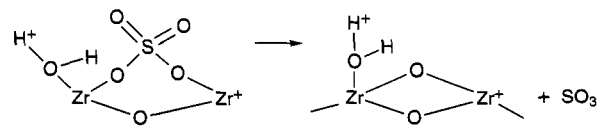

The loss of SO_2 implies the reduction of S^{6+} to S^{4+} with a corresponding oxidation of some Zr or O species, but the authors[634] were unable to offer a scheme to illustrate that.

In order to deal with those difficulties Clearfield et al.[632] have proposed the following scheme:

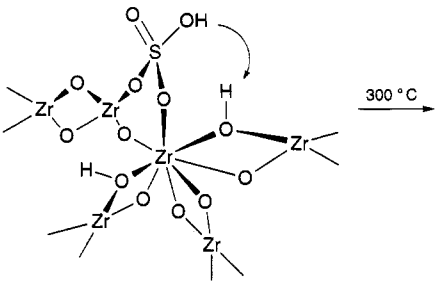

I

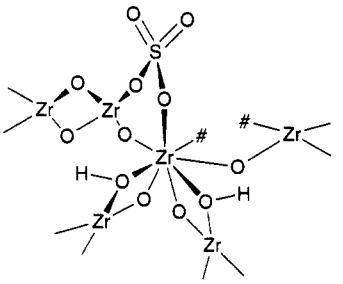

II

The authors proposed that in sulfuric acid media the predominant species is bisulfate. This ion could displace a single bridge. On heating, an adjacent hydroxyl could interact with the bisulfate ion to split out water leading to structure II. However, the hydroxyl group could also interact with an adjacent OH bridge to split out water and leave the bisulfate ion intact. Thus strong Brönsted and Lewis acid sites would be present on that structure. The presence of both type of sites have, indeed, been seen by IR and pyridine adsorption measurements,[644] and it has been proposed that Brönsted acid centers can be present only if sulfates, and possibly polysulfates, are present on the top terminations of the scale—like ZrO_2 crystallites, i.e., on regular patches of low index crystal planes.

With respect to their acidity CO adsorption at room temperature led to an IR spectrum with a peak at 2200 cm^{-1} characteristic of CO adsorbed on strong acid sites.[642,647,648] Large H-1 chemical shifts suggest that the sulfated zirconia catalyst presents protonic superacidity, this property being related to the structure of surface sulfated species.[649] Most of the measurement using indicators show that these materials fall in the superacidity region. However, this has been contested by Hall et al.,[650] claiming that they have not observed superacidity on sulfated zirconia catalysts. The limitations of Hammett's indicators for measuring the acid strength of sulfated oxides have been presented by several authors[636,651] who have shown that even the nonsulfated ZrO_2 is already in the superacid region using the Hammett indicator technique, while it is inactive for butane isomerization.

Recently, Lin and Hsu[59] have proposed a new approach for detecting superacidity on these catalysts by means of temperature-programmed desorption of substituted benzenes. Using such a procedure it was shown that sulfated zirconium oxides present superacid sites. However, the method has been contested by Jatia et al.,[62] who have shown that the TPD peak used by the former authors[59] to claim superacidity comes from CO_2, SO_2, and O_2 formed by oxidation of adsorbed benzene on the samples.

Very recently Vedrine et al.[652] introduced a new model for SO_4^{2-}/ZrO_2 catalyst which indicates that the acidity does not fall in the superacidity range but corresponds to that of H_2SO_4. The authors indicate that from the IR spectra of SO_4^{2-}/ZrO_2 activated at 600 °C and 2 wt % sulfur content, one can see the SO_3 species associated to 1387 and 1027 cm^{-1} bands corresponding to a Lewis site with a band at 1459–1464 cm^{-1} for adsorbed pyridine. This SO_3 species was reversibly transformed upon water adsorption into adsorbed H_2SO_4 species associated to 1320, 1200, and 1055 cm^{-1} bands and to pyridinium species at 1542 cm^{-1}. On these bases, the authors have proposed the following equilibrium to occur:

$$(SO_3)_{ads} + H_2O \rightleftarrows (SO_3, H_2O)_{ads} \rightleftarrows (H_2SO_4)_{ads} \rightleftarrows H_3O^+ + (HSO_4^-)_{ads}$$

$$(HSO_4^-)_{ads} + H_2O \rightleftarrows H_3O^+ + (SO_4^{2-})_{ads}$$

This is supported by theoretical calculations using molecular complex models which show that sulfated zirconia corresponds to H_2SO_4 on ZrO_2 with an acid strength about equal to that of H_2SO_4, which is in the lower limit of superacidity.[648,653] This model, while very suggestive, needs to take into account the role of the metal which undoubtedly indicates that there is a direct correlation between the acid strength of the SO_4^{2-}/MO_2 catalyst and the electronegativity of the metal, in such a way that the following order of acid strength has been observed:[639,654–656] $SO_4^{2-}/ZrO_2 > SO_4^{2-}/SnO_2 > SO_4^{2-}/TiO_2 > SO_4^{2-}/Fe_2O_3 > SO_4^{2-}/Al_2O_3$.

In order to increase both acidity and stability, complex oxides have been sulfated. In this way it has been shown that the introduction of a small amount of WO_3 in SO_4^{2-}/ZrO_2 not only enhances the acid strength of the catalyst but also introduces Brönsted acidity. This indicates that Brönsted acidity may result in this system from the OH groups bonded to tungsten atoms on the catalyst surface through the following structure:[657]

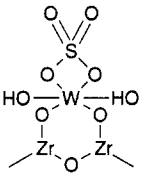

In this case, WO_3 and SO_4^{2-} cooperate to enhance the acidity of ZrO_2.

One limitation of sulfated oxide solid acids is their lack of stability, and the improvement of this is of paramount interest for future catalytic applications. In this sense, a new class of solid superacids, sulfated metal oxides containing Fe, Mn, and Zr have been developed,[658–661] which shows higher stability than sulfated ZrO_2, while are able to isomerize *n*-butane at near room temperature with a rate 3 orders of magnitude greater than sulfated zirconia. These results have been reproduced by Jatia et al.[62] who also found that the addition of either Fe or Mn

increases the catalytic activity with the Fe impregnated sample showing an order of magnitude greater activity than the Mn impregnated material. The combination of Fe and Mn enhances the catalytic activity over the singly impregnated solids and the sulfate concentration plays an important role in optimizing the activity of the doubly impregnated zirconia.

In conclusion, it can be said that a new type of solid acid catalysts with relatively high surface areas and strong acidities are obtained by treating some transition metal oxides by H_2SO_4 or $(NH_4)_2SO_4$. The acid strength could be controlled by changing the electronegativity of the metal as well as by introducing multimetal systems. Both types of acid sites, Brönsted and Lewis, are present on these catalysts, and they remain stable at temperatures up to 600 °C. The acidity and surface area strongly depend on the preparation procedure, i.e. impregnation, and calcination. Finally, the exact nature of the acid sites is still controversial, and it even is questioned if superacid sites, i.e. sites with acidity higher than 100% H_2SO_4, are really formed. Nevertheless, they are very active catalysts for carboniogenic reactions and this aspect will be discussed below.

Superacid Oxides. Another way to overcome the unstability of the sulfated oxide catalysts at high temperature is to try to develop strong acidity on nonsulfated promoted oxides. In this sense it has been shown[662,663] that ZrO_2 has weak acid sites which are able to catalyze carbenium ion reactions such as double-bond isomerization, dehydrations, etc., and the acidic characteristic of the oxide depends on preparation and calcination conditions. However, Arata and Hino[664-667] have shown that by impregnating $Zr(OH)_4$ with a salt of tungsten or molybdenum followed by calcination in air at high temperatures acid sites of $H_0 \leq -14.52$ are formed. Thus, $Zr(OH)_4$ was impregnated with aqueous ammonium metatungstate $[(NH_4)_6(H_2W_{12}O_{40})\cdot nH_2O]$ or molybdic acid (H_2MoO_4) dissolved in ammonia water followed by drying and calcination at 600−1000 °C. As it occurred in the case of sulfated ZrO_2, it has to be avoided the crystallization of ZrO_2 from $Zr(OH)_4$. Consequently, the hydroxide should not be heated at temperatures above 300 °C.

The interaction of W or Mo with ZrO_2 during calcination retards the evolution of the tetragonal form, as occurred with the introduction of SO_4^{2-}. However, with W and Mo the crystallographic phase transformation of ZrO_2 is completely a tetragonal form when calcining up to 900 °C and a monoclinic form after calcination at 1000 °C. It would appear then that tungsten and molybdenum oxides combine with zirconium oxides to create superacid sites at the time when a tetragonal system is formed.[664,666] MoO_3-$(WO_3)/ZrO_2$ catalysts have been prepared by different methods including a conventional impregnation technique, a molten salt method, and calcination of zirconium hydroxide impregnated with Mo(W) salt. Among them the third one gives the strongest acidities, which are lower than those obtained with sulfated zirconia.[668]

As observed with the sulfate superacids when calcined at high temperatures, the surface areas of WO_3/ZrO_2 and MoO_3/ZrO_2 catalysts are larger then those of pure ZrO_2 (Table 25).[637] Moreover the optimum amount of W (13 wt %) and Mo (6.6 wt %) which strongly interacts with ZrO_2 is equivalent to the amount of S (2.2 wt %) that as the sulfate, strongly interacts with ZrO_2 in monolayer. All these facts are a clear indication that the type of interaction, and species formed cannot be too different from those obtained on SO_4^{2-}/ZrO_2 catalysts.

Table 25. Surface Area of WO_3/ZrO_2 and MoO_3/ZrO_2 Catalysts[637]

calcination temp (°C)	surface area ($m^2\ g^{-1}$)		
	WO_3/ZrO_2	MoO_3/ZrO_2	ZrO_2
600	44	68	34
700	39	60	15
800	35	58	6
900	30	7	2

3. Hydrocarbon Reactions on Superacids Oxides and Sulfated Oxides

Dehydration of Alcohols and Hydration of Olefins. Dehydration of alcohols is a reaction which does not need strong acid sites. In fact the relatively weak acid sites present in untreated ZrO_2 are able to carry out this type of reaction[669-675] in a very selective way. Practical use has been made of the selectivity of ZrO_2 and other pure oxides for dehydration of alcohols; and for instance, Koei chemicals obtains allylamine by the selective dehydration of 1-amino-2-propanol using ZrO_2 as catalyst:[676]

$$H_2NCH_2CH(OH)CH_3 \rightarrow H_2NCH_2CH{=}CH_2 + H_2O$$

As was said above, the SO_4^{2-} treatment of oxides produces a decrease in the amount of weak acid sites while new very strong acid sites are formed. Then, since in the case of alcohol dehydration all weak and strong acid sites can be active, it can be expected that the activity should correlate with the total number of acid sites better than only with the number of the very strong. For instance when the catalytic activity for 2-propanol dehydration of a series of TiO_2, TiO_2−SiO_2 and SO_4^{2-}/TiO_2, and SO_4^{2-}/TiO_2-SiO_2 catalysts was compared it was found that although the acidity of SO_4^{2-}/TiO_2 is the highest, its catalytic activity is relatively low.[677] SO_4^{2-}/Fe_2O_3 catalysts have also been used to dehydrate ethanol, 2-propanol, and 2-butanol at 170−250 °C,[678-680] showing a higher activity than amorphous silica−alumina, and much higher activity that the Fe_2O_3 in the absence of SO_4^{2-}. One advantage of SO_4^{2-}/metal oxide catalysts is that it is possible, in some cases, to combine the acidic properties of the sulfated catalyst with the oxidation activity of the metal oxides to carry out, in one pot, dehydration and oxidation reactions. For instance, cyclohexanol is dehydrated and oxidized on SO_4^{2-}/SnO_2 catalysts to give high yields of cyclohexanone (Table 26).[678] The results show that the amount of cyclohexanone formed was increased by the sulfate treatment and the addition of water, and selectivities to cyclohexanone higher than 95% could be obtained.

If the strong acidities of sulfated oxides do not present any advantage with respect to dehydration

Table 26. Dehydration and Oxidation of Cyclohexanol over SO_4^{2-}/SnO_2 at 623 K and 54 h Reaction Time

catalyst	additive	conv (%)	selectivity (%) cyclohexane	cyclohexanone
SO_4^{2-}/SnO_2[a]	none	8.3	14.5	85.5
	O_2[b]	4.3	17.1	82.9
	H_2O[c]	23.3	4.8	95.2
SnO_2	none	2.0	31.3	68.7
	O_2[b]	4.7	20.5	79.5
	H_2O[c]	3.2	43.0	57.0

[a] Calcination temperature: 823 K. [b] Dried air was used. [c] A mixture of cyclohexanol and wt % water was feed.

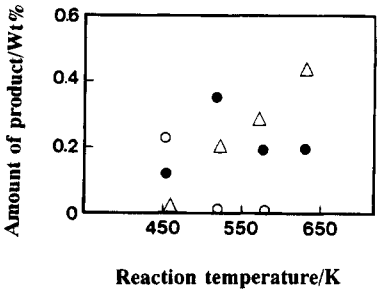

Figure 31. Effect of reaction temperature on product distribution of ethene hydration on SO_4^{2-}/SnO_2, reaction time 5 h: (○) ethanol; (●) acetaldehyde; (△) acetone.

of alcohols, it can however be of interest to catalyze the hydration of olefins since at low reaction temperatures the equilibrium composition favors the formation of alcohol. Indeed, high activities and selectivities to ethanol were obtained during hydration of ethylene on SO_4^{2-}/ZrO_2 and TiO_2–ZnO containing small amount of SO_4^{2-} catalysts. The main inconvenience of sulfated oxides as hydration catalysts is their gradual deactivation owing to the loss of SO_4^{2-} by dissolution in water occurring during the reaction. The results given in Figure 31[681] indicate that higher yields and selectivities of ethanol are obtained at low temperatures, but oxidative dehydrogenation of the alcohol occurred at higher temperatures on SO_4^{2-}/SnO_2 catalysts.

Esterification and Acylation Reactions. Esterification of organic acids and alcohols is a type of reaction which is not highly demanding from the point of view of acid strength and can be catalyzed by relatively weak acid sites present in unsulfated ZrO_2.[682] Sulfation of ZrO_2 strongly decreases the activity for the esterification of acetic acid and methanol due to the decrease in total amount of acid sites. On the other hand, the formation of very strong acid sites during the sulfation can also catalyze the dehydration of the alcohol giving the corresponding olefin.[683,684] The extent of the side reaction will be decreased by diminishing the electronegativity of the metal to be sulfated. In Table 27[685] it is shown that the initial activity of SO_4^{2-}/TiO_2 is the highest of any catalyst studied, but it decays rapidly with time. Indeed, after 2 h of use the activity of SO_4^{2-}/TiO_2 is already lower than that of niobic acid, which on the other hand remain unchanged after 60 h of use. The deactivation of SO_4^{2-}/TiO_2 has also been observed during the esterification of phthalic acid with *n*-octyl alcohol, and the decay was associated to the elimination of sulfate ion on the surface. At

Table 27. Catalytic Activities of Several Solid Acids for Vapor-Phase Esterification of Acetic Acid and Ethanol

catalyst	reaction temp (K)	based on ethanol conversion (%)	selectivity (%)
niobic acid	393	72	100
	413	86	100
cation-exchange resin	413	50	98
SO_4^{2-}/ZrO_2	413	56	90
SO_4^{2-}/TiO_2	413	100	95
SiO_2–Al_2O_3	413	14	98
ZSM-5	393	82	92
	413	99	72
$H_3PW_{12}O_{40}$ on carbon	393	83	99.7

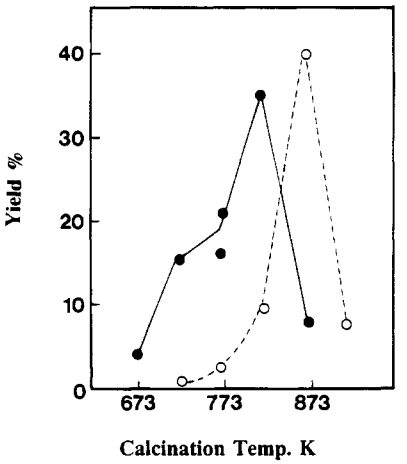

Figure 32. Activities of two samples of ZrO_2–SO_4^{2-} catalysts prepared by impregnation with H_2SO_4 (●), and $(NH_4)_2SO_4$ (○) followed by calcining at different temperatures, for the acylation of chlorobenzene with chlorobenzoyl chloride.

the same time if the calcination temperature of the SO_4^{2-}/ZrO_2 catalyst was increased by 150 °C, the activity remained unchanged for the repeated operation without observing sulfate elimination owing to a stronger sulfate–metal interaction.[637,684] Other esterification reactions studied using SO_4^{2-}/TiO_2 and SO_4^{2-}/ZrO_2 as catalysts are ethanol and acrylic acid, and methanol and salicylic acid.[637,684]

In conclusion, it appears that sulfated oxides are not the most adequated catalysts for esterification reactions since the most stable SO_4^{2-}/ZrO_2 catalysts are less active and selective than others such as niobic acid and supported heteropoly acids, while other more active and selective such as SO_4^{2-}/TiO_2 are rapidly deactivated due to the loss of SO_4^{2-}.

In the case of Friedel–Crafts acylations the reaction can be performed with an acid chloride, an anhydride, or an organic acid as acylating reagents and with $AlCl_3$ as catalyst but used in stoichiometric amounts. Thus, the disadvantages of this catalyst due to wastes and corrosion problems have been tried to be overcome by the use of SO_4^{2-}/ZrO_2, which has very strong acid sites needed for this reaction. A direct correlation between acylation activity and concentration of the very strong acid sites has been found on SO_4^{2-}/ZrO_2 catalysts. Indeed, the results from Figure 32[686] show that different calcination temperatures of 823 and 873 K for samples prepared

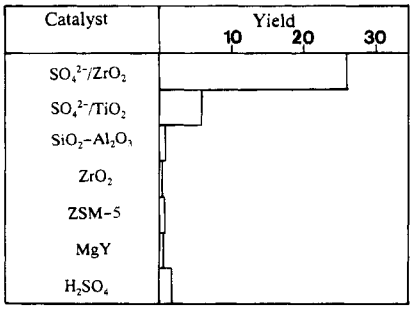

Figure 33. Catalytic acylation of *o*-chlorobenzoyl chloride with chlorobenzene by solid acids and H_2SO_4 at 406 K.

by sulfation with H_2SO_4 and $(NH_4)_2SO_4$ respectively, in order to obtain the maximum activity.

On the basis of the strong acidity of SO_4^{2-}/ZrO_2, it has been used as catalyst for acylation of *o*-chlorobenzoyl chloride with chlorobenzene and its activity is superior to that of any other known inorganic solid oxide base catalyst, and H_2SO_4:[686]

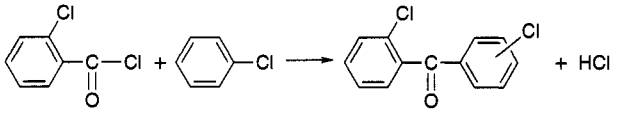

Indeed, results from Figure 33 clearly show that SO_4^{2-}/ZrO_2 is more active that either H_2SO_4 acid or zeolites.

The use carboxylic acids as acylating agents is of great interest, but it should be considered that in that case acid sites stronger than $H_0 = -15$ are needed for the formation of the acylium cation (RCO^+). If one takes into account that acid sites of $H_0 = -16$ have been found on SO_4^{2-}/ZrO_2 it is not surprising that it has been found to be able to carry out acylations of toluene using anhydrides and carboxylic acids, with the order of reactivity[637,684,687] $(PhCO)_2O$ > $PhCO_2H$ > $PhCO_2Et$ > $PhCO_2Me$.

Contrary to what has been observed on $FeSO_4$, in the case of SO_4^{2-}/ZrO_2 the acylation reaction completely stopped when the solid catalyst was separated from the reaction mixture. Thus, it appears that SO_4^{2-}/ZrO_2 acts as a true heterogeneous acid catalyst.[686] When the electronegativity of the metal changes, the activity of the sulfated catalyst for the acylation reaction also changes. In this sense while the sulfated Al_2O_3 is active for benzoylation of benzene with both benzoyl chloride and benzoic acid, its activity is smaller than that of SO_4^{2-}/ZrO_2.[688] The authors suggest that the benzoyl cation ($PhCO^+$) from a benzoyl chloride molecule is generated on a Brönsted site created by adsorption of water on Lewis sites of the catalyst.

In conclusion, sulfated zirconia appears as a very promising solid catalyst for carrying out acylation reactions. However, questions related to catalyst lifetimes remain unanswered.

Isomerization Reactions. Cis–trans and double-bond isomerization of butenes are catalyzed by Brönsted acid sites of relatively low acid strength, being the reaction intermediate a *sec*-butyl cation formed by the addition of the proton. The same intermediate is often involved in the case of Lewis solid acids, but in this case protonic acid is induced by the reaction of the olefin on the Lewis acid site. Due to the low acid demand of this reaction, it appears that sulfated oxides would not be the most adequate catalysts, and the studies of isomerization of olefins on them are scarce. In the case of SO_4^{2-}/Fe_2O_3 the IR of adsorbed 1-butene has provided information on the nature of interaction between the olefin and the sulfated catalyst.[689] Thus, upon adsorption at room temperature, the presence of C=C stretching and CH_3 bending vibration in the 1400–1700 cm^{-1} region indicate that 1-butene adsorbs molecularly, probably forming a π complex.[690] When increasing the temperature to 420–520 K, the original peak disappears and new broad peaks appear in 1550–1700 cm^{-1} region which may indicate the formation of π-allyl intermediates. If this is so, it is then possible that 1-butene adsorbs on Fe site (Lewis acid site) forming an allyl species between 420 and 520 K. When the sample is heated further in He flow some of the adsorbed 1-butene does not simply desorb but reacts with the sulfate ion to promote its decomposition.[689] Hence an IR band at 1350 cm^{-1} appears to be due to the following intermediate of the sulfate decomposition:

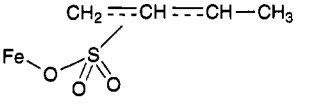

It appears then that if the olefin isomerization reaction is carried out at temperatures above 520 K there is the possibility that catalyst deactivates by chemical decomposition of sulfate groups.

The cis–trans isomerization of 2-butene has been used as a test reaction to evaluate the acidity of NiO–TiO_2 treated by different mineral acids,[691] based on the idea that the activity increases either with increasing acid strength and/or acid amount. In that case the high catalytic activities of modified catalysts were correlated with the increase of acid strength by the different inductive effects of the anions of the treating acids, which follow the order of acid strength and catalytic activity: SO_4^{2-} > PO_4^{3-} > BO_3^{3-} > SeO_4^{2-}.

If olefin isomerization is an uninteresting reaction to be catalyzed by sulfated superacid catalysts, the branching isomerization of short chain *n*-alkanes is of practical interest. Indeed, the reaction of isomerization of *n*-butane to isobutane, is carried out commercially on chlorinated aluminas. Due to thermodynamic reasons, it is of interest to carry out the reaction at temperatures as low as possible, and this would be achieved by using superacids as catalysts.

When *n*-butane is reacted in a liquid superacid, molecular H_2, methane, and ethane are observed as reaction products. Their formation is explained by the attack of a H^+ either to a C–H or a C–C bond to form a carbonium ion, in which the incorporated H^+ forms a two-electron three-center intermediate, and this intermediate liberates one hydrogen or an alkane molecule and leaves a carbenium ion. This carbenium ion may undergo skeletal rearrangement and yield alkane isomers:[692]

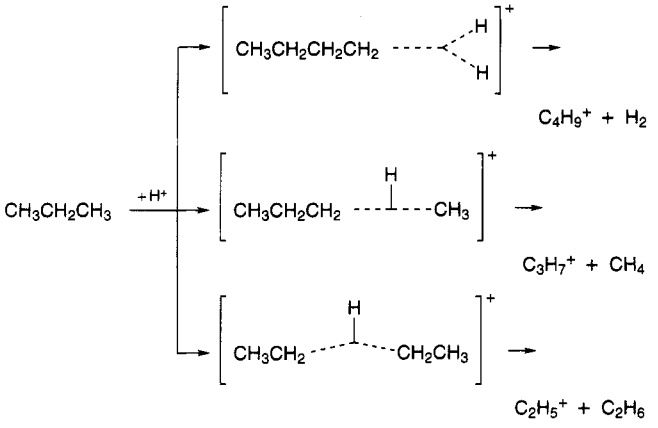

In the case of solid superacids of the sulfated oxide type, *n*-butane is selectively isomerized to isobutane at reaction temperatures up to 150 °C. On the basis of the idea that intermediate carbenium, but no carbonium ions, can lead to branching isomerization, it has been proposed that it is an abstraction of hydride ion by a Lewis acid site which initiates the reaction to form a butyl carbenium ion, followed by the methyl migration to yield a 2-methylpropyl carbenium ion, and finally isobutane is formed by the addition of hydride ion to a carbenium ion.[693] These conclusions were confirmed by deuterium tracer investigations.[693] However, as was seen for zeolites, isobutane can also be formed through an oligomerization-cracking mechanism which can also be carried out on Brönsted acid sites.

In the case of sulfated oxides, which can isomerize *n*-butane even at room temperature, both types of acid sites, i.e. Brönsted and Lewis acid sites, have been detected by pyridine adsorption. Even though there is still discussion on the type of active site involved in the isomerization of *n*-butane on these catalysts, it appears that the presence of both types of sites are necessary for the reaction to occur. In fact, it has been suggested that the superacidity may arise from the presence of Brönsted sites whose acidity is enhanced by the presence of strong neighboring Lewis acid sites.[633,636] These conclusions are supported by the correlation between acidity and catalytic activity, and the maximum rate for *n*-butane transformation is found to correspond to a Brönsted/Lewis ratio, measured from the intensity of pyridine IR bands, close to 1, hence to the monolayer of sulfur species. Moreover, it has been shown[652] that in the presence of excess of water (e.g. 0.6×10^3 Pa partial pressure) the activity of a SO_4^{2-}/ZrO_2 catalyst for *n*-butane isomerization dropped to zero. Furthermore, if no water was present in the reaction media, by drying the *n*-butane by passing through a molecular sieve column, the activity was also shown to decrease by 20% to 30%. If the normal feed, containing traces of water, was used again, the catalytic activity was recovered. On the other hand Pinna et al.[694] have claimed on the basis of selective and reversible CO adsorption results that strong Lewis acid sites from SO_4^{2-}/ZrO_2 intervene in the isomerization of *n*-butane since CO selectively poisons Lewis acid sites and in parallel the activity drops to zero. Activity is recovered upon desorption of CO.

After all these results, one is tempted to compare the behavior of SO_4^{2-}/ZrO_2 with that of $HF-SbF_5$ and $AlCl_3$. In the case of the $HF-SbF_5$ superacid system, this also involves both Brönsted and Lewis acid sites with their ratio equal to one. In the case of $AlCl_3$ which is very active for *n*-paraffin isomerization, it requires the presence of low amounts of moisture to proceed as catalyst. When small amounts of H_2O are present in the reaction media, some of the $AlCl_3$ molecules become hydrolyzed and the final catalytic system consists of HCl-$AlCl_3$, which again contains Brönsted–Lewis acid sites.

Finally, it is worth pointing out that at high hydrogen pressures an inhibition of the rate of isomerization occurs. This property is consistent with a mechanism involving Brönsted sites.[695]

Thus, it can be concluded that the variables in catalyst preparation which were shown above to control acidity of these systems are also going to control the catalytic activity for *n*-butane isomerization.[633,636]

One of the important variables which controls acidity in sulfated oxides catalyst preparation is the nature of the oxide. In this sense, SO_4^{2-}/ZrO_2 is more active than SO_4^{2-}/TiO_2 catalyst.[623] An increase in catalyst stability, surface acidity, and, therefore, catalytic activity for *n*-butane isomerization has been obtained by Hsu et al.[658-660] by using a sulfated oxide containing iron, manganese and zirconium. The sulfated zirconia promoted with iron and manganese is capable of isomerizing *n*-butane to isobutane at near room temperature with rates approximately 2–3 orders of magnitude greater than sulfated zirconia.[62,660]

Unfortunately, the isomerization activity of sulfated oxide catalysts decreased along the time on stream due to catalyst decay. It has been presented[696,697] that catalyst deactivation occurs not only by coke deposition but by reduction of the oxidation state of sulfur in the surface complex. High H_2 pressures can inhibit coke deposition and prolong the life of the catalyst.[698] This was much prolonged by preparing a bifunctional catalyst by supporting Pt on SO_4^{2-}/ZrO_2, and introducing H_2 in the reaction media.

Bifunctional Sulfated Oxide Catalysts. The isomerization of *n*-butane, as well as *n*-pentane and *n*-hexane which form the light straight run (LSR) gasoline, are important reactions in the refinery. Those isomerizations are commercially carried out on bifunctional catalysts containing chlorinated alumina as the acid component and Pt as the dehydrogenating–hydrogenating function. In the case of LSR Pt/zeolites, they are also used commercially owing to the higher stability presented by zeolitic catalysts to the presence of some water and sulfur in the feed. However, the lower acid strength of zeolites with respect to chlorinated alumina requires the use of ~100 °C higher reaction temperatures in the former with the corresponding decrease in branched products and therefore on the octane of the resulting product. Taking all this into account it could be expected that SO_4^{2-}/ZrO_2 catalyst containing Pt could act as an adequate isomerization catalyst for *n*-butane and LSR, since it can work at low temperatures and it is not poisoned by traces of water in the feed. Indeed, high conversions for isomerization of

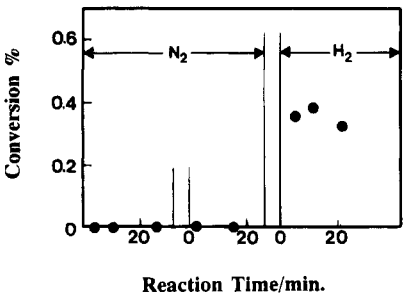

Figure 34. Effect of carrier gas on catalytic activity of Pt–SO_4^{2-}/ZrO_2 for skeletal isomerization of pentane.

C_5/C_6 have been reported using Pt–SO_4^{2-}/ZrO_2 catalysts.[699] The addition of Pt produces a strong increase in catalyst duration at 140 °C, 20 kg cm^{-2} total pressure and a molar ratio of H_2 to n-C_5 equal to 1–5. On these catalysts, Pt exists in the metallic state in reasonable large crystals and no detectable change in the valence state of Pt occurs during catalyst use.[700] H_2 also plays a role on keeping the activity since even in absence of Pt the catalyst deactivation is significantly reduced if the H_2 pressure is high enough.[698] However the role of H_2 may not be limited to avoid deactivation by hydrogenating hydrogen-deficient poison precursor,[699] and Ebitani et al.[701] have presented the possibility of H_2 intervening in protonic acid sites generation. These authors claim that protonic acid sites can also be originated from molecular hydrogen. To explain this they suggest that molecular hydrogen dissociates on the Pt to hydrogen atoms which undergo spillover on the SO_4^{2-}/ZrO_2 and convert to an H^+ and e^- or H^-, the H^+ acting as catalytic site for acid catalyzed reactions. In this case the Lewis acid sites would act as acceptors of an H^- or e^-, and as a result of that the Lewis acid site is weakened. This suggestion was made on the basis of the observation that when n-pentane isomerization was carried out in a N_2 stream no conversion was obtained, while a conversion was obtained when the gas switched to hydrogen (Figure 34).[701] An important fact observed by Ebitani et al. is that the bifunctional catalysis, if any, is very small on Pt-SO_4^{2-}/ZrO_2 catalysts, and therefore the role of Pt will not be to carry out the dehydrogenation–hydrogenation of paraffins as it occurs in a conventional bifunctional catalyst. If this is so, we can oversee another mechanism to explain the role of H_2 on these catalysts during alkane isomerization. Indeed, we have presented very recently[702] that on monofunctional acid catalysts, on the basis of zeolites, at lower reaction temperatures the controlling step can be the desorption of the carbocations. Then, under these circumstances, H_2 can act as a hydrogen transfer agent which facilitates the desorption of organic cation while regenerating the acid site. The H_2 being activated on the surface of the catalyst:

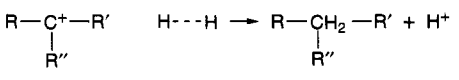

The final result was also an increase on the ratio of isomerization/cracking ratio.

When Pt was introduced on the catalyst, a much larger activation of the H_2 occurs on it, thus facilitating the above reaction. The kinetic results obtained

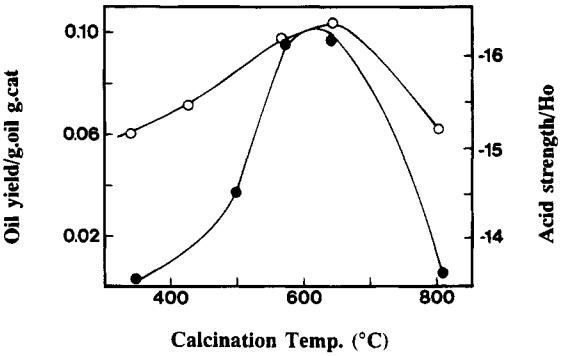

Figure 35. Changes in activity (●) and acid strength (○) of SO_4^{2-}/ZrO_2 as a function of calcination temperature, at 150 °C isobutane/butene ratio of 1.8.

by changing H_2 partial pressure, hydrocarbon partial pressure, and reaction temperature could be explained by such a mechanism.[702] If this was so on zeolites which have weaker acid sites (shorter average lifetime of carbocations) and good hydrogen transfer activity, one should expect it to occur even more so on the SO_4^{2-}/ZrO_2 type catalyst.

Our model would also be supported by the result obtained by Iglesia et al.[703,704] who have showed that the addition of small amounts of adamantane (which increases hydride transfer and carbenium ion termination rates) to n-heptane increases isomerization rates by a factor of 3 and inhibits undesirable cracking reactions. In their case, dihydrogen also acts as a hydride source in alkane isomerization catalysis but it requires the additional presence of metals which can catalyze H_2 dissociation.

In conclusion, it could be postulated that when Pt is introduced in SO_4^{2-}/ZrO_2 superacid catalysts and H_2 is used in the reaction, not only the life of catalyst is longer but also better activities and selectivities are achieved, by decreasing the average lifetime of the carbocations on the surface, due to the presence of activated H_2 which acts as a hydride transfer agent. For practical applications, the catalyst should retain activity for at least a one year period and should be regenerated afterward.

Reactions Involving Formation and Cracking of C–C Bonds. Owing to the strong acid sites present on sulfated oxides, they have been tested as possible alternatives of HF and H_2SO_4 for alkylation of paraffins and olefins. In this way they have been used to react methane and ethylene to produce C_3 to C_7 products[705] or, more importantly from a practical short-term point of view, to alkylate isobutane and butene to produce alkylation gasoline.[706–708] Calcination temperature plays an important role on acid properties and therefore on alkylation activity. It was found (Figure 35)[706] that a maximum in alkylation occurs at calcination temperatures of 650 °C for SO_4^{2-}/ZrO_2 and 550 °C for SO_4^{2-}/TiO_2.

However, it has been found[707,708] that on SO_4^{2-}/ZrO_2, together with alkylation of isobutane and butene, oligomerization of butene and cracking of alkylate products also occur on these catalysts. The recracking of alkylates can be decreased by decreasing the reaction temperature (Figure 36), and high activity and selectivity to the desired trimethylpentanes is obtained on sulfated zirconia catalyst, with

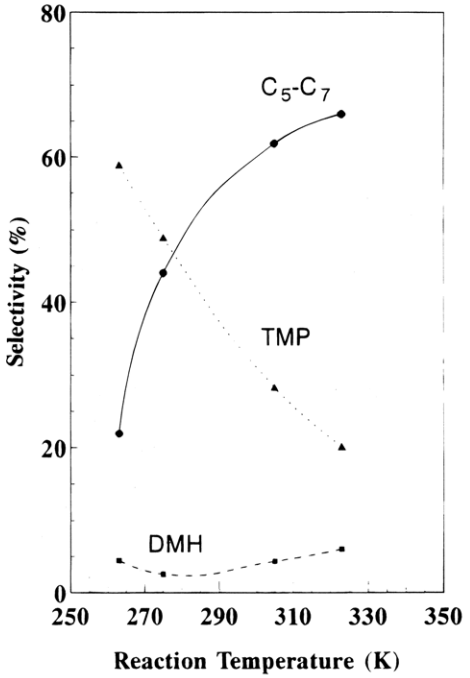

Figure 36. Effect of reaction temperature on cracking (C_5-C_7) dimerization (OMH) and alkylation (TMP) selectivities in the isobutane/2-butene alkylation on SO_4^{2-}/ZrO_2 superacid (1 min TOS).

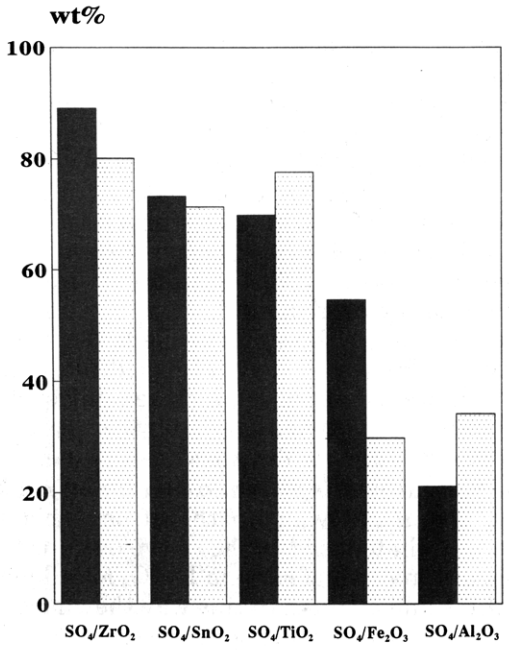

Figure 37. Initial (1 min TOS) 2-butene conversion (■) and TMP selectivity (□) in isobutane/2-butene alkylation on different sulfated metal oxides at 305 K reaction temperature.

results better than those obtained on zeolite catalysts. However, SO_4^{2-}/ZrO_2 has a major drawback as an alkylation catalyst, and this is rapid deactivation.[707] We have tried to change the product distribution and catalyst life by modifying reaction conditions, as well as the acid strength of the catalyst. The latter was done by changing the nature of the sulfated oxide. Results from Figure 37,[709] where the activity of sulfated zirconia, titania, SnO_2, Fe_2O_3, and Al_2O_3 was compared for alkylation of isobutane/butene, indicate that the order of activity is the same than the order of acidity: $ZrO_2 > SnO_2 \simeq TiO_2 > Fe_2O_3 > Al_2O_3$. No large differences in catalyst deactivation were observed.

In conclusion, superacid sulfated oxides are active and selective catalysts for performing alkylation of isobutane/butene at low temperatures. The behavior of SO_4^{2-}/ZrO_2 is not very different from that of H_2SO_4, with the indication that for this reaction the catalyst may be acting as "supported sulfuric acid".

If sulfated oxides are able to carry out C−C bond formation, they should also catalyze the reverse reaction, i.e. C−C bond rupture. In this sense and as has been found for any of the reactions described up to now, a correlation exits between calcination temperature (acidity) and cumene cracking. Again, two different maxima were found for SO_4^{2-}/ZrO_2 and SO_4^{2-}/TiO_2, being lower by ~100 °C the calcination temperature required for achieving the maximum on SO_4^{2-}/TiO_2.[710]

In the case of paraffin cracking, hexadecane has been used as a representative test molecule of the long-chain alkanes present in gasoil feeds. Practically all the reported studies[711,712] conclude that sulfated zirconia was much less active than a similar material containing Pt, and cracking increased with both reaction temperature and reaction time.

Two aspects on the behavior of Pt-SO_4^{2-}/ZrO_2 catalysts for hydrocracking of long chain *n*-alkanes are worth pointing out. The first one is that despite the presence of very strong acid sites it is possible to obtain up to 70% of the hydroisomerized products with two or more alkyl substituents, provided that a low enough reaction temperature is used. When the reaction temperature is increased above 100 °C, hydrocracked products strongly increase with a very high selectivity for isoparaffin products. It appears, therefore, that on the catalysts *n*-hexadecane is first isomerized into multibranched products which are then cracked more easily:

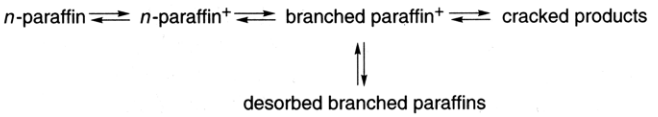

The second aspect to be noticed is that the cracked products are shifted on Pt−SO_4^{2-}/ZrO_2 toward long-chain products. The amount of long-chain cracked products ($\geq C_8$) obtained on SO_4^{2-}/ZrO_2 is much greater than on either amorphous silica−alumina or zeolites,[634] with the ratio of C_n/C_{16-n} ($n > 8$) much larger on the former. This supports the idea that together with cracking, addition and, specially, oligomerization reactions also occur:[634]

$$C_4H_9^+ + C_5H_{10} \rightarrow C_9H_{19}^+$$

$$2C_4H_9^+ \rightarrow C_8H_{17}^+ + H^+$$

In conclusion, it appears that it is worth investigating the possibilities of these catalysts for hydroisomerization and hydrocracking of long-chain paraffins and waxy products, in the sense that they allowed the reaction to be performed at lower temperatures with the benefits in formation of branched products. In the case of catalytic cracking we do not oversee practical possibilities due to their relatively

low thermal and hydrothermal stability which do not allow regeneration by coke burning in the presence of steam.

Other Reactions Requiring Superacids Sites Carried Out on Sulfated Oxides: Electrophilic Chlorination of Methane. Activation of methane is a subject of actual interest in many laboratories. Besides the extensive work carried out on the oxidative coupling of methane,[713-715] electrophilic conversions offer interesting possibilities.[716] Thus, under superacidic conditions, methane reacts with SbF_5/Cl_2 in SO_2ClF at −78 °C to give methyl chloride in high selectivity, but with low levels of conversion.[717] TaF_5/Nafion-H, SbF_5/graphite, and even zeolites have been used as catalyst for the chlorination of methane.[718,719] When the reaction was carried out on SO_4^{2-}/ZrO_2 catalysts, it was found[720] that the conversion increases with reaction temperature from 200 to 235 °C, while, in contrast to what occurs on zeolites, selectivity decreases. More specifically, at temperatures below 225 °C SO_4^{2-}/ZrO_2 gives selectivities ≥80% in methyl chloride. Above 225 °C chloroform is formed, but no Cl_4C is observed. Addition of Fe and Mn to sulfated zirconia improves methyl chloride selectivity but decreases conversion. However, it should be considered that in order to discuss selectivity effects the results should be compared at the same level of conversion. It has been proposed[720] that the mechanism of the reaction on SO_4^{2-}/ZrO_2 might be the same as that the proposed over oxyhalide or supported Lewis superacid catalysts:

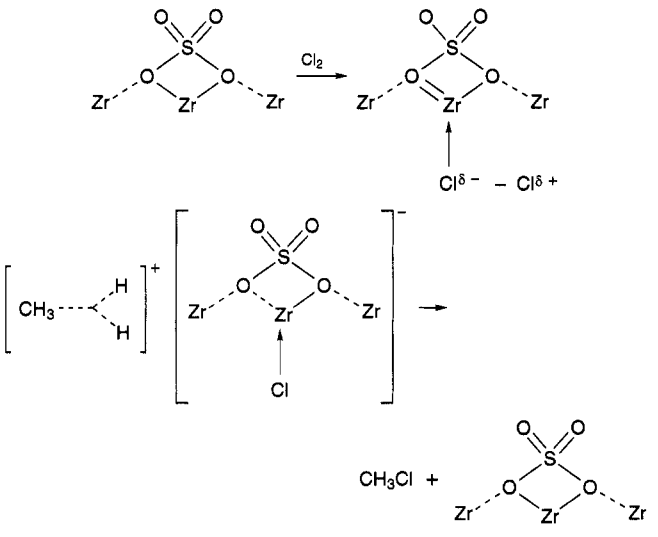

Cl_2 is polarized at the Lewis centers of the catalyst and chlorination of methane takes place under electrophilic conditions.

One important limitation of the sulfated oxide catalysts is that leaching of the metal by HCl occurs with the corresponding loss of catalyst with time on stream.

Hydrocarbon Reactions on Superacid Metal Oxides. It was presented above that zirconia–tungsten and zirconia–molybdena oxides, calcined at temperatures between 600 and 1000 °C, show strong acid sites. When used as catalysts, they are able to carry out the benzoylation of toluene with benzoic anhydride, isomerization of *n*-heptane, and oligomerization of 1-decene.[637] In these cases the maximum in activity was obtained for very high temperatures, close to 800 °C, but in all cases and as occurred before, their catalytic activity follows the trend of acidity. This type of oxide will offer new opportunities in catalysis, especially for reactions which require highly thermally stable catalysts.

IV. General Conclusions

It appears today that a large variety of solid acids within a large scale of acidities $+3.5 \geq H_0 \geq -16$ and with high surface areas can be prepared. This offers the possibility for selecting a catalyst with the adequate acid strength for almost any particular acid-catalyzed reaction. This situation has been made possible by the large amount of work performed by researchers from different areas. In this way NMR, IR, EPR, Raman, and XPS spectroscopists have characterized the nature and different types of acid sites, which have been modeled by a specialist in quantum chemistry. On the basis of those as well as on adsorption studies, researchers in Material Sciences have made possible the preparation of solid acids, based on inorganic oxides, within different range of acid strengths. On top of that and in collaboration with catalytic specialists, acidity has been coupled with adequate surface and pore size properties in order to optimize catalytic activity and selectivity in a large variety of reactions with organic compounds. In this sense, zeolites and zeotypes have represented a revolution in the field of acid catalysis, not only because of the rationalization on the nature of the acid sites achieved, but also because of the practical catalytic results achieved with these materials. Their use has completely changed the scheme in refining and petrochemistry and, now, is opening new possibilities in the field of fine chemicals. However, their practical use is still limited to reactions requiring acidities lower than $H_0 = -10$ (unless high reaction temperatures can be used). Owing to this, there is strong incentive to develop new solid acid catalysts based on inorganic solids, with very strong acid sites. In this sense, heteropoly acids and their acid salts offer new possibilities for carrying out more demanding reactions at lower temperatures. Their possibilities will be expanded in the near future if structures with controlled, stable micropores with sizes in the range of reactant molecules could be prepared. In this case there is no doubt that a combination of acidity, molecular sieve properties, and chirality can open new and exciting possibilities to these materials.

Finally, when stable stronger acidities are required, activated oxides and sulfated oxides can offer clear advantages. These materials, make available superacid sites on the surface of solid catalysts. However, their performance has to be improved in order to avoid undesired parallel reactions and catalyst deactivation. Efforts should be made to decrease the acid strength heterogeneity of these materials, which involve the presence of acid sites of weak, medium, strong, and very strong acid sites. Their possibilities as a real counterpart of unfriendly HF and H_2SO_4 acid catalysts would strongly be increased if they could be prepared with only very strong acid sites on the surface.

Acknowledgments. Financial support by the Dirección General de Investigación Científica y Técnica of Spain (Project MAT 94-0359-CO2-01) is gratefully acknowledged.

V. References

(1) 1. Hammett, L. P.; Deyrup, A. J. *J. Am. Chem. Soc.* **1932**, *54*, 2721.
(2) Tanabe, K.; Misono, M.; Ono, Y.; Hattori, H. *Stud. Surf. Sci. Catal.* **1989**, *51*, 6.
(3) Walling, C. *J. Am. Chem. Soc.* **1950**, *72*, 1164.
(4) Benesi, H. A. *J. Am. Chem. Soc.* **1956**, *78*, 5490.
(5) Tanabe, K. *Solid Acid and Bases, Their Catalytic Properties*; Academic Press: New York, 1970.
(6) Forni, L. *Catal. Rev.* **1973**, *8*, 65.
(7) Benesi, H. A.; Winquist, B. H. C. *Adv. Catal.* **1978**, *27*, 97.
(8) Tanabe, K. *Catalysis: Science and Technology*; Anderson, J. R., Boudart, M., Eds.; Spring-Verlag: Berlin, 1981; Vol. 2, Chapter 5.
(9) Arata, K.; Hino, M. *Mater. Chem. Phys.* **1991**, *26*, 213.
(10) Hino, M.; Arata, K. *J. Chem. Soc., Chem. Commun.* **1987**, 1259.
(11) Matsuhashi, H.; Hino, M.; Arata, K. *Appl. Catal.* **1990**, *59*, 205.
(12) Guo, C.; Liao, S.; Quian, Z.; Tanabe, K. *Appl. Catal. A* **1994**, *107*, 239.
(13) Guo, C.; Yao, S.; Cao, J.; Qian, Z. *Appl. Catal. A* **1994**, *107*, 229.
(14) Take, J.; Nomizo, Y.; Yoneda, Y. *Bull. Chem. Soc. Jpn.* **1973**, *46*, 3568.
(15) Balikova, M. *React. Kinet. Catal. Lett.* **1975**, *2*, 323.
(16) Hirschler, A. E. *J. Catal.* **1963**, *2*, 428.
(17) Forni, L. *Adv. Catal.* **1974**, *8*, 65.
(18) Leftin, H. P.; Hobson, M. C. *Adv. Catal.* **1963**, *14*, 115.
(19) Drushel, H. V.; Sommers, A. L. *Anal. Chem.* **1966**, *38*, 1723.
(20) Arnett, E. M. *Progr. Org. Chem.* **1963**, *1*, 223.
(21) Arnett, E. M.; Scorrano, G. *Adv. Phys. Org. Chem.* **1976**, *13*, 83.
(22) Farcasiu, D.; Marino, G.; Miller, G.; Kastrup, R. V. *J. Am. Chem. Soc.* **1989**, *111*, 7210.
(23) Chen, F. R.; Coudurier, G.; Joly, J. F.; Vedrine, J. C. *J. Catal.* **1993**, *143*, 616.
(24) Arnett, E. M.; Quirk, R. P.; Larsen, J. W. *J. Am. Chem. Soc.* **1970**, *92*, 3977.
(25) Arnett, E. M.; Haaksma, R. A.; Chwala, B.; Healy, M. H. *J. Am. Chem. Soc.* **1986**, *108*, 4888.
(26) Farcasiu, D.; Ghenciu, A. *J. Org. Chem.* **1991**, *56*, 6050.
(27) Farcasiu, D.; Ghenciu, A. *J. Am. Chem. Soc.* **1993**, *115*, 10901.
(28) Gold, V.; Mah, T. *J. Chem. Soc., Perkin Trans. 2* **1991**, 812.
(29) Borekova, E. G.; Topchieva, K. V.; Piguzova, L. I. *Kinet. Katal.* **1964**, *5*, 903.
(30) Turkevich, J.; Nozaki, F.; Stamires, D. *Proc. Int. Congr. Catal.* **1965**, *3*, 586.
(31) Romanovskii, V. B.; Thong, H. S.; Topchieva, K. V. *Kinet. Katal.* **1966**, *7*, 179.
(32) Murell, L. L.; Dispenziere, N. C., Jr. *J. Catal.* **1989**, *117*, 275.
(33) Brown, H. C.; Johanneson, R. B. *J. Am. Chem. Soc.* **1953**, *75*, 16.
(34) Knozinger, H.; Krietenbrink, H.; Ratnasamy, P. *J. Catal.* **1977**, *48*, 436.
(35) Murell, L. L.; Grenoble, D. C.; Baker, R. T. K.; Prestidge, E. B.; Fung, S. C.; Chianelli, R. R.; Cramer, S. P. *J. Catal.* **1983**, *79*, 23.
(36) Reitsma, H. J.; Boelhouwer, C. J. *J. Catal.* **1974**, *33*, 39.
(37) Unger, K. K.; Kittelman, U. R.; Kries, W. K. *J. Chem. Tech. Biotechnol.* **1981**, *31*, 435.
(38) Murell, L. L.; Dispenziere, N. C., Jr. *Catal. Lett.* **1989**, *2*, 329.
(39) Soled, S. L.; McVicker, G. B.; Murell, L. L.; Sherman, L. G.; Dispenziere, N. C., Jr.; Hsu, S. L.; Waldman, D. *J. Catal.* **1988**, *111*, 286.
(40) Vedrine, J. C.; Auroux, A.; Bolis, V.; Dejaifve, P.; Naccache, C.; Wierzchowski, P.; Derouane, E. G.; Nagy, J. B.; Gilson, J. P.; van Hooff, J. H. C.; van den Berger, J. P.; Wolthuizen, J. *J. Catal.* **1988**, *36*, 323.
(41) Auroux, A.; Yin, Y. S.; Vedrine, J. C. *Appl. Catal.* **1988**, *36*, 323.
(42) Kapustin, G. I.; Brueva, T. R.; Klyachko, A. L.; Beran, S.; Wichterlova, B. *Appl. Catal.* **1988**, *42*, 239.
(43) Thamm, H. *J. Phys. Chem.* **1987**, *91*, 8.
(44) Spiewak, B. E.; Handy, B. E.; Sharma, S. B.; Dumesic, J. A. *Catal. Lett.* **1994**, *23*, 207.
(45) Cardona-Martínez, N.; Dumesic, J. A. *J. Catal.* **1991**, *128*, 23; *Adv. Catal.* **1992**, *38*, 149.
(46) Parrillo, D. J.; Lee, C.; Gorte, R. J. *Appl. Catal. A* **1994**, *110*, 67.
(47) Parrillo, D. J.; Gorte, R. J. *Catal. Lett.* **1992**, *16*, 17.
(48) Yori, J. C.; Krasnogor, L. M.; Castro, A. A. *React. Kinet. Catal. Lett.* **1986**, *32*, 27.
(49) Karge, H. G.; Schweckendied, J. In *Proceedings of the 5th International Symposium on Heterogeneous Catalysis*, Varna Bulgaria, 1983; Shopov, D., *et al.*, Eds.; Publishing House of the Bulgarian Acad. Sci.: Sofia, 1983; p 429.
(50) Juskelis, M. V.; Slanga, J. P.; Roberie, T. G.; Peters, A. W. *J. Catal.* **1992**, *138*, 391.
(51) Kofke, T. J. G.; Gorte, R. J.; Farneth, W. E. *J. Catal.* **1988**, *114*, 34.
(52) Shimazu, K.; Hattori, H.; Tanabe, K. *J. Catal.* **1977**, *48*, 302.
(53) Koubek, J.; Volf, J.; Pasek, J. *J. Catal.* **1975**, *38*, 385.
(54) Takahashi, M.; Iwasawa, Y.; Ozasawara, S. *J. Catal.* **1976**, *45*, 15.
(55) Mieville, R. L.; Meyers, B. L. *J. Catal.* **1982**, *74*, 196.
(56) Ghosh, A. K.; Curthoys, G. *J. Phys. Chem.* **1984**, *88*, 1130.
(57) Tapp, N. J.; Milestone, N. B.; Bibby, D. M. *Stud. Surf. Sci. Catal.* **1988**, *37*, 393.
(58) Auroux, A. *Stud. Surf. Sci. Catal.* **1988**, *37*, 385.
(59) Lin, C. H.; Hsu, C. Y. *J. Chem. Soc., Chem. Commun.* **1992**, 1479.
(60) Farcasiu, D.; Fisk, S. L.; Melchior, M. T.; Rose, K. D. *J. Org. Chem.* **1982**, *47*, 453.
(61) Choudhary, V. R.; Srinivasan, K. R.; Sigh, A. P. *Zeolites* **1990**, *10*, 16.
(62) Jatia, A.; Chang, C.; MacLeod, J. D.; Okubo, T.; Davis, M. E. *Catal. Lett.* **1994**, *25*, 21.
(63) Dondur, V.; Karge, H. G. *Surf. Sci.* **1987**, *189*, 873. Karge, H. G.; Dondur, V. *J. Phys. Chem.* **1990**, *94*, 765.
(64) Karge, H. G. *Catalysis and Adsorption by Zeolites*; Öhlmann, G., *et al.*, Eds.; Elsevier Science Publishers B. V.: Amsterdam, 1991; p 133.
(65) Sharma, S. B.; Meyers, B. L.; Chen, D. T.; Miller, J.; Dumesic, J. A. *Appl. Catal. A* **1993**, *102*, 253.
(66) Delgass, W. N.; Haller, G. L.; Kellerman, R.; Lunsford, J. H. *Spectroscopy in Heterogeneous Catalysis*; Academic Press: New York, 1979.
(67) Haller, G. T. *Catal. Rev.-Sci. Eng.* **1981**, 477.
(68) Ward, J. W. *J. Catal.* **1970**, *17*, 355; *18*, 248.
(69) Anderson, M. W.; Klinowski, J. *Zeolites* **1986**, *6*, 455.
(70) Lohse, U.; Löffler, E.; Hunger, M.; Stöckner, J.; Patzelova, V. *Zeolites* **1987**, *7*, 11.
(71) Klinowski, J.; Hamdan, H.; Corma, A.; Fornés, V.; Hunger, M.; Freud, D. *Catal. Lett.* **1989**, *3*, 263.
(72) Dombrowski, D.; Hoffman, J.; Fruwert, J.; Stock, T. *J. Chem. Soc., Faraday Trans. 1* **1985**, *81*, 2257.
(73) Dwyer, J.; Karim, K.; Kayali, W.; Milward, D.; O'Malley, P. J. *J. Chem. Soc., Chem. Commun.* **1988**, 594.
(74) Parry, E. P. *J. Catal.* **1963**, *2*, 371.
(75) Basila, M. R.; Kantner, T. R.; Rhee, K. H. *J. Phys. Chem.* **1964**, *68*, 3197.
(76) Hughes, T. R.; White, H. M. *J. Phys. Chem.* **1967**, *71*, 2192.
(77) Datka, J.; Turek, A. M.; Jehng, J. M.; Wachs, I. E. *J. Catal.* **1992**, *135*, 186.
(78) Emeis, C. A. *J. Catal.* **1993**, *141*, 347.
(79) Chiche, B. H.; Fajula, F.; Garrone, E. *J. Catal.* **1994**, *146*, 460.
(80) Ferwerda, R.; Van der Maas, J. H. *Proc. 13 th Int. Conf. on Raman Spectroscopy*; Kiefer, W., *et al.*, Eds.; John Wiley & Sons: New York, 1992.
(81) Hardin, A. H.; Klemes, M.; Morrow, B. A. *J. Catal.* **1980**, *62*, 316.
(82) Corma, A.; Fornés, V.; Rey, F. *Zeolites* **1993**, *13*, 56.
(83) Knözinger, H.; Kriltenbrink, H.; Ratnasamy, P. *J. Catal.* **1977**, *48*, 436.
(84) Corma, A.; Rodellas, C.; Fornés, V. *J. Catal.* **1984**, *88*, 374.
(85) Lercher, J. A.; Noller, H.; Ritter, G. *J. Chem. Soc., Faraday Trans. 1* **1981**, *77*, 621.
(86) Jacobs, P. A. *Catal. Rev.-Sci. Eng.* **1982**, *24*, 415.
(87) Busca, G.; Lorenzelli, V. *Mater. Chem.* **1982**, *7*, 89.
(88) Kazansky, V. B.; Yu Borovkov, V.; Kustov, L. M. *Proc. 8th Int. Congr. Catal.*; Verlag Chemie: Weinheim, 1984; Vol. 3, p 3.
(89) Ghiotti, G.; Garrone, E.; Morterra, C.; Boccuzzi, F. *J. Phys. Chem.* **1979**, *83*, 2863.
(90) Beebe, T. P.; Gelin, P.; Yates, J. T. *Surf. Sci.* **1984**, *148*, 526.
(91) Paukshtis, E. A.; Soltanov, R. I.; Yurchenko, E. N. *React. Kinet. Catal. Lett.* **1982**, *19*, 105.
(92) Izaki, M. I.; Knözinger, H. *Mater. Chem. Phys.* **1987**, *17*, 201.
(93) Morterra, C.; Cerrato, G.; Emanuel, C.; Bolis, V. *J. Catal.* **1993**, *142*, 349.
(94) Maache, M.; Janin, A.; Lavalley, J. C.; Joly, J. F.; Benazzi, E. *Zeolites* **1993**, *13*, 419.
(95) Paukshtis, E. A.; Yurchenko, E. N. *React. Kinet. Catal. Lett.* **1982**, *19*, 105.
(96) de la Betta, G.; Fubini, B.; Ghiotti, G.; Morterra, C. *J. Catal.* **1976**, *43*, 90.
(97) Tsyganenko, A. A.; Denisenko, L. A.; Zwerev, S. M.; Filiminov, V. N. *J. Catal.* **1985**, *94*, 10.
(98) Zecchina, A.; Escalona, E.; Otero, C. *J. Catal.* **1987**, *107*, 244.
(99) Izaki, M. I.; Knözinger, H. *Spectrochim. Acta* **1987**, *43A*, 1455.
(100) Soltanov, R. I.; Paukshtis, E. A.; Yurchenko, E. N. *Kinet. Catal.* **1982**, *23*, 135.
(101) Paukshtis, E. A.; Soltanov, P. I.; Yurchenko, E. N.; Jirátová, K. *Collect. Czech. Chem. Commun.* **1982**, *47*, 2044.
(102) Izaki, M. I.; Vielhaber, B.; Knözinger, H. *J. Phys. Chem.* **1986**, *90*, 3176.

(103) Morterra, C.; Garrone, E.; Bolis, V.; Fubini, B. *Spectrochim. Acta* **1987**, *43A*, 1577.
(104) Scarano, D.; Zecchina, A. *Spectrochim. Acta* **1987**, *43A*, 1441.
(105) Scarano, D.; Zecchina, A.; Reller, A. *Surf. Sci.* **1988**, *198*, 11.
(106) Shanon, R. D. *Acta Crystallogr.* **1976**, *A32*, 751.
(107) Dzwigaj, S.; Briend, M.; Shikholeslami, A.; Peltre, M. J.; Barthomeuf, D. *Zeolites* **1990**, *10*, 157.
(108) Barthomeuf, D. In *Zeolite Microporous Solids: Synthesis, Structure and Reactivity*; Derouane, E. G., *et al.*, Eds.; Kluwer Academic Publishers: Netherlands, 1992; p 193.
(109) Su, B. L.; Barthomeuf, D. *Zeolites* **1993**, *13*, 626; *J. Catal.* **1993**, *139*, 81.
(110) Janin, A.; Lavalley, J. C.; Macedo, A.; Raatz, F. *ACS Symp. Ser.* **1988**, *368*, 117.
(111) Claydon, M. F.; Sheppard, N. *J. Chem. Soc., Chem. Commun.* **1969**, 1431.
(112) Pelmenschikov, A. G.; Vansanten, R. A.; Janchen, J.; Meifer, E. *J. Phys. Chem.* **1993**, *97*, 11071.
(113) Jolly, F. Ph.D. Thesis, Université de Caen, 1994.
(114) Knozinger, H.; KrietenBrink, M. *J. Chem. Soc., Faraday Trans. 1* **1975**, *71*, 2421.
(115) Soltanov, R. I.; Paukshtis, E. A.; Yurchenko, E. N. *React. Kinet. Catal. Lett.* **1987**, *34*, 421.
(116) Angell, C. L.; Howell, M. W. *J. Phys. Chem.* **1969**, *73*, 2551.
(117) Thomas, J. M.; Klinowski, J. *Adv. Catal.* **1985**, *33*, 256.
(118) Mastikhin, V. M.; Mudrakovsky, I. L.; Nosov, A. V. *Prog. NMR Spectrosc.* **1991**, *23*, 259.
(119) Brunner, E.; Ernst, H.; Freude, D.; Frohlich, T.; Hunger, M.; Pfeifer, H. *J. Catal.* **1991**, *127*, 34.
(120) Haw, J. F.; Richardson, B. R.; Oshiro, I. S.; Lazo, N. D.; Speed, J. D. *J. Am. Chem. Soc.* **1989**, *111*, 2052.
(121) Freude, D.; Oehme, W.; Schniedel, H.; Staudte, B. *J. Catal.* **1977**, *49*, 123.
(122) Freude, D.; Pfeifer, H.; Ploss, W.; Staudte, B. *J. Mol. Catal.* **1981**, *12*, 1.
(123) Freude, D. *Adv. Colloid Interface Sci.* **1985**, *23*, 21.
(124) Pfeifer, H.; Freude, D.; Hunger, M. *Zeolites* **1985**, *5*, 274.
(125) Pfeifer, H.; Freude, D.; Kärger, J. *Z. Phys. Chem. Leipzig* **1988**, *269*, 320.
(126) Pfeifer, H. *J. Chem. Soc., Faraday Trans. 1* **1988**, *84*, 3777.
(127) Hunger, M.; Freude, D.; Pfeifer, H. *Catal. Today* **1988**, *3*, 507.
(128) Ernst, H. *Z. Phys. Chem. Leipzig* **1988**, *269*, 1073.
(129) Datka, J.; Geerlings, P.; Mortier, W.; Jacobs, P. *J. Phys. Chem.* **1985**, *89*, 3488.
(130) Sauer, J. *J. Phys. Chem.* **1987**, *91*, 2315.
(131) Yoshida, S.; Kawakami, H. *Proc. Int. Symp. Acid-Base Catal.*, Sapporo; Tanabe, K., *et al.*, Eds.; Kodansha: Tokyo, 1988; p 123.
(132) Freude, F.; Brunner, E.; Pfeifer, H.; Prager, D.; Jerschkewitz, H. G.; Lohse, U.; Oehlman, G. *Chem. Phys. Lett.* **1987**, *139*, 225.
(133) Freude, D.; Klinowski, J.; Amdan, H. *Chem. Phys. Lett.* **1988**, *149*, 355.
(134) Hunger, M.; Freude, D.; Pfeifer, H.; Bremer, H.; Jank, M.; Wendlandt, K. P. *Chem. Phys. Lett.* **1983**, *100*, 29.
(135) Ernst, H.; Freude, D.; Wolf, I. *Chem. Phys. Lett.* **1993**, *212*, 588.
(136) Batamack, P.; Doremieux-Morin, C.; Vincent, R.; Fraissard, J. *J. Phys. Chem.* **1993**, *97*, 9779.
(137) Haw, J. F.; Chuang, I. S.; Hawkins, B. L.; Maciel, G. E. *J. Am. Chem. Soc.* **1983**, *105*, 7206.
(138) Michel, D.; Germanus, A.; Pfeifer, H. *J. Chem. Soc., Faraday Trans. 1* **1982**, *78*, 237.
(139) Maciel, G. E.; Haw, J. F.; Chuang, I. S.; Hawkins, B. L.; Early, T. E.; McKay, D. R.; Petrakis, L. *J. Am. Chem. Soc.* **1983**, *105*, 5529.
(140) Ripmeester, J. A. *J. Am. Chem. Soc.* **1983**, *105*, 2925.
(141) Bosacek, V.; Freude, D.; Gründer, W.; Meiler, W.; Pfeifer, H. *Z. Phys. Chem. Leipzig* **1984**, *265*, 241.
(142) Freude, D.; Pfeifer, H.; Schmidt, A.; Standte, B. *Z. Phys. Chem. Leipzig* **1984**, *265*, 250.
(143) Mastikhin, V. M.; Mudrakowsky, I. L.; Filimonova, S. V. *Chem. Phys. Lett.* **1988**, *149*, 175.
(144) Farcasiu, D.; Ghenciu, A.; Miller, G. *J. Catal.* **1992**, *134*, 118.
(145) Biaglow, A. I.; Gorte, R. J.; Kokotailo, G. T.; White, D. *J. Catal.* **1994**, *148*, 779.
(146) Mastikhin, V. M.; Mudrakovsky, I. L.; Nosov, A. V.; Mashkina, A. V. *J. Chem. Soc., Faraday Trans.* **1989**, *85*, 2819.
(147) Rothwell, W. P.; Shen, W.; Lunsford, J. H. *J. Am. Chem. Soc.* **1984**, *106*, 2452.
(148) Lunsford, J. H.; Rothwell, W. P.; Shen, W. *J. Am. Chem. Soc.* **1985**, *107*, 1540.
(149) Baltusis, L.; Frye, J. S.; Maciel, G. E. *J. Am. Chem. Soc.* **1986**, *108*, 7119.
(150) Defosse, C.; Canesson, P. *J. Chem. Soc., Faraday Trans. 1* **1976**, *72*, 2565.
(151) Lahtinen, J.; Vehanen, A. *Catal. Lett.* **1991**, *8*, 67.
(152) Schrader, D. M.; Jean, Y. C. *Positron and Positronium Chemistry*; Elsevier: Amsterdam, 1988.
(153) Huang, W. F.; Huang, D. C.; Tseng, P. K. *Catal. Lett.* **1994**, 26, 269.
(154) Houdry, E.; Joseph, A. *Bull. Assoc. Fr. Tech. Pet.* **1956**, *117*, 177.
(155) Courty, P.; Marcilly, Ch. *Preparation of Catalysts III*; Amsterdam: Elsevier, 1983; p 485.
(156) Tanabe, K.; Sumiyoshi, T.; Shibata, K.; Kiyoura, T.; Kitagawa, J. *Bull. Chem. Soc. Jpn.* **1974**, *47*, 1064.
(157) Thomas, C. L. *Ind. Eng. Chem.* **1949**, *41*, 2564.
(158) Tamele, K. *Disc. Faraday Soc.* **1950**, *8*, 270.
(159) Grabowski, W.; Misono, M.; Yoneda, Y. *J. Catal.* **1980**, *61*, 103.
(160) Hawakami, H.; Yoshida, S.; Yonezawa, T. *J. Chem. Soc. Faraday Trans.* **1984**, *280*, 205.
(161) Zhidomirov, G. M.; Kazansky, V. B. *Adv. Catal.* **1986**, *34*, 131.
(162) Fripiat, J. J. *Natl. Conf. Clays Clay Minerals* **1963**, *12*, 327.
(163) de Kimpl, C.; Gastuche, M. C.; Brindley, G. W. *Am. Mineral* **1961**, *46*, 1370.
(164) Plank, C. J.; Drake, L. C. *J. Colloid Sci.* **1947**, *2*, 399.
(165) Manton, M. R. S.; Davidtz, J. C. *J. Catal.* **1979**, *60*, 156.
(166) Corma, A.; Fornés, V.; Pérez-Pariente, J.; Rey, F.; Rawlence D. *Appl. Catal.* **1990**, *63*, 145.
(167) Bellusi, G.; Perego, C.; Carati, A.; Peratello, S.; Previde Massara, E.; Perego, G. *Stud. Surf. Sci. Catal.* **1994**, *85*, 84A.
(168) Yanagisawa, T.; Shimizu, T.; Kuroda, K.; Kato, C. *Bull. Chem. Soc. Jpn.* **1990**, *63*, 988; *J. Chem. Soc., Chem. Commun.* **1993**, 680.
(169) Beck, J. S.; Chu, C. T. W.; Johnson, I. D.; Kresge, C. T.; Leonowicz, M. E.; Roth, W. J.; Vartuli, J. C. WO 91/11390, 1991.
(170) Beck, J. S.; Vartuli, J. C.; Roth, W. J.; Leonowicz, M. E.; Kresge, C. T.; Schmitt, K. D.; Chu, C. T. W.; Olson, D. H.; Sheppard, E. W.; McCullen, S. B.; Higgins, J. B.; Schlenker, J. L. *J. Am. Chem. Soc.* **1992**, *114*, 10834.
(171) Beck, J. S.; Calabro, D. C.; McCullen, S. B.; Pelrine, B. P.; Schmitt, K. D.; Vartuli, J. C. U.S. Patent 5145816, 1992.
(172) Kolodziejski, W.; Corma, A.; Navarro, M. T.; Pérez-Pariente, J. *Solid State NMR* **1993**, *2*, 253.
(173) Corma, A.; Fornés, V.; Navarro, M. T.; Pérez-Pariente, J. *J. Catal.* **1994**, *148*, 569.
(174) Tanabe, K.; Misono, M.; Ono, Y.; Hattori, M. *Stud. Surf. Sci. Catal.* **1989**, *51*.
(175) Beck, J. S.; Calabro, D. C.; McCullen, S. B.; Pelrine, B. P.; Schmitt, K. D.; Vartuli, J. C. U.S. Patent 5200058, 1993.
(176) Le, Q. N.; Thomson, R. T. U.S. Patent 5191144, 1993.
(177) Le, Q. N.; Thomson, R. T. U.S. Patent 5232580, 1993.
(178) Peri, J. B. *Disc. Faraday Soc.* **1971**, *52*, 55.
(179) Campelo, J. M.; Marinas, J. M.; Mendioroz, S.; Pajares, J. A. *J. Catal.* **1986**, *101*, 484.
(180) Tada, A.; Yoshida, M.; Hirai, M. *Nippon Kagaku Kaishi* **1973**, 1739.
(181) Flanigen, E. M. *Stud. Surf. Sci. Catal.* **1991**, *58*, 1.
(182) Wilson, S. T.; Lok, B. M.; Mesina, C. A.; Cannan, T. R.; Flanigen, E. M. *J. Am. Chem. Soc.* **1982**, *104*, 1146.
(183) Lok, B. M.; Messina, C. A.; Patton, R. L.; Gajek, R. T.; Cannan, T. R.; Flanigen, E. M. *J. Am. Chem. Soc.* **1984**, *106*, 6092.
(184) Flanigen, E. M.; Lok, B. M.; Patton, R. L.; Wilson, S. T. In *New Developments in Zeolite Science and Technology*, Proc. 7th. Int. Zeolite Conf.; Murakami, Y., Lijima, A., Ward, J. W., Eds.; Kodanska Elsevier: Tokyo, 1986; p 103.
(185) Davis, M. E.; Montes, C.; Hathaway, P. E.; Garces, J. M. *Stud. Surf. Sci. Catal.* **1989**, *49*, 199.
(186) Huo, Q.; Xu, R.; Li, S.; Ma, Z.; Thomas, J. M.; Jones, R. H.; Chippendale, A. M. *J. Chem. Soc., Chem. Commun.* **1992**, 875.
(187) Estermann, M.; McCusker, L. B.; Baerlocher, C.; Merrouche, A.; Kessler, H. *Nature 352*, **1991**, 320.
(188) Weisz, P. B. *Chemtech* **1973**, *3*, 498.
(189) Post, M. F. M. *Stud. Surf. Sci. Catal.* **1991**, *58*, 391.
(190) Chen, N. Y.; Haag, W. O. In *Hydrogen Effects in Catalysis*; Paal, Z., Menon, P. G., Eds.; Marcel Dekker: New York, 1988; p 695.
(191) Weisz, P. B. *Chemtech* **1982**, *12*, 424.
(192) Weisz, P. B. *Pure Appl. Chem.* **1980**, *52*, 2091.
(193) Haag, W. O.; Chen, N. Y. In *Catalyst Design Progress and Perspectives*; Hegedus, L. L., Ed.; John Wiley & Sons: New York, 1987; Chapter 6.
(194) Gorring, R. L. *J. Catal.* **1973**, *31*, 13.
(195) Theodorou, D. N.; Wei, J. *J. Catal.* **1983**, *83*, 205.
(196) Nelson, P. H.; Kaiser, A. B.; Bibby, D. M. *J. Catal.* **1991**, *127*, 101.
(197) Moore, R. M.; Katzer, J. R. *AICHE J.* **1972**, *18*, 816.
(198) Satterfield, C. N.; Katzer, J. R.; Vieth, W. R. *Ind. Eng. Chem. Fundam.* **1971**, *10*, 478.
(199) Karger, J.; Pfeifer, H. *Int. Zeolite Conf.* **1992**, *9*, B.22.
(200) Derouane, E. G.; Gabelica, Z. *J. Catal.* **1980**, *65*, 486.
(201) Weisz, P. B.; Frilette, V. J. *J. Phys. Chem.* **1960**, *64*, 382.
(202) Barrer, R. M. *J. Colloid Sci.* **1966**, *21*, 416.
(203) Dessau, R. M. *ACS Symp. Ser.* **1980**, *135*, Chapter 6.
(204) Narita, E.; Horiguchi, N.; Okabe, T. *Chem. Lett.* **1985**, 787.
(205) Fajula, F.; Bourgeat-Lami, E.; Des Courières, T.; Anglerot, D. Eur. Patent 0 488 867 A1, 1992.
(206) Corma, A.; Llopis, F.; Monton, J. B. *Proc. Int. Congr. Catal.* (Guczi, L., Solymosi, F., Tetenyi, P., Eds.) **1993**, *10*, 1145.
(207) Venuto, P. B.; Hamilton, L. A.; Landis, P. S.; Wise, J. J. *J. Catal.* **1966**, *5*, 81.
(208) Venuto, P. B.; Wu, E. L. *J. Catal.* **1969**, *15*, 205.
(209) Venuto, P. B.; Landis, P. S. *J. Catal.* **1966**, *6*, 237.

(210) Parton, R. F.; Jacobs, J. M.; van Ooteghem, H.; Jacobs, P. A. *Stud. Surf. Sci. Catal.* **1988**, *46*, 211. Parton, R. F.; Jacobs, J. M.; Huybrechts, D. R.; Jacobs, P. A. *Stud. Surf. Sci. Catal.* **1988**, *46*, 163.
(211) Corma, A.; García, H.; Iborra, S.; Primo, J. *J. Catal.* **1989**, *78*, 120.
(212) Corma, A.; Faraldos, M.; Mifsud, A. *Appl. Catal.* **1989**, *47*, 125.
(213) Corma, A.; Faraldos, M.; Martínez, M.; Mifsud, A. *J. Catal.* **1990**, *122*, 230.
(214) Uytterhoeven, J. B.; Christner, L. G.; Hall, W. K. *J. Phys. Chem.* **1965**, *69*, 2117.
(215) Hansford, R. S. *Ind. Eng. Chem.* **1947**, *39*, 849.
(216) Peri, J. B. *J. Catal.* **1976**, *41*, 227.
(217) Mikheikin, I. D.; Lumpov, A. I.; Zhidomirov, G. M.; Kazansky, V. B. *Kinet. Katal.* **1978**, *19*, 1053.
(218) Mikheikin, I. D.; Senchenya, I. N.; Lumpov, A. I.; Zhidomirov, G. M.; Kazansky, V. B. *Kinet. Katal.* **1979**, *20*, 496.
(219) Mortier, W. J.; Sauer, J.; Lercher, J. A.; Noller, H. *J. Phys. Chem.* **1984**, *88*, 905.
(220) Mortier, W. J. *Proc. Zeolite Conf.* **1984**, *6*, 734.
(221) Gutmann, V. *The Donor Acceptor Approach to May molecular Interactions*; Plenum Press: New York, 1978.
(222) Rabo, J. A.; Gajda, G. *J. Catal. Rev. Sci. Eng.* **1990**, *31*, 385.
(223) Rabo, J. A. *Prepr. Int. Congr. Catal.* **1993**, *10*, 1 (Guczi, L., Solymosi, F., Tetenyi, P., Eds.).
(224) van Santen, R. A.; de Man, A. J. M.; Jacobs, W. P. J. H.; Teunissen, E. H.; Kramer, G. J. *Catal. Lett.* **1991**, *9*, 273.
(225) Corma, A.; Fornés, V.; Pérez-Pariente, J. *J. Chem. Soc., Chem. Commun.* **1993**, *8*, 676.
(226) Doremieux-Morin, C.; Batamack, P.; Martin, C.; Bregeault, J. M.; Fraissard, J. *Catal. Lett.* **1991**, *9*, 403.
(227) Czjzek, M.; Jobic, H.; Fitch, A. N.; Vogt, T. *J. Phys. Chem.* **1992**, *96*, 1535.
(228) Freude, D.; Klinowski, J. *J. Chem. Soc., Chem. Commun.* **1988**, 1411.
(229) Sauer, J.; Kölmel, C. M.; Hill, J. R.; Ahlrichs, R. *Chem. Phys. Lett.* **1989**, *164*, 193.
(230) Kazansky, V. B. *Stud. Surf. Sci. Catal.* **1994**, *85*, 251.
(231) van Santen, R. A. *Stud. Surf. Sci. Catal.* **1994**, *85*, 273.
(232) Scherzer, J.; Bass, J. L.; Hunter, F. D. *J. Phys. Chem.* **1975**, *79*, 1194.
(233) Keir, D.; Lee, E. F. P.; Rees, L. V. C. *Zeolites* **1988**, *8*, 3.
(234) Karge, H. G. In *Zeolite Microporous Solids: Synthesis, Structure and Reactivity*; Derouane, E. G., Lemos, F., Naccache, C., Ribeiro, F. R., Eds.; NATO ASI Ser. 352; Plenum: New York, 1991; p 273.
(235) Liang, S. M. C.; Cay, I. D. *J. Catal.* **1980**, *66*, 294.
(236) Rabo, J. A.; Pickert, P. E.; Stamires, D. N.; Boyle, J. E. *Proc. Int. Cong. Catal.* **1960**, *2*, 2055.
(237) Kerr, G. T. *J. Catal.* **1982**, *77*, 307.
(238) Ward, J. W.; Hansford, R. C. *J. Catal.* **1964**, *13*, 364.
(239) Flanigen, E. M. *Stud. Surf. Sci. Catal.* **1991**, *58*, 13.
(240) Freude, D.; Hunger, M.; Pfeifer, H.; Schwieger, W. *Chem. Phys. Lett.* **1986**, *128*, 62.
(241) Barthomeuf, D.; Beaumont, R. *J. Catal.* **1973**, *30*, 288.
(242) Kramer, G. J.; van Santen, R. A. *J. Am. Chem. Soc.* **1993**, *115*, 2887.
(243) Pine, L. A.; Maher, P. J.; Wachter, W. A. *J. Catal.* **1984**, *85*, 466.
(244) Mikousky, R. J.; Marshall, J. F. *J. Catal.* **1976**, *44*, 170.
(245) Beagley, B.; Dwyer, J.; Fitch, F. R.; Mann, R.; Walters, J. *J. Phys. Chem.* **1984**, *88*, 1744.
(246) Peters, A. W. *Book of Abstracts*, 183rd ACS National Meeting, Las Vegas, NV, Spring 1982; American Chemical Society: Washington, DC, 1982; p 482.
(247) Mortier, W. J. *J. Catal.* **1978**, *55*, 138.
(248) Jacobs, P. A. *Catal. Rev. Sci. Eng.* **1982**, *24*, 415.
(249) Mortier, W. J. *Stud. Surf. Sci. Catal.* **1986**, *28*, 423.
(250) Mortier, W. J. *Stud. Surf. Sci. Catal.* **1988**, *37*, 253.
(251) van Genechten, K. A.; Mortier, W. J. *Zeolites* **1988**, *8*, 273.
(252) Chu, C. T. W.; Chang, C. D. *J. Phys. Chem.* **1985**, *89*, 1569.
(253) Dompas, D. H.; Mortier, W. J.; Kenter, O. C. H.; Janssen, M. J. G.; Verduijn, J. P. *J. Catal.* **1991**, *129*, 19.
(254) Corma, A.; Fornés, V.; Herrero, E.; Martínez, A.; Prieto, J. *Prepr. Am. Chem. Soc. Div. Petrol. Chem.* **1987**, *32*, 369.
(255) Mirodatos, C.; Barthomeuf, D. *J. Chem. Soc., Chem. Commun.* **1981**, 39.
(256) Corma, A.; Fornés, V.; Martínez, A.; Melo, F.; Pallota, O. *Stud. Surf. Sci. Catal.* **1988**, *37*, 495.
(257) Garralón, G.; Corma, A.; Fornés, V. *Zeolites* **1988**, *9*, 84.
(258) Haag, W. O.; Lago, R. M. Eur. Patent 34444, 1981.
(259) Sendoda, Y.; Ono, Y. *Zeolites* **1988**, *8*, 101.
(260) Corma, A.; Fornés, V.; Martínez, A.; Orchillés, A. V. *ACS Symp. Ser.* **1988**, *368*, 542.
(261) Corma, A. *Stud. Surf. Sci.* **1989**, *49*, 49.
(262) Corma, A.; Fornés, V.; Rey, F. *Appl. Catal.* **1990**, *59*, 267.
(263) Corma, A.; Frontela, J.; Lázaro, J.; Pérez, M. *Prepr.—Am. Chem. Soc., Div. Pet. Chem.* **1991**, *36*, 833.
(264) Peters, A. *Catal. Lett.*, in press.
(265) Szostak, R. *Stud. Surf. Sci. Catal.* **1991**, *58*, 153.
(266) Gilson, J. P.; Edwards, G. C.; Peters, A. W.; Rajagopalan, K.; Wormsbecher, R. F.; Roberie, T. G.; Shatlock, M. P. *J. Chem. Soc., Chem. Commun.* **1987**, 91.
(267) Sanz, J.; Fornés, V.; Corma, A. *J. Chem. Soc., Faraday Trans. 1* **1988**, *84*, 3113.
(268) Janin, A.; Maache, M.; Lavalley, J. C.; Joly, J. F.; Raatz, F.; Szydlowsky, N. *Zeolites* **1991**, *11*, 391.
(269) Kerr, G. T. *J. Phys. Chem.* **1968**, *72*, 2594.
(270) Skeels, G. W.; Breck, D. W. *Proc. Int. Zeol. Conf.* (Olson, D., Bisio, A., Eds.) **1984**, *6*, 87.
(271) Garralón, G.; Fornés, V.; Corma, A. *Zeolites* **1988**, *8*, 268.
(272) Beyer, H. K.; Belenkaya, I. In *Catalysis by Zeolites*; Imelik, I., *et al.*, Eds.; Elsevier: Amsterdam, 1980; p 203.
(273) Datka, J.; Boczen, M.; Rymarowicz, P. *J. Catal.* **1988**, *114*, 368.
(274) Sauer, J. *Chem. Rev.* **1989**, *89*, 199.
(275) Sauer, J.; Kölmel, C. M.; Hill, J. R.; Ahlrichs, R. *Chem. Phys. Lett.* **1989**, *164*, 193.
(276) Nicholas, J. B.; Winans, R. E.; Harrison, R. J.; Iton, L. E.; Curtiss, L. A.; Hopfinger, A. J. *J. Phys. Chem.* **1992**, *96*, 10247.
(277) Limatrakul, J.; Hannongbua, S. *J. Mol. Struct. (Theochem)* **1993**, *280*, 139.
(278) Carson, R.; Cooke, E. M.; Dwyer, J.; Hinchliffe, A.; O'Malley, P. J. In *Zeolites as Catalysts, Sorbents and Detergents Builders*; Karge, H. G., Weitkamp, J., Eds.; Elsevier: Amsterdam, 1989; p 39.
(279) Kassab, E.; Seiti, K.; Allavena, M. *J. Phys. Chem.* **1988**, *92*, 6705.
(280) Sierra, L.; Saldarriaga, C.; Davis, M. *J. Am. Chem. Soc.* **1987**, *109*, 2686.
(281) Olson, D. H.; Dempsey, E. *J. Catal.* **1969**, *13*, 221.
(282) Mortier, W. J.; Pluth, J. J.; Smith, J. V. *J. Catal.* **1967**, *45*, 367.
(283) Bosacek, V.; Beran, S.; Jirak, Z. *J. Phys. Chem.* **1981**, *85*, 3856.
(284) Haag, W. O.; Lago, R. M.; Weisz, P. B. *Faraday Discuss.* **1982**, *72*, 317.
(285) Frilette, V. J.; Haag, W. O.; Lago, R. M. *J. Catal.* **1981**, *67*, 218.
(286) Csicsery, S. M. *ACS Monograph* **1976**, *171*, 680.
(287) Csicsery, S. M. *Zeolites* **1984**, *4*, 202.
(288) Csicsery, S. M. *J. Catal.* **1987**, *108*, 433.
(289) Derouane, E. G. *J. Catal.* **1986**, *100*, 541.
(290) Derouane, E. G. *Stud. Surf. Sci. Catal.* **1980**, *4*, 5.
(291) Derouane, E. G. *Stud. Surf. Sci. Catal.* **1984**, *19*, 1.
(292) Dwyer, J. *Chem. Ind.* **1984**, *7*, 229.
(293) Jacobs, P. A.; Martens, J. A. *Stud. Surf. Sci. Catal.* **1986**, *28*, 23.
(294) Hammon, U.; Kokotailo, G. T.; Riekert, L.; Zhou, J. Q. *Zeolites* **1988**, *8*, 338.
(295) Derouane, E. G.; Gabelica, Z. *J. Catal.* **1980**, *65*, 486.
(296) Mirodatos, C.; Barthomeuf, D. *J. Catal.* **1985**, *93*, 246.
(297) Derouane, E. G. *Chem. Phys. Lett.* **1987**, *142*, 200; Derouane, E. G. In *Guidelines to the Mastering of Zeolite properties*; Barthomeuf, D., *et al.*, Eds.; Nato ASI Ser. 221; Plenum: New York, 1990; p 250.
(298) Derouane, E. G.; André, J. M.; Lucas A. A. *J. Catal.* **1988A**, *110*, 58.
(299) Corma, A.; Zicovich-Wilson, C. M.; Viruela, P. *J. Phys. Chem.* **1994**, *98*, 10863.
(300) van Santen, R. A. In *Guidelines for Mastering the Properties of Molecular Sieves*; NATO ASI Ser. 221; Plenum: New York, 1990; p 201.
(301) Pearson, R. G. *J. Am. Chem. Soc.* **1963**, *85*, 3533.
(302) Pearson, R. G. *Chem. Eng. News* **1965**, *43*, 90.
(303) Pearson, R. G. *Chem. Br.* **1967**, *3*, 103.
(304) Langemaeker, W.; de Decker, M.; Geerlings, P.; Raeymaekers, P. *J. Mol. Struct. (THEOCHEM)* **1990**, *66*, 115.
(305) Parr, R. G.; Donnelly, R. A.; Palke, W. E. *J. Phys. Chem.* **1978**, *68*, 3801.
(306) Parr, R. G.; Yang, W. *J. Am. Chem. Soc.* **1984**, *106*, 4049.
(307) Lee, Ch.; Yang, W.; Parr, R. G. *J. Mol. Struct. (THEOCHEM)* **1988**, *163*, 205.
(308) Baekelandt, B. G.; Mortier, W. J.; Lievens, J. L.; Schoonheydt, R. A. *J. Am. Chem. Soc.* **1991**, *113*, 6730.
(309) Corma, A. In *Guidelines for Mastering the Properties of Molecular Sieves*; Barthomeuf, D., *et al.*, Eds.; NATO ASI Series; Plenum Press: New York, 1990; p 299.
(310) Corma, A.; Sastre, G.; Viruela, P.; Zikovich-Wilson, C. *J. Catal.* **1992**, *136*, 521.
(311) Corma, A.; Llopis, F.; Viruela, P.; Zikovich-Wilson, C. *J. Am. Chem. Soc.* **1994**, *116*, 134.
(312) Corma, A.; Zikovich-Wilson, C.; Viruela, P. *J. Phys. Org. Chem.* **1994**, *7*, 364.
(313) Corma, A.; Viruela, P.; Zikovich-Wilson, C. To be published.
(314) Wendlant, K. P.; Bremer, H. In *Proceedings of the 8th. Int. Congress of Catalysis*; Verlag Chemie: Weingheim, 1988; Vol. IV, p 507.
(315) Corma, A.; Sastre, E.; Sastre, G.; Viruela, P.; Zikovich-Wilson, C. *Proc. 9th. Int. Zeolite Conf.*, Montreal, 1992; von Ballmoos, *et al.*, Ed.; Butterworth-Henemann: Washington, 1993; p 379.
(316) Olah, G. A.; Prakash, G. K. S.; Sommer, J. *Superacids*; John Wiley & Sons: New York, 1985.
(317) Olah, G. A.; Prakash, G. K. S.; Williams, R. E.; Field, J. D.; Wade, D. *Hypercarbon Chemistry*; John Wiley & Sons: New York, 1987.

(318) Lombardo, E. A.; Dereppe, J. M.; Marcelin, G.; Hall, W. K. *J. Catal.* **1988**, *114*, 167.
(319) Xu, T.; Haw, J. F. *J. Am. Chem. Soc.* **1994**, *116*, 7753.
(320) Aronson, M. T.; Gorte, R. S.; Farneth, W. E.; White, D. *J. Am. Chem. Soc.* **1989**, *111*, 840.
(321) Sommer, J.; Hachoumy, M.; Garin, F. *J. Am. Chem. Soc.* **1994**, *116*, 5491. Sommer, J.; Hachoumy, M.; Garin, F.; Barthomeuf, D.; Vedrine, J. *J. Am. Chem. Soc.* **1995**, *117*, 1135–136.
(322) Haw, J. F.; Richardson, B. R.; Oshiro, I. S.; Lazo, N. D.; Speed, J. A. *J. Am. Chem. Soc.* **1989**, *111*, 2052.
(323) van der Berg, J. P.; Wolthnizen, J. P.; Clague, A. D. H.; Hays, G. R.; Huis, R.; van Hoff, J. B. *J. Catal.* **1983**, *80*, 130.
(324) Rabo, J. A.; Gajda, G. J. In *Guidelines for Mastering the Properties of Molecular Sieves*; Barthomeuf, D., *et al.*, Eds.; Plenum Press: New York, 1990; Vol. 221, p 273.
(325) Kazansky, V. B.; Senchenya, I. N. *J. Catal.* **1989**, *119*, 108; *Catal. Lett.* **1991**, *8*, 317.
(326) Kazansky, V. B. *Acc. Chem. Res.* **1991**, *24*, 379.
(327) Viruela, P.; Zicovich-Wilson, C. M.; Corma, A. *J. Phys. Chem.* **1993**, *97*, 13713.
(328) Teunissen, E. H.; van Santen, R. A.; Jansen A. P. J.; van Duijneveldt, F. B. *J. Phys. Chem.* **1993**, *97*, 203.
(329) Venuto, P. B.; Landis, P. S. *Adv. Catal.* **1968**, *18*, 259.
(330) Venuto, P. B. *Microporous Mater.* **1994**, *2*, 297.
(331) Holderich, W. F.; Hesse, M.; Neuman, F. *Angew. Chem., Int. Ed. Engl.* **1988**, *27*, 226.
(332) Hölderich, W. F.; van Bekkum, H. *Stud. Surf. Sci. Catal.* **1991**, *58*, 631.
(333) Chen, N. Y.; Garwood, W. E.; Dwyer, F. G. *Shape Selective Catalysis in Industrial Applications*; Marcel Dekker Inc.: New York, 1987.
(334) Maxwell, I. E.; Stork, W. H. J. *Stud. Surf. Sci. Catal.* **1991**, *58*, 571.
(335) Corma, A. *Catal. Lett.* **1993**, *22*, 33.
(336) Ozaki, A.; Kimura, K. *J. Catal.* **1964**, *55*, 394.
(337) Lemberton, J. L.; Perot, G.; Guisnet, M. *Proc. 7th. Int. Congr. Catal.*, Tokyo 1980; Kodansha: Tokyo (Elsevier: Amsterdam), 1981; p 993.
(338) Misono, M.; Tani, N.; Yoneda, Y. *J. Catal.* **1978**, *55*, 314.
(339) Hightower, J.; Hall, W. K. *J. Phys. Chem.* **1967**, *71*, 1014.
(340) Jacobs, P. A. *Carboniogenic Activity of Zeolites*; Elsevier: Amsterdam, 1977.
(341) Corma, A.; Romanach, M.; Sanchez, F.; Auguet, A. SP 8900384, 1989.
(342) Choudary, V. R. *Chem. Ind. Dev.* **1974**, 32.
(343) Szabo, J.; Parrotey, J.; Szabo, G.; Duchet, J. C.; Cornet, D. *J. Mol. Catal.* **1991**, *67*, 79.
(344) Janssen, M. J. G.; Mortier, W. J.; van Oorschot, W. M. WO Patent Appl. 18851, 1991.
(345) Zubowa, H. L.; Richter, M.; Roost, U.; Parlitz, B.; Fricke, R. *Catal. Lett.* **1993**, *19*, 67.
(346) Gaffney, A. M.; Jones, A. U.S. Patent 5107050, 1992.
(347) Gajda, G. J. U.S. Patent 5132484, 1992.
(348) Simon, M. W.; Xu, W. Q.; Suib, S. L.; O'Young, C. L. *Microporous Mater.* **1994**, *2*, 477.
(349) Asensi, M. A.; Corma, A.; Martínez, A. To be published.
(350) Simon, M. W.; Suib, S. L.: O'Young, C. L. *J. Catal.* **1994**, *147*, 484.
(351) Xu, W. Q.; Yin, Y. G.; Suib, S. L.; O'Young, C. L.; *J. Catal.* **1984**, *150*, 34.
(352) Grandvallet, P.; de Jong, K. P.; Mooiwer, H. H.; Kortbeek, A. G. T. G.; Kraushaar-Czarnetzki, B. EP 501577, 1992.
(353) Mooiweer, H. H.; de Jong, K. P.; Kraushaar-Czarnetzki, B.; Storkan, W. H. J.; Krutzen, B. C. H. *Stud. Surf. Sci.* **1994**, *84*, 2327.
(354) Weisz, P. B. *Adv. Catal.* **1962**, *13*, 137.
(355) Guisnet, M.; Alvarez, F.; Gianetto, G.; Perot, G. *Catal. Today* **1987**, *1*, 415. Ribeiro, F.; Marcilly, Ch.; Guisnet, M. *J. Catal.* **1982**, *78*, 275; **1982**, *78*, 267.
(356) Koradia, P. B.; Kiouski, J. R.; Asim, M. Y. *J. Catal.* **1980**, *66*, 290.
(357) Guisnet, M.; Fouche, V.; Belloum, M.; Bournouille, J. P.; Travers, C. *Appl. Catal.* **1991**, *71*, 283.
(358) Fajula, F.; Boulet, M.; Coq, B.; Rajaofanova, V.; Figueras, F.; Des Courieres, T. *Proc. 10th. Int. Congr. Catal.*; Guczi, L., Solymosi, F., Tetenyi, P., Eds.; Akademiai Kiado: Budapest, 1993; p 1007.
(359) Leu, L. J.; Hou, L. Y.; Kang, B. C.; Li, C. P.; Wu, S. T.; Wu, J. C. *Appl. Catal.* **1991**, *69*, 49.
(360) Jacobs, P. A.; Martens, J. A.; Weitkamp, J.; Beyer, H. K. *Faraday Discuss. Chem. Soc.* **1981**, *72*, 353.
(361) Chen, N. Y.; Degnan, T. F.; Weisz, P. B. EP 363531, 1990.
(362) Schweizer, A. E. U.S. Patent 4992617 and 4992402, 1991.
(363) Brehm, A.; Kromminga, T.; Stoeckel, V. *DECHEMA Mongr.* **1989**, *118*, 171.
(364) Coq, B.; Rajaofanova, V.; Chauvin, B.; Figueras, F. *Appl. Catal.* **1991**, *69*, 341.
(365) Martens, J. A.; Tielen, M.; Jacobs, P. A. *Stud. Surf. Sci. Catal.* **1989**, *46*, 49.
(366) Parton, R.; Uytterhoeven, L.; Martens, J. A.; Jacobs, P. A.; Froment, G. F. *Appl. Catal.* **1991**, *76*, 131.
(367) Martens, J. A.; Tielen, M.; Jacobs, P. A.; Weitkamp, J. *Zeolites* **1984**, *4*, 98.
(368) Cortés, A.; Corma, A. *J. Catal.* **1978**, *51*, 388.
(369) Lanewala, M. A.; Bolton, A. *J. Org. Chem.* **1969**, *34*, 3107.
(370) Csicsery, S. M. *J. Org. Chem.* **1969**, *34*, 338.
(371) Corma, A.; Sastre, E. *J. Catal.* **1991**, *129*, 177.
(372) Gnep, N. S.; Tejada, J.; Guisnet, M. *Bull. Soc. Chim. Fr. I* **1982**, 5. Olson, D. H.; Haag, W. O. *ACS Symp. Ser.* **1984**, *248*, 275.
(373) Martens, J. A.; Pérez-Pariente, J.; Sastre, E.; Corma, A.; Jacobs, P. A. *Appl. Catal.* **1988**, *45*, 85.
(374) Csicsery, S. M. *J. Catal.* **1987**, *108*, 433.
(375) Kim, M. H.; Chen, C. Y.; Davis, M. E. *ACS Symp. Ser.* **1993**, *517*, 222.
(376) Solinas, V.; Monaci, R.; Marougiu, B.; Forni, L. *Appl. Catal.* **1984**, *9*, 109.
(377) Weitkamp, J.; Neuber, N. *Stud. Surf. Sci.* **1991**, *60*, 291.
(378) Matsuda, T.; Yogo, K.; Mogi, Y.; Kikuchi, E. *Chem. Lett.* **1990**, 1085.
(379) Weitkamp, J.; Ernst, S. *Catal. Today* **1994**, *19*, 107.
(380) Olah, G. A. *J. Am. Chem. Soc.* **1972**, *94*, 808.
(381) Olah, G. A.; Mo, Y. K.; Olah, J. A. *J. Am. Chem. Soc.* **1973**, *95*, 4939.
(382) Haag, W. O.; Dessau, R. M. *Proc. 8th. Int. Congr. Catal.* **1984**, *II*, 305.
(383) Corma, A.; Planelles, J.; Sanchez-Marin, J.; Tomás, F. *J. Catal.* **1985**, *92*, 284.
(384) Greensfelder, B. S.; Voge, H. H.; Good, G. M. *Ind. Eng. Chem.* **1957**, *49*, 742.
(385) Poustma, M. L. *ACS Monograph* **1976**, *117*, 505 (Rabo, J. A., Ed.).
(386) Planelles, J.; Sanchez-Marin, F.; Tomás, F.; Corma, A. *J. Mol. Catal.* **1985**, *32*, 365.
(387) Barthomeuf, D.; Mirodator, C. *Prepr. Am. Chem. Soc. Petrol. Div.* **1989**, *34*, 714.
(388) Abbot, J.; Head, J. D. *J. Catal.* **1990**, *125*, 187.
(389) Tung, S. E.; Mc.Ininch, E. *J. Catal.* **1968**, *10*, 166.
(390) Chen, F. R.; Fripiat, J. J. *J. Phys. Chem.* **1993**, *97*, 5796.
(391) Greensfelder, B. S.; Voge, H. H.; Good, G. M. *Ind. Eng. Chem.* **1949**, *41*, 2573.
(392) Wojciechowski, B. W.; Corma, A. *Catalytic Cracking: Catalyst, Chemistry and Kinetics*; Marcel Dekker: New York, 1986.
(393) Venuto, P. B.; Habib, E. T. *Fluid Catalytic Cracking with Zeolite Catalysts*; Marcel Dekker: New York, 1979.
(394) Corma, A.; Lopez Agudo, A. *React. Kinet. Catal. Lett.* **1981**, *16*, 253.
(395) Abbot, J.; Wojciechowsky, B. W. *J. Catal.* **1987**, *107*, 571.
(396) Corma, A.; Mocholí, F.; Orchillés, V.; Koermer, G. S.; Madon, R. J. *Appl. Catal.* **1991**, *67*, 307.
(397) van Klink, A. J. E. M.; Hartkamp, M. B.; O'Connor, P. *Prepr.-Am. Chem. Soc., Pet. Div.* **1989**, *34*, 728.
(398) Good, G. M.; Voge, H. H.; Greensfelder, B. S. *Ind. Eng. Chem.* **1947**, *39*, 1032.
(399) Corma, A.; Wojciechowski, B. W. *Catal. Rev. Sci. Eng.* **1982**, *24*, 1.
(400) Corma, A.; Miguel, P. J.; Orchillés, A. V.; Koermer, G. *J. Catal.* **1994**, *145*, 181.
(401) Gianetto, G.; Guisnet, M.; Porot, G. *J. Chem. Soc., Chem. Commun.* **1989**, 3225.
(402) Frilette, V. J.; Haag, W. O.; Lago, R. M. *J. Catal.* **1981**, *67*, 218.
(403) Anderson, C. D.; Dwyer, F. G.; Koch, G.; Niiranen, P. *Proc. Iberoamerican Symp. on Catal.* **1984**, *9*.
(404) Roberie, T. G.; Young, G. W.; Chin, D. S.; Wormsbecher, R. F.; Habib, E. T. *NPRA Ann. Meeting*, 1992, New Orleans; NPRA: Washington DC, 1992; AM-92–43.
(405) Chen, N. Y.; Garwood, G. E. *J. Catal.* **1978**, *52*, 453.
(406) Nayak, V. S.; Moffat, J. B. *Appl. Catal.* **1990**, *60*, 87.
(407) Madon, R. J. *J. Catal.* **1991**, *129*, 275.
(408) Schipper, P. H.; Dwyer, F. G.; Sparell, P. T.; Mizrahi, S.; Herbst, J. A. *ACS Symp. Ser.* **1988**, *375*, 64.
(409) Chen, N. Y.; Ketkar, A. B.; Nace, P. M.; Kam, A. Y.; Kennedy, C. R.; Ware, R. A. EP 186446B1, 1991.
(410) Bonetto, L.; Camblor, M. A.; Corma, A.; Pérez-Pariente, J. *Appl. Catal.* **1992**, *82*, 37.
(411) Bonetto, L.; Corma, A.; Herrero, E. *Proc. Int. Zeol. Conf.* **1992**, *10*.
(412) Martens, J. A. Ph.D. Catholic University Leuven, Belgium, Dec, 1985. Jacobs, P. A.; Martens, J. A.; Weitkamp, J.; Beyer, H. K. *Faraday Disc. Chem. Soc.* **1982**, *72*, 353.
(413) Corma, A.; Martínez, A. *Catal. Rev. Sci. Eng.* **1993**, *35*, 483.
(414) Kirsch, F. W.; Potts, J. D. *Prepr.—Am. Chem. Soc., Div. Pet. Chem.* **1970**, *15*, A-109.
(415) Kirsch, F. W.; Potts, J. D.; Barmby, D. S. *J. Catal.* **1972**, *27*, 142.
(416) Huang, T. J.; Yurchak, S. *ACS Symp. Ser.* **1977**, *55*, 75.
(417) Weitkamp, J. *Stud. Surf. Sci.* **1980**, *5*, 65.
(418) Weitkamp, J. *Proc. Int. Zeol. Conf.* **1980**, *5*, 858. Rees, L. Ed., Wiley, N. Y.
(419) Chu, Y. F.; Chester, A. W. *Zeolites* **1986**, *6*, 195.

(420) Corma, A.; Martínez, A.; Martínez, C. *J. Catal.* **1994**, *146*, 185.
(421) Corma, A.; Gómez, V.; Martínez, A. *Appl. Catal.* **1994**, *119*, 83.
(422) Corma, A.; Martínez, A.; Martínez, C. *Catal. Lett.* **1994**, *28*, 187.
(423) Leonowicz, M. E.; Lawton, J. A.; Lawton, S. L.; Rubin, M. K. *Science* **1994**, *264*, 1910.
(424) van den Berg, J. P.; Wolthuizen, J. P.; Claque, A. D. H.; Hays, G. R.; Huis, R.; van Hoof, J. H. C. *J. Catal.* **1983**, *80*, 130.
(425) van den Berg, J. P.; Wolthuizen, J. P.; van Hoof, J. H. C. *J. Catal.* **1983**, *80*, 139.
(426) Haw, J. F.; Richardson, B. R.; Oshiro, I. S.; Lazo, N. D.; Speed, J. A. *J. Am. Chem. Soc.* **1989**, *111*, 2052.
(427) Richardson, B. R.; Lazo, N. D.; Schettler, P. D.; White, J. L.; Haw, J. F. *J. Am. Chem. Soc.* **1990**, *112*, 2886.
(428) White, J. L.; Lazo, N. D.; Richardson, B. R.; Haw, J. F. *J. Catal.* **1990**, *125*, 260.
(429) Weeks, T. S.; Bolton, A. P. *J. Chem. Soc., Faraday Trans. 1* **1976**, *70*, 1676.
(430) Galya, L. G.; Occelli, M. L.; Hsu, J. T.; Young, D. C. *J. Mol. Catal.* **1985**, *32*, 391.
(431) Pellet, R. J.; Rabo, J. A.; Long, G. N.; Coughlin, P. K. *N. Am. Mtg. Catal. Soc.* **1987**, *10*, Paper No. B-2.
(432) Garwood, W. E. *ACS Symp. Ser.* **1983**, *218*, 383.
(433) Tabak, S. A.; Krambeck, F. J.; Garwood, W. E. *AICHE J.* **1986**, *32*, 1526.
(434) Tabak, S. A. AICHE Nat. Mtg. Philadelphia, 1984.
(435) Tabak, S. A.; Avidan, A. A.; Krambeck, F. J. Book of Abstracts, 191st National Meeting of the American Chemical Society, New York, Spring 1986; American Chemical Society: Washington, DC, 1986.
(436) Beech, J. M, Jr.; Ragonese, F. P.; Stoos, J. A.; Yurchak, S. Can. Patent Appl. CA 2030034, 1991.
(437) van den Berg, B. P.; Roebschlaeger, K. H. W. EU Patent Appl. 439865, 1990.
(438) Hall, A. H. P.; Winstanley, A. W. Brit UK Patent Appl. GB2246141, 1992.
(439) Tabak, S. A.; Krambeck, F. J.; Garwood, W. E. *AICHE J.* **1986**, *32*, 1529.
(440) Quann, R. J.; Green, L. A.; Tobak, S. A.; Krambeck, F. J. *Ind. Eng. Chem. Res.* **1988**, *27*, 567.
(441) Wilshier, K. G.; Smart, P.; Western, R.; Moles, T.; Behrsing, T. *Appl. Catal.* **1987**, *31*, 345.
(442) O'Connor, C. T.; Schwarz, S.; Kojima, M. *Stud. Surf. Sci. Catal.* **1991**, *65*, 491.
(443) Chu, C. T. W. U.S. Patent 4956514, 1990.
(444) Keville, K. M.; Huss, A., Jr.; Hussain, A.; Del Rossi, K. J.; Chu, C. T. W. WO 9314048, 1992.
(445) Le, N. Q.; Thomson, R. T. U.S. Patent 5134241, 1992.
(446) Weitkamp, J. *Acta Phys. Chem. (Szeged)* **1985**, *31*, 271.
(447) Ren, C. F.; Coudurier, G.; Naccache, C. *Stud. Surf. Sci. Catal.* **1986**, *28*, 733.
(448) Coughlan, B.; Keane, M. A. *J. Catal.* **1992**, *138*, 164.
(449) Lukyanov, D. B.; Shtral, V. I. *Prepr.—Am. Chem. Soc., Div. Pet. Chem.* **1991**, *36*, 693.
(450) Dwyer, F. G. In *Catalysis of Organic Reactions*; Moser, W. R., Ed.; Marcel Dekker: New York, 1981; p 39.
(451) Kaeding, W. W.; Young, L. B.; Prapas, A. G. *Chemtech* **1982**, *12*, 556.
(452) Kaeding, W. W.; Chu, C.; Young, L. B.; Weinstein, B.; Butter, S. A. *J. Catal.* **1981**, *67*, 159.
(453) Brenan, J. A.; Garwood, W. E.; Yurchak, S.; Lee, W. *Proc. Int. Sem. on Alternative Fuels* **1981**, 19.1 (Germain, A., Ed.).
(454) Young, L. B. U.S. Patent 4301317, 1981.
(455) Dart, C. B.; Davis, M. E. *Catal. Today* **1994**, *19*, 151.
(456) Sugi, Y.; Toba, M. *Catal. Today* **1994**, *19*, 187.
(457) Sugui, Y.; Matsuzaki, T.; Hanaoka, T.; Takenchi, K.; Tokoro, T.; Takenchi, G. *Stud. Surf. Sci. Catal.* **1991**, *60*, 303.
(458) Lee, G. S.; Maj, J. J.; Rocke, S. C.; Garcés, J. M. *Catal. Lett.* **1989**, *2*, 243.
(459) Katayama, A.; Toba, M.; Takeuchi, G.; Mizukami, F.; Niwa, S.; Mitamura, S. *J. Chem. Soc., Chem. Commun.* **1991**, 39.
(460) Mizukami, F.; Katayama, A.; Mitamura, S.; Toba, M. Jpn. Tokyo Kokai 91176429, 1991.
(461) Takeuchi, G.; Okazaki, M.; Yamaye, M.; Kito, T. *Sekiyu Gakkaishi* **1991**, *34*, 531.
(462) Takeuchi, G.; Okazaki, H.; Yamaye, M.; Kito, T. *Appl. Catal.* **1991**, *76*, 49.
(463) Pope, M. T.; Muller, A. *Angew Chem., Int. Ed. Engl.* **1991**, *30*, 34.
(464) Evans, H. T., Jr. *Perspectives in Structural Chemistry*; Dunitz, J. D., Ibers, J. A., Eds.; Wiley and Sons: New York, 1971; Vol. 4, p 1.
(465) Tsigdinos, G. A. *Top. Curr. Chem.* **1978**, *76*, 1.
(466) Keggin, J. F. *Proc. R. Soc. London* **1934**, *A144*, 75.
(467) Lipscomb, W. N. *Inorg. Chem.* **1965**, *4*, 132.
(468) Jun, P.; Lun-Yu, Q.; Ya-guang, Ch. *Inorg. Chim. Acta* **1991**, *183*, 157.
(469) Rocchiccioli-Deltcheff, C.; Thouvenot, R.; Franck, R. *Spectrochim. Acta* **1976**, *32A*, 587.
(470) Misono, M. *Kagaku no Ryoiki* **1981**, *35*, 519.
(471) Misono, M.; Mizuno, N.; Katamura, K.; Kasai, A.; Konishi, Y.; Sakata, K.; Okuhara, T.; Yoneda, Y. *Bull. Chem. Soc. Jpn.* **1982**, *55*, 400.
(472) Rocchiccioli-Deltcheff, C.; Fournier, M.; Franck, R. *Inorg. Chem.* **1983**, *22*, 207.
(473) Zuolong, Y.; Shufang, L.; Furong, H.; Shunli, W.; Guilin, Z.; Suxian, Z. *Kexue Tongbao* **1987**, *32*, 1540.
(474) Bielanski, A.; Malecka, A. *J. Chem. Soc., Faraday Trans. 1* **1989**, *85*, 2847.
(475) Lange, G.; Hahn, H.; Dehnicke, K. *Z. Naturforsch.* **1969**, *24B*, 1498.
(476) Kasprazak, M. S.; Leroi, G. E.; Crouch, S. R. *Appl. Spectros.* **1982**, *36*, 285.
(477) Mandal, K. C.; Ozanam, F.; Chazalviel, J. N. *J. Electroanal. Chem.* **1992**, *336*, 153.
(478) Bruckman, K.; Haber, J.; Serwicka, E. M.; Yurchenko, E. N.; Lazarenko, T. P. *Catal. Lett.* **1990**, *4*, 181.
(479) Bank, J.; Schwenk, Z. *Phys. B* **1975**, 75.
(480) English, A. D.; Jesson, J. P.; Klemperer, W. G.; Mamouneas, T.; Messerle, L.; Shum, W.; Tramontano, A. *J. Am. Chem. Soc.* **1975**, *97*, 4785.
(481) Kazanskii, L. P.; Spitsyn, V. I. *Dokl. Akad. Nauk SSR, Phys. Chem.* **1975**, *223*, 721.
(482) Kazanskii, L. P.; Fedotov, M. A.; Ptushkina, M. N.; Spitsyn, V. I. *Dokl. Akad. Nauk SSSR, Phys. Chem.* **1975**, *224*, 1029.
(483) Pope, M. T.; O'Donnell, S. E.; Prados, R. A. *J. Chem. Soc., Chem. Commun.* **1975**, 22.
(484) O'Donnell, S. E.; Pope, M. T. *J. Chem. Soc., Dalton Trans.* **1976**, 2290.
(485) Kazanski, L. P. *Koord. Khim.* **1977**, *3*, 327.
(486) Sergienko, U. S.; Porai-Koshits, M. A.; Fedotov, M. A.; Yurchenko, E. N.; Kuznetsova, L. I. *Zh. Strukt. Khim.* **1977**, *18*, 976.
(487) Pope, M. T.; Baker, L. C. W. *J. Chem. Soc., Chem. Commun.* **1979**, 777.
(488) Acerete, R.; Hammer, C. F.; Baker, L. C. W. *J. Am. Chem. Soc.* **1979**, *101*, 267.
(489) Gansow, G. A.; Ho, R. K. C.; Kempler, W. G. *J. Organomet. Chem.* **1980**, *187*, C27.
(490) Jeannin, Y.; Martín-Frére, J. *J. Am. Chem. Soc.* **1981**, *103*, 1664.
(491) Le Febure, J.; Chauveau, F.; Doppelt, P. *J. Am. Chem. Soc.* **1981**, *103*, 4589.
(492) Finke, R. G.; Droege, M.; Hutchisson, J. R.; Gansow, D. *J. Am. Chem. Soc.* **1981**, *103*, 1587.
(493) Knoth, W. H.; Harlow, R. L. *J. Am. Chem. Soc.* **1981**, *103*, 4265.
(494) Knoth, W. H.; Farlee, R. D. *Inorg. Chem.* **1984**, *23*, 4765.
(495) Pope, M. T. *Heteropoly and Isopoly Oxometalates*; Springer: New York, 1983.
(496) Black, J. B.; Clayden, N. J.; Griffiths, L.; Scott, J. D. *J. Chem. Soc., Dalton Trans.* **1984**, 2765.
(497) Barrows, J. N.; Jameson, G. B.; Pope, M. T. *J. Am. Chem. Soc.* **1985**, *107*, 1771.
(498) Day, V. W.; Kempler, W. G. *Science* **1985**, May 3, 533.
(499) Farneth, W. E.; Staley, R. H.; Domaille, P. J.; Farlee, R. D. *J. Am. Chem. Soc.* **1987**, *109*, 4018.
(500) Kanda, Y.; Lee, K. Y.; Nakata, S.; Asakoa, S.; Misono, M. *Chem. Lett.* **1988**, 139.
(501) Okuhara, T.; Arai, T.; Ichiki, T.; Lee, K. Y.; Misono, M. *J. Mol. Catal.* **1989**, *55*, 293.
(502) Acerete, R.; Casañ-Pastor, N.; Bas-Serra, J.; Baker, L. C. W. *J. Am. Chem. Soc.* **1989**, *111*, 6049.
(503) Barrows, J. N.; Pope, M. T. *Adv. Chem. Ser.* **1990**, *226*, 403.
(504) Serwicka, E. M.; Grey, C. P. *Colloids Surf.* **1990**, *45*, 69.
(505) Mastikhin, M.; Kulikov, S. M.; Nosov, A. V.; Kozhevnikov, I. V.; Mudrakovsky, I. L.; Timofeeva, M. N. *J. Mol. Catal.* **1990**, *60*, 65.
(506) Lee, K. Y.; Arai, T.; Nakata, S.; Asaoka, S.; Okuhara, T.; Misono, M. *J. Am. Chem. Soc.* **1992**, *114*, 2836.
(507) Okuhara, T.; Misono, M. In *Dynamic Process on Solid Surfaces*; Tamarn, K., Ed.; Plenum Press: New York, 1993; Chapter 10, p 259.
(508) Misono, M.; Okuhara, T. *CHEMTECH* **1993**, *23*, 23.
(509) Bonardet, J. L.; McGarvey, G. B.; Moffat, J. B.; Fraissard, J. *Colloids Surf. A* **1993**, *72*, 191.
(510) So, H.; Pope, M. T. *Inorg. Chem.* **1972**, *11*, 1441.
(511) Pope, M. T.; Muller, A. *Angew Chem., Int. Ed. Engl.* **1991**, *30*, 34.
(512) Wu, H. *J. Biol. Chem.* **1920**, *43*, 189.
(513) Linz, A. *Ind. Eng. Chem. Anal. Ed.* **1942**, *15*, 459.
(514) Tsigdinos, G. A. *Ind. Eng. Chem. Prod. Res. Dev.* **1974**, *13*, 267.
(515) *Gmelin Handbuch der Anorganischen Chemie*; Verlag Chemie: Berlin, 1933; System number 54 (Tungsten).
(516) *Gmelin Handbuch der Anorganischen Chemie*; Verlag Chemie: Berlin, 1935; System number 53 (Molybdenum).
(517) North, E. O. *Inorganic Synthesis*; Booth, H. S., Ed.; McGraw Hill: New York, 1939; Vol. 1, pp 127 and 129.
(518) Malaprade, L. *Nouveau Traite de Chimie Minerale*; Pascale, P., Ed.; Masson et cie: Paris, 1959; Vol. 14.
(519) *Handbook of Preparative Inorganic Chemistry*, 2nd ed.; Brauer, G., Ed.; Academic Press Inc.; New York, 1986; Vol. 2.
(520) Pope, M. T.; Varga, G. M., Jr. *Inorg. Chem.* **1966**, *5*, 1249.

(521) Pope, M. T.; Papaconstantinou, E. *Inorg. Chem.* **1967**, *6*, 1147.
(522) Jolly, W. L. *The Synthesis and Characterization of Inorganic Compounds*; Prentice Hall, Inc.: New Jersey, 1970.
(523) Fuchs, J. *Z. Naturforsch.* **1973**, *B28*, 389.
(524) Tsigdinos, G. A. *Top. Curr. Chem.* **1978**, *76*, 1.
(525) Filowitz, M.; Ho, R. K. C.; Kemplerer, W. G.; Shum, W. *Inorg. Chem.* **1979**, *18*, 93.
(526) Tourné, G. *Bull. Soc. Chim. Fr.* **1982**, *3*, 69.
(527) Baker, L. C. W.; Lebioda, L.; Grochouski, J.; Mukherjee, H. G. *J. Am. Chem. Soc.* **1980**, *102*, 3274.
(528) Brown, D. H. *J. Chem. Soc.* **1962**, 3189.
(529) Misono, M.; Konishi, Y.; Furuta, M.; Yoneda, Y. *Chem. Lett.* **1978**, 709.
(530) Niiyama, H.; Saito, Y.; Yoshida, S.; Echigoya, E. *Nippon Kagaku Kaishi* **1982**, *4*, 569.
(531) McGarvey, G. B.; Moffat, J. B. *J. Catal.* **1991**, *130*, 483.
(532) Moffat, J. B. *J. Mol. Catal.* **1989**, *52*, 169.
(533) Bonardet, J. L.; McGarvey, G. B.; Moffat, J. B.; Fraissard, J. *Colloids Surf. A* **1993**, *72*, 191.
(534) Ito, T.; Fraissard, J. *J. Phys. Chem.* **1982**, *76*, 5225.
(535) Tatsumisago, M.; Kishida, K.; Minami, T. *Solid State Ion* **1993**, *59*, 171.
(536) Kozhevnikov, I. V.; Sinnema, A.; Jansen, R. J. J.; van Bekkum, H. *Catal. Lett.* **1994**, *27*, 187.
(537) Izumi, Y.; Hasebe, R.; Urabe, K. *J. Catal.* **1983**, *84*, 402.
(538) Igarashi, S.; Masuda, T.; Ogino, Y. *J. Jpn. Pet. Inst.* **1979**, *22*, 331; **1980**, *23*, 30.
(539) Kozhevnikov, I. V.; Sinnewa, A.; Jansen, R. J. J.; Pamin, K.; van Bekkum, H. *Catal. Lett.* **1995**, *30*, 241.
(540) Izumi, Y.; Urabe, K.; Onaka, M. *Zeolite, Clay and Heteropoly Acid in Organic Reactions*; Kodansha/VCH: Tokyo, 1992; p 99.
(541) Jansen, R. J. J.; van Veldhuizen, H. M.; van Bekkum, H. *Recl. Trav. Chim. Pays-Bas* **1994**, *113*, 115.
(542) Ono, Y. In *Perspectives in Catalysis*; Thomas, J. M., Zamaraev, K. I., Eds.; Blackwell: London, 1992; p 431.
(543) Lee, K. Y.; Mizuno, N.; Okuhara, T.; Misono, M. *Bull. Chem. Soc. Jpn.* **1989**, *62*, 1731.
(544) Chidichimo, G.; Golemme, A.; Imbardelli, D.; Santoro, E. *J. Phys. Chem.* **1990**, *94*, 6826.
(545) Kazanskii, L. P.; Fedotov, M. A.; Spitsyn, V. I. *Dokl. Acad. Nauk SSSR*, **1977**, *233*, 152.
(546) Klemperer, W. G.; Shum, W. *J. Am. Chem. Soc.* **1977**, *99*, 3544; **1978**, *100*, 4891.
(547) Brown, G. M.; Noe-Spirlet, M. R.; Bushing, W. R.; Levy, H. A. *Acta Crystallogr. B* **1977**, *33*, 1038.
(548) Niiyama, H.; Saito, Y.; Echigoya, E. In *Proc. 7th Int. Congr. Catal.*, Tokyo; Elsevier: Amsterdam, 1981; p 1416.
(549) Niiyama, H.; Saito, Y.; Yoshida, S.; Echigoya, E. *Nippon Kagaku Kaishi* **1982**, 569.
(550) Baba, T.; Sakai, J.; Ono, Y. *Bull. Chem. Soc. Jpn.* **1982**, *55*, 2633.
(551) Baba, T.; Nomura, M.; Ono, Y.; Kansaki, Y. *J. Chem. Soc., Faraday Trans.* **1992**, *88*, 71.
(552) Baba, T.; Watanabe, H.; Ono, Y. *J. Phys. Chem.* **1983**, *87*, 2406.
(553) Hayashi, H.; Moffat, J. B. *J. Catal.* **1982**, *77*, 473.
(554) Serwicka, E. M.; Bruckman, K.; Haber, J.; Paukshtis, E. A.; Yurchenko, E. N. *Appl. Catal.* **1991**, *73*, 153.
(555) Bielanski, A.; Cichowlas, A.; Kostrzewa, D.; Malecka, A. *Z. Phys. Chem.* N. F. **1990**, *167*, 93.
(556) Ghosh, A. K.; Moffat, J. B. *J. Catal.* **1986**, *101*, 238.
(557) Misono, M. *Stud. Surf. Sci.* **1985**, *20*, 147.
(558) Misono, M.; Konishi, Y.; Furuta, M.; Yoneda, Y. *Chem. Lett.* **1978**, 709.
(559) Furuta, M.; Sakata, K.; Misono, M.; Yoneda, Y. *Chem. Lett.* **1979**, 31.
(560) Okuhara, T.; Kasai, A.; Ayakawa, N.; Yoneda, Y.; Misono, M. *J. Catal.* **1983**, *83*, 121.
(561) Ai, M. *J. Catal.* **1981**, *71*, 88.
(562) Misono, M.; Mizuno, N.; Katamura, K.; Kasai, A.; Konishi, Y.; Sakata, K.; Okuhara, T.; Yoneda, Y. *Bull. Chem. Soc. Jpn.* **1982**, *55*, 400.
(563) Misono, M. *Proc. 4th Climax Int. Conf. Chem. and Uses of Mo*; Climax Mo Comp., **1982**: p 289 (Berry, H. F., Mitchell, P. C. H., Eds.).
(564) Misono, M.; Okuhara, T. *CHEMTECH* **1993**, *23*, 23.
(565) Okuhara, T.; Misono, M. *Dynamic Processes on Solid Surfaces*; Tamarn, K., *et al.*, Ed.; Plenum Press: New York, 1993; p 259.
(566) Feng, X. L. C.; Lefebvre, F. *Catal. Lett.* **1993**, *22*, 387.
(567) Okuhara, T.; Tatematsu, S.; Lee, K. Y.; Misono, M. *Bull. Chem. Soc. Jpn.* **1989**, *62*, 717.
(568) Misono, M. In *Polyoxometallates*; Pope, M. T., Müller, A., Eds.; Kluwer Academic Pub.: Netherlands, 1994; p 255. 107. Lee, K. Y.; Arai, T.; Nakata, S.; Asaoka, S.; Okuhara, T.; Misono, M. *J. Am. Chem. Soc.* **1992**, *114*, 2836.
(569) Misono, M. *Catal. Rev. Sci. Eng.* **1987**, *29*, 269.
(570) Misono, M. *Proc. 10th Int. Congr. Catal.*; Akademiaki Kiodo: Budapest, 1993; p 69.
(571) Okuhara, T.; Mizuno, N.; Lee, K. Y.; Misono, M. *Acid Base Catalysis*; Kodansha: Tokyo, 1989; p 421.
(572) Okuhara, T.; Hashimoto, T.; Misono, M.; Yoneda, Y.; Niiyama, M.; Saito, Y.; Echigoya, E. *Chem. Lett.* **1983**, 573.
(573) Highfield, J. G.; Moffat, J. B. *J. Catal.* **1986**, *98*, 245.
(574) Okuhara, T.; Misono, M. In *Dynamic Processes on Solid Surfaces*; Tamarn, K., Ed.; Plenum Press: New York, 1993; Chapter 10, p 259.
(575) Kanda, Y.; Lee, K. Y.; Nakata, S.; Asaoka, S.; Misono, M. *Chem. Lett.* **1988**, 139.
(576) Knozinger, H. *Angew Chem., Int. Ed. Engl.* **1968**, *7*, 791.
(577) Misono, M.; Okuhara, T.; Ichiki, T.; Arai, T.; Kanda, Y. *J. Am. Chem. Soc.* **1987**, *109*, 5535.
(578) Okuhara, T.; Arai, T.; Ichiki, T.; Lee, K. Y.; Misono, M. *J. Mol. Catal.* **1989**, *55*, 293.
(579) Otake, M.; Onoda, T. *Shokubai* **1975**, *17*, 13.
(580) Orita, H.; Hayakawa, T.; Shimizu, M.; Takehira, K. *Appl. Catal.* **1991**, *77*, 133.
(581) Schwegler, M. A.; Vinke, P.; Vandereijk, M.; van Bekkum, H. *Appl. Catal.* **1992**, *80*, 41.
(582) Hasik, M.; Pron, A.; Kulszewiczbajer, I.; Pozniczek, J.; Bielanski, A.; Piwowarska, Z.; Dziembaj, R. *Synth. Met.* **1993**, *55*, 972.
(583) Hashimoto, K.; Matsumura, Y.; Fukuchi, M.; Kera, Y. *Catal. Lett.* **1993**, *19*, 375.
(584) Nomiya, K.; Miwa, M. *Sikei Daigaku Kogaku Hokoku* **1982**, *33*, 2221.
(585) Misono, M.; Sakata, K.; Yoneda, Y.; Lee, W. Y. *Proc. 7th Int. Congr. Catal.*; Kodansha: Tokyo (Elsevier: Amsterdam), 1981; p 1047.
(586) Misono, M.; Nojiri, N. *Appl. Catal.* **1990**, *64*, 1.
(587) Izumi, Y.; Kawasaki, Y.; Tani, M. Jpn. Kokai 44-34798, 1969.
(588) Izumi, Y.; Kawasaki, Y.; Tani, M. U.S. Patent 3,758,615, 1973.
(589) Izumi, Y.; Kawasaki, Y.; Tani, M. Jpn. Tokkyo Koho, 49-36203, 1974.
(590) Onoue, Y.; Mizutani, Y.; Akiyama S.; Izumi, Y. *CHEMTECH* **1978**, 432.
(591) Aoshima, A.; Yamamatsu, S.; Yamaguchi, T. *Nippon Kagaku Kaishi* **1990**, 233.
(592) Knifton, J. F. *Appl. Catal. A* **1994**, *109*, 247.
(593) Bhutada, S. R.; Pangarkar, V. G. *J. Chem. Tech. Biotechnol.* **1986**, *36*, 61.
(594) Izumi, Y.; Urabe, K. *Chem. Lett.* **1981**, 663.
(595) Guttmann, A. T.; Graselli, R. K. *Appl. Catal.* **1983**, *8*, 57.
(596) Izumi, Y.; Matsuo, R.; Urabe, K. *J. Mol. Catal.* **1983**, *18*, 299.
(597) Baba, T.; Ono, Y. *Appl. Catal.* **1986**, *22*, 321.
(598) Hu, C. W.; Hashimoto, M.; Okuhara, T.; Misono, M. *J. Catal.* **1993**, *143*, 437.
(599) Schwegler, M. A.; van Bekkum, H. *Appl. Catal.* **1991**, *74*, 191.
(600) Thorat, T. S.; Yadav, V. M.; Yadav, G. D. *Appl. Catal. A* **1992**, *A90*, 73.
(601) Ozaki, A.; Kimura, K. *J. Catal.* **1964**, *3*, 395.
(602) Hightower, J.; Hall, W. K. *J. Am. Chem. Soc.* **1967**, *89*, 778.
(603) Hightower, J.; Hall, W. K. *J. Phys. Chem.* **1967**, *71*, 1014.
(604) Matsuda, T.; Sato, M.; Kanno, T.; Miura, H.; Sugiyama, K. *J. Chem. Soc., Faraday Trans. 1* **1981**, *77*, 3107.
(605) Olah, G. A.; Shen, J.; Schlosberg, R. H. *J. Am. Chem. Soc.* **1973**, *95*, 4957.
(606) Hattori, H.; Takahashi, O.; Takagi, M.; Tanabe, K. *J. Catal.* **1981**, *68*, 132.
(607) Na, K.; Okuhara, T.; Misono, M. *Chem. Lett.* **1993**, *7*, 1141.
(608) Suzuki, S.; Kogai, M.; Ono, Y. *Chem. Lett.* **1984**, 699.
(609) Ono, Y.; Taguchi, M.; Gerile, S.; Suzuki, S.; Baba, T. *Stud. Surf. Sci. Catal.* **1985**, *20*, 167.
(610) Sebulsky, R. T.; Henke, A. M. *Ind. Eng. Chem. Proc. Des. Dev.* **1971**, *10*, 272.
(611) Izumi, Y.; Natsume, M.; Takamine, H.; Tamaoki, I.; Urabe, K. *Bull. Chem. Soc. Jpn.* **1989**, *62*, 2159.
(612) Kozhevnikov, I. V.; Tsyganok, A. I.; Timofeeva, M. N.; Kulikov, S. M.; Sidel'nikov, V. N. *Kinet. Katal.* **1992**, *33*, 430.
(613) Okuhara, T.; Misono, M. *J. Synth. Org. Chem. Jpn.* **1993**, *51*, 128.
(614) Soeda, H.; Okuhara, T.; Misono, M. *Chem. Lett.* **1994**, *5*, 909.
(615) Kricheldorf, H. R.; Engelhardt, J. *J. Polym. Sci. Part A, Polym. Chem.* **1990**, *28*, 2335.
(616) Nishimura, T.; Okuhara, T.; Misono, M. *Appl. Catal.* **1991**, *73*, L7.
(617) Okuhara, T.; Nishimura, T.; Watanabe, H.; Misono, M. *J. Mol. Catal.* **1992**, *74*, 247.
(618) Nowinska, K.; Fiedorow, R.; Adamiec, J. *J. Chem. Soc., Faraday Trans.* **1991**, *87*, 749.
(619) Nomiya, K.; Sasa, S.; Miwa, M. *Chem. Lett.* **1980**, 1075.
(620) Ohgoshi, S.; Kanai, J.; Sugimoto, M. EU. Patent Appl. 561284 A1, 1993.
(621) Okuhara, T.; Yamashita, M.; Na, K.; Misono, M. *Chem. Lett.* **1994**, *8*, 1451.
(622) Hino, M.; Arata, K. *Chem. Lett.* **1979**, 1259.
(623) Hino, M.; Arata, K. *J. Chem. Soc., Chem. Commun.* **1979**, 1148.
(624) Hino, M.; Arata, K. *J. Chem. Soc., Chem. Commun.* **1980**, 851.
(625) Tanabe, K.; Itoh, M.; Morishige, K.; Hattori, H. In *Preparation of Catalysts*; Delmol, B., Jacobs, P. A., Poncelet, G., Eds.; Elsevier: Amsterdam, 1976; p 65.
(626) Jin, T.; Machida, M.; Yamaguchi, T.; Tanabe, K. *Inorg. Chem.* **1984**, *23*, 4396.
(627) Jin, T.; Yamaguchi, T.; Tanabe, K. *J. Phys. Chem.* **1986**, *90*, 4794.

(628) Serrete, G. P. D.; Khazisdey, A.; Clearfield, A. *Book of Abstracts*, 206th National Meeting of the American Chemical Society, Chicago, Fall, 1993; American Chemical Society: Washington, DC, 1993; p 197.
(629) Hino, M.; Arata, K. *Chem. Lett.* **1979**, *477*.
(630) Arata, K.; Hino, M. *Appl. Catal.* **1990**, *59*, 197.
(631) Corma, A.; López-Nieto, J. M.; Juan-Rajadell, M. I. *Appl. Catal. A* **1994**, *116*, 151.
(632) Clearfield, A.; Serrete, G. P. D.; Khazi-Syed, A. H. *Catal. Today* **1994**, *20*, 295.
(633) Nascimento, P.; Akratopoulou, C.; Oszagyan, M.; Coudurier, G.; Travers, C.; Joly, J. F.; Vedrine, J. C.; Hall, W. K.; Wender, I.; Fripat, J. J.; Morterra, C.; Conner, W. C.; Pinna, F.; Hightower, J. W.; Dejong, K. P. *Stud. Surf. Sci. Catal.* **1993**, *75*, 1185.
(634) Davis, B. H.; Keogh, R. A.; Srinivasan, R. *Catal. Today* **1994**, *20*, 219.
(635) Chokkaram, S.; Srinivasan, R.; Milburn, D. R.; Davis, B. H. *J. Colloid Int. Sci.* **1994**, *165*, 160.
(636) Chen, F. R.; Coudurier, G.; Joly, J. F.; Vedrine, J. C. *J. Catal.* **1993**, *143*, 616.
(637) Arata, K. *Adv. Catal.* **1990**, *37*, 165.
(638) Norman, C. J.; Goulding, P. A.; McAlpine, I. *Catal. Today* **1994**, *20*, 313.
(639) Matsuhashi, H.; Hino, M.; Arata, K. *Appl. Catal.* **1990**, *59*, 205.
(640) Hino, M. Ph.D. Thesis Hokkaido Univ., 1982.
(641) Lee, J. S.; Park, D. S. *J. Catal.* **1989**, *120*, 46.
(642) Bensitel, M.; Saur, O.; Lavalley, J. C.; Morrow, B. A. *Mater. Chem. Phys.* **1988**, *19*, 147.
(643) Yamaguchi, T. *Appl. Catal.* **1990**, *61*, 1.
(644) Vesteghem, H.; Jaccon, T.; Lecomte, A. *Rev. Phys. Appl.* **1989**, *24*, C4-59.
(645) Parera, J. M. *Catal. Today* **1992**, *15*, 481.
(646) Yamaguchi, T.; Tanabe, K.; Kung, Y. C. *Mater. Chem. Phys.* **1986**, *16*, 67.
(647) Morterra, C.; Cerrato, G.; Bolis, V. *Catal. Today* **1993**, *17*, 505.
(648) Morterra, C.; Cerrato, G.; Emanuel, C.; Bolis, V. *J. Catal.* **1993**, *142*, 349.
(649) Riemer, T.; Spielbauer, D.; Hunger, M.; Mekhemer, G. A. H.; Knozinger, H. *J. Chem. Soc., Chem. Commun.* **1994**, 1181.
(650) Umansky, B.; Engelhardt, J.; Hall, W. K. *J. Catal.* **1991**, *127*, 128.
(651) Mukaida, K.; Miyoshi, T.; Satoh, T. In *Acid-Base Catalysis*; Tanabe, K., *et al.*, Eds.; Kodansha: Tokyo, 1989; p 363.
(652) Akratopoulou, C.; Babou, F.; Coudurier, G.; Vedrine, J. C. *Simp. Iberoamer. de Catal.* **1994**, *XIV*, 837 (12–16 Sept., Concepción Chile).
(653) Babou, F.; Bigot, B.; Sautet, P. *J. Phys. Chem.* **1993**, *97*, 11501.
(654) Arata, K.; Hino, M.; Yamagata, N. *Bull. Chem. Soc. Jap.* **1990**, *63*, 244.
(655) Waqif, M.; Bachelier, J.; Saur, O.; Lavalley, J. C. *J. Mol. Catal.* **1992**, *72*, 127.
(656) Tanabe, K.; Misono, M.; Ono, Y.; Hattori, H. *Stud. Surf. Sci. Catal.* **1989**, 51.
(657) Yinyan, H.; Gailian, Z.; Wenpu, Z. *Rare Met.* **1992**, *11*, 185.
(658) Hollstein, E. J.; Wei, J. T.; Hsu, C. Y. U.S. Patent 4918041, 1990; 4956519, 1990.
(659) Hsu, C. Y.; Patel, V. K.; Vahlsing, D. H.; Wei, J. J.; Myers, H. K., Jr. U.S. Patent 5019671, 1991.
(660) Hsu, C. Y.; Heimbuch, C. R.; Armes, C. T.; Gates, B. C. *J. Chem. Soc., Chem. Commun.* **1992**, 1645.
(661) Adeeva, V.; Lei, G. D.; Sachtler, W. M. H. *Appl. Catal. A* **1994**, *118*, L11–L15.
(662) Nakano, Y.; Iizuka, T.; Hattori, H.; Tanabe, K. *J. Catal.* **1979**, *57*, 1.
(663) Yamaguchi, T. *Catal. Today* **1994**, *20*, 1999.
(664) Arata, K.; Hino, M. Jpn. Patent 63-114790, 1988.
(665) Hino, M.; Arat, K. *J. Chem. Soc., Chem. Commun.* **1988**, 1259.
(666) Arata, K.; Hino, M. *Proc. Int. Congr. Catal.* **1988**, *9*, 1727.
(667) Hino, M.; Arata, K. *Chem. Lett.* **1989**, 971.
(668) Arata, K.; Hino, M. *Shokubai* **1989**, *31*, 477.
(669) Kochloefl, K.; Kraus, M.; Bazant, U. *Proc. Int. Congr. Catal.* **1968**, *4*, 490.
(670) Davis, B. H. *J. Colloid Interface Sci.* **1976**, *3*, 115.
(671) Davis, B. H.; Ganesan, P. *Ind. Eng. Chem. Prod. Res. Dev.* **1979**, *18*, 191.
(672) Hayashi, H.; Kurokawa, K.; Hosokawa, W.; Tanaka, T.; Okazi, T. *J. Catal.* **1980**, *66*, 49.
(673) Davis, B. H. *J. Org. Chem.* **1982**, *47*, 900.
(674) Davis, B. H. *J. Catal.* **1983**, *79*, 58.
(675) Franklin, R.; Goulding, P.; Haviland, J.; Joyner, R. W.; McAlpine, I.; Moles, P.; Norman, C.; Nowell, T. *Catal. Today* **1991**, *10*, 405.
(676) Kagaku, K. Eur. Patent 0433959, 1991.
(677) Sohn, J. R.; Jang, H. J. *J. Catal.* **1992**, *136*, 267.
(678) Hino, M.; Arata, K. *Chem. Lett.* **1979**, 963.
(679) Arata, K.; Hino, M. *Bull. Chem. Soc. Jpn.* **1980**, *53*, 535.
(680) Tanabe, K.; Kayo, A.; Yamaguchi, T. *J. Chem. Soc., Chem. Commun.* **1981**, 602.
(681) Matsuhashi, H.; Hino, M.; Arata, K. *Appl. Catal.* **1990**, *59*, 205.
(682) Kazama, Y.; Shimamura, Y.; Hiyama, O. Jpn. Kokai Tokkyo Koho 74-10591; *Chem. Abstr.* **1974**, *81*, P1357535.
(683) Hino, M.; Arata, K. *Chem. Lett.* **1981**, 1671.
(684) Arata, K.; Hino, M. *Shokubai (Catalysts)* **1983**, *25*, 124.
(685) Tanabe, K.; Misono, M.; Ono, Y.; Hattori, H. *Stud. Surf. Sci. Catal.* **1989**, *51*, 285.
(686) Tanabe, K.; Yamaguchi, T.; Akiyama, K.; Mitho, A.; Iwabuchi, K.; Isogai, K. *Proc. 8th Intern. Congr. Catal.*; Verlag Chemie: Weinheim, 1984, Vol. 5, 601.
(687) Hino, M.; Arata, K. *J. Chem. Soc., Chem. Commun.* **1985**, 112.
(688) Arata, K.; Hino, M. *Appl. Catal.* **1990**, *59*, 197.
(689) Lee, J. S.; Yeom, M. H.; Park, D. S. *J. Catal.* **1990**, *126*, 361.
(690) Kokes, R. J.; Dent, A. C. *Adv. Catal.* **1970**, *22*, 1.
(691) Sohn, J. R.; Pae, Y. I.; Jang, H. J.; Park, M. Y. *J. Catal.* **1991**, *127*, 449.
(692) Olah, G. A.; Halpern, Y.; Shen, J.; Mo, I. K. *J. Am. Chem. Soc.* **1973**, *95*, 4960.
(693) Takahashi, O.; Hattori, H. *J. Catal.* **1981**, *68*, 144.
(694) Pinna, F.; Signoretto, M.; Strukul, G.; Cerrato, G.; Mortera, C. *Catal. Lett.* **1994**, *26*, 339.
(695) Sommer, J.; Bukala, J. *Acc. Chem. Res.* **1993**, *26*, 370.
(696) Yori, J. C.; Luy, J. C.; Parera, J. M. *Catal. Today* **1989**, *5*, 493.
(697) Yori, J. C.; Luy, J. C.; Parera, J. M. *Appl. Catal.* **1989**, *46*, 103.
(698) Garin, F.; Andriamasinoro, D.; Abdulsamad, A.; Sommer, J. *J. Catal.* **1991**, *131*, 199.
(699) Hosoi, T.; Shimidzu, T.; Itoh, S.; Baba, S.; Takaoka, H.; Imai, T.; Yokoyama, N. *Prepr.—Am. Chem. Soc., Div. Pet. Chem.* **1988**, *33*, 562.
(700) Zhao, J.; Huffman, G. P.; Davis, B. H. *Catal. Lett.* **1994**, *24*, 385.
(701) Ebitani, K.; Konishi, J.; Hattori, H. *J. Catal.* **1991**, *130*, 257.
(702) Meusinger, J.; Corma, A. *J. Catal.*, in press.
(703) Iglesia, E.; Kramer, G. M.; Gates, W. E.; Ernst, R. H. Eur. Patent Appl. 0507518 A2, 1992.
(704) Iglesia, E.; Soled, S. L.; Kramer, G. M. *J. Catal.* **1993**, *144*, 238.
(705) Surrell, M. S. *Appl. Catal.* **1987**, *34*, 109.
(706) Guo, C. X.; Yao, S.; Cao, J. H.; Qian, Z. H. *Appl. Catal.* **1994**, *107*, 229.
(707) Corma, A.; Martínez, A.; Martínez, C. *J. Catal.* **1994**, *146*, 185.
(708) Corma, A.; Juan-Rajadell, M. I.; López-Nieto, J. M.; Martínez, A.; Martínez, C. *Appl. Catal. A* **1994**, *111*, 175.
(709) Corma, A.; Juan-Rajadell, M. J.; López-Nieto, J. M.; Martínez, A.; Martínez, C. Unpublished results.
(710) Arata, K.; Hino, H.; Yamagata, N. *Bull. Chem. Soc. Jpn.* **1990**, *63*, 244.
(711) Wen, M. Y.; Wender, I.; Tierney, J. W. *Energy Fuels* **1990**, *4*, 372.
(712) Keogh, R. A.; Sparks, D.; Hu, J.; Wender, I.; Tierney, J. W.; Wang, W.; Davis, B. H. *Energy Fuels.* **1994**, *8*, 755.
(713) Lee, J. S.; Oyama, T. *Catal. Rev. Sci. Eng.* **1988**, *30*, 249.
(714) Amenomiya, Y.; Birss, V. I.; Goledzinowski, M.; Galuszka, J.; Sanger, A. R. *Catal. Rev. Sci. Eng.* **1991**, *32*, 163.
(715) Wolf, E. E., Ed. *Methane Conversion by Oxidative Processes: Fundamental and Engineering Aspects*; Van Nostrand Reinhold: New York, 1992.
(716) Olah, G. A. *Acc. Chem. Res.* **1987**, *20*, 422.
(717) Olah, G. A.; Mo, Y. M. *J. Am. Chem. Soc.* **1972**, *74*, 6864.
(718) Olah, G. A.; Gupta, B.; Farina, M.; Felberg, J. D.; Ip, W. M.; Husain, A.; Karpeles, R.; Lammerstsma, K.; Melhotra, A. K.; Trivedi, N. J. *J. Am. Chem. Soc.* **1985**, *107*, 7097.
(719) Bucsi, I.; Olah, G. A. *Catal. Lett.* **1992**, *16*, 27.
(720) Batamack, P.; Bucsi, I.; Molnar, A.; Olah, G. A. *Catal. Lett.* **1994**, *25*, 11.

CR9400931